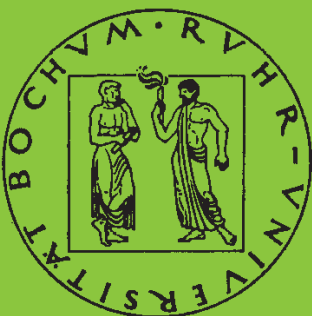


**Mitteilungen aus dem Institut für Mechanik**

**J. Chroscielewski  
J. Makowski  
H. Stumpf**

**Finte Elements for Irregular Nonlinear  
Shells**

Heft Nr. 96



**RUHR-UNIVERSITÄT BOCHUM**

**RUHR-UNIVERSITÄT BOCHUM**

**J. CHRÓŚCIELEWSKI**

**J. MAKOWSKI**

**H. STUMPF**

**Finite Elements**

**for**

**Irregular Nonlinear Shells**

**MITTEILUNGEN AUS DEM INSTITUT FÜR MECHANIK NR. 96**

**1994**

**Herausgeber:**  
**Institut für Mechanik der Ruhr-Universität Bochum**  
**Schriftenreihe**  
**Universitätsstr. 150**  
**44780 Bochum**

© o. Prof. Dr.-Ing H. Stumpf

Dr. inż. J. Chróścielewski

Dr. inż. J. Makowski

Alle Rechte, auch das der Übersetzung in fremde Sprachen, vorbehalten.  
Ohne Genehmigung der Autoren ist es nicht gestattet, dieses Heft ganz  
oder teilweise auf fotomechanischem Wege (Fotokopie, Mikrokopie) zu  
vervielfältigen oder in elektronischen Medien zu speichern.

## Contents

<b>Introduction .....</b>	<b>1</b>
---------------------------	----------

### Chapter I

<b>Concepts in finite element analysis of shells .....</b>	<b>7</b>
--	----------

1. Formulation of shell elements..... 7
2. Classical  $C^0$  shell elements ..... 13
3. Other types of shell finite elements ..... 18
4. Folds, junctions and shell intersections ..... 21

### Chapter II

<b>Boundary value problems of irregular shells.....</b>	<b>26</b>
---	-----------

1. Shell structures and shell theory ..... 26
2. General theory of irregular shells ..... 33
3. Field equations and side conditions ..... 37
4. Weak form of the momentum balance laws..... 43
5. Iterative solution of nonlinear problems ..... 47
6. Parametrization of rotations..... 51

### Chapter III

<b>Finite element approximations.....</b>	<b>55</b>
---	-----------

1. Preliminaries ..... 55
2. Discretization of the undeformed configuration ..... 60
3. Displacement/rotation based shell elements ..... 65
4. Stress resultant mixed shell elements ..... 73
5. Stress resultant semi-mixed shell elements ..... 78
6. Assumed strain shell elements..... 80

**Chapter IV**

<b>Numerical analysis of linearly elastic shells .....</b>	<b>85</b>
1. Tested shell finite elements .....	85
2. Smooth shell problems .....	91
3. Folds and kinks in shell structures .....	106
4. Folded plate structures .....	118
5. Irregular shell structures .....	126
<b>References.....</b>	<b>132</b>

## Introduction

In spite of significant progress in the finite element analysis of shell structures, the search for reliable and efficient elements capable to represent the general nonlinear behavior of shell structures with arbitrary geometry, loading, boundary conditions, and material properties still appears as a challenging task. The vast number of papers published on the subject is perhaps the best measure of the encountered difficulties.<sup>1</sup> It seems to be a general agreement that presently there exists a fairly large number of shell elements, which are reliable for the analysis of some classes of problems if used with care. However, none of those elements meets a common acceptance to be superior to others and the search for a general applicable shell element appears as an endless task.<sup>2</sup> To some extent this is so, since quite often the elements are formulated on the basis of special techniques without formal mathematical justification, and relatively few elements have allowed a rigorous mathematical stability and error analysis. Also the lack of an access to exact analytical solutions makes it difficult to assess various shell element formulations.

Generally, three distinct classes of shell elements can be distinguished: (I) Flat triangular or quadrilateral elements formed by the superposition of stretching behavior (plane stress element) and bending behavior (plate element), (II) Curved elements formulated on the basis of various specialized shell theories, usually Kirchhoff-Love or Mindlin-Reissner type theories, (III) Elements derived from the isoparametric 3D brick element by the use of the degeneration method. The elements of each class have their own advantages and deficiencies. Actually, nearly all existing shell elements are formulated on the basis of quite restrictive assumptions. In particular, it is usually assumed that:

1. The through-the-thickness material fibres remain straight during deformation.
2. The through-the-thickness material fibres preserve their length during deformation.

---

<sup>1</sup>The survey articles by GALLAGHER [1976], BELYTSCHKO [1986], WEMPNER [1989], YANG, SAIGAL AND LIAW [1990], and the recent works cited throughout this work give a rather complete account of the earlier efforts, current trends and an extensive bibliography in the field.

<sup>2</sup>Cf. TAYLOR [1988].

Moreover, it is nearly the rule that the formulation is based on strong smoothness assumptions. Specifically, one typically assumes, implicitly rather than clearly stated, that:

- A. A shell is geometrically represented by a smooth regular surface (called a shell reference surface).
- B. A deformation of the reference surface is described by an injective, globally invertible and smoothly differentiable map.
- C. All static and kinematic variables are smoothly differentiable fields over the shell reference surface.

The assumption 1), when combined with the assumptions A)–C) and with the standard finite element discretization, leads to elements with five degrees-of-freedom per node, three translational and two rotational ones. As a result, an essential difficulty one encounters in the analysis of general engineering structures, which are typically composed of rod-like and plate/shell-like segments interconnected pointwise at joints and along junctions in a widely varying manner to form, in overall, fairly complex structures. Folded plates, multicell box girders, stiffened prismatic or non-prismatic shells, shell structures sustained by columns and stiffened with beams or plates are typical examples.

In turn, the assumption 2) precludes an application of the formulated elements to large strain problems, which are characterized by highly nonlinear through-the-thickness deformation. A large strain deformation is typical for rubber-like materials, which are usually incompressible or nearly so. An attempt to extend standard finite element formulations to such problems is accompanied by essential difficulties due to appearance of an unknown pressure.<sup>3</sup>

The aforementioned problems are just a few among many others. From the careful study of the literature, it becomes apparent that difficulties in the finite element analysis of shell structures with arbitrary geometry, loading, boundary conditions, etc., center around the following three main issues:

- I) Shell theory - reduction of an otherwise three-dimensional problem of continuum mechanics to the one having coordinates of a certain surface as the only independent variables.

---

<sup>3</sup> See HUGHES AND CARNOY [1983], PARISCH [1983]. The formulations presented in these papers account for large membrane strains but still excludes large bending strains.

- II) Discretization - finite element approximation of an otherwise two-dimensional continuum problem.
- III) Irregularities - treatment of shell branches and shell intersections, stiffeners, reinforcements, shell-to-rod transitions, etc.

The aim of this work is to present a systematic treatment of all three issues with emphasis on their different nature. Our starting point will be the shell theory developed in the accompanying paper.<sup>4</sup> Actually, the shell theory developed in that paper resolves the first and third issue. In this way we can actually concentrate on the formulation of shell finite elements. It may be noted that the formulation of shell elements is essentially independent of the manner the underlying shell theory was formulated. However, the physical meaning of the finite element solutions is strongly related to the basic concepts which underlay the development of the shell theory. This fact is particularly important in the case of the shell theory formulated in Part I, which substantially differs from the approaches usually adopted in the formulation of shell finite elements. For this reason we find it necessary to present below a short summary of the main concepts, within which the shell theory was developed in that work.

The main virtues of the approach applied in Part I are:

- It draws a clear distinction between the general physical laws, which are independent of specific material properties and the specific construction of the shell, and the constitutive relations, which define particular classes of shells.
- The mechanical balance laws for shells are derived by direct specification of the laws of continuum mechanics for a shell-like body with no simplifying hypotheses and/or ad hoc postulates of whatsoever nature. In effect, various simplifying assumptions underlying the classical derivation of basic shell governing equations are avoided.
- The kinematics of the shell is the outcome of the formulation and not a basic assumption or a postulate of the theory as it is the case in other formulations of shell theory.
- Displacements, rotations and strains are not restricted in any way as to their magnitude. There is also no thinness assumption.

---

<sup>4</sup> MAKOWSKI AND STUMPF [1994], hereafter referred to as Part I. The shell theory developed in that paper provides an essential refinement and substantial generalization of our earlier studies, MAKOWSKI AND STUMPF [1988,1990].



- Independent kinematical variables of the shell theory consist of the displacement field of a shell reference surface and a proper orthogonal tensor specifying independent mean rotations of the shell cross sections. This feature is particularly important from the computational point of view.<sup>5</sup>
- The only approximate character of the theory may appear in the form of two-dimensional constitutive equations.

Moreover, the regularity assumptions required in the formulation are far weaker than one typically adopts. In particular:

- The shell reference surface needs not be smooth but solely piecewise smooth or a union of such surfaces.
- The deformation of the shell reference surface needs not be smooth but solely piecewise smooth or even piecewise continuous.
- Various kinematic and static variables appearing in the shell theory are admitted to suffer jump discontinuity across curves on the shell reference surface.

In effect, the shell theory formulated within this approach, is rich enough to account for extension (compression), flexure, transverse shear and an arbitrary through-the-thickness deformation. Thus it is applicable to large strain problems aside large displacement/rotation problems. The underlying kinematic model of this theory coincides with a geometric surface (a shell reference surface), each point of which has extra degrees of freedom of the rigid body. In effect, all shell finite elements developed in this work include the drilling rotation formulated on the firm foundation of an exact (in defined sense) shell theory. By implication, these elements have all six degrees of freedom at each node, three translational and three rotational ones. As such, they are equally applicable to smooth as well as to irregular shell structures containing folds, branches, kinks, column supports, stiffeners, etc.

Moreover, the relaxed regularity assumption adopted in Part I, yields not only the field equations of the shell (equilibrium equations, kinematic relations, etc.), but also static and kinematic jump conditions due to non-smoothness of the shell reference surface or non-smoothness of various static and kinematic variables. In addition, the resultant stress couple vectors include all three components along any basis on the reference surface. By implication, the developed shell theory makes it possible to satisfy rigorously static jump conditions. This is in contrast with

---

<sup>5</sup> See CHRÓSCIELEWSKI, MAKOWSKI AND STUMPF [1992,1994].

various other attempts to develop shell finite elements with drilling degree-of-freedom. An element enriched by this degree-of-freedom makes it applicable to non-smooth shell structures, but it does not allow to satisfy static jump conditions. Let us note that the formulation of shell finite elements is based on a suitable variational principle. Accordingly, static jump conditions do not enter the formulation explicitly.

We now outline the contents of this work. In Chapt. I we provide a very short and selective overview of the basic concepts in the finite element analysis of shells. Chapt. II contains the summary of the complete set of shell governing equations together with the formulation of the momentum balance law in a weak form (principle of virtual displacements). On this basis we next present a general iterative procedure which is needed in the solution of nonlinear shell problems. The corresponding variational principles with relaxed regularity requirements are formulated in Chapt. III. These principles provide the mathematical basis for the formulation of different classes of shell finite elements. In the formulation are included a displacement/rotation based Lagrange family of finite elements, a stress resultant based mixed and a semi-mixed family of elements as well as so-called assumed strain elements. Finally, in Chapt. IV we present the numerical analysis of linearly elastic shells. In order to obtain a still deeper insight into the problem a Lagrange family of standard degenerated shell elements with five degrees of freedom per node and an element with six degrees of freedom per node, based on the von Karman plate theory, are considered as well. Their limited range of applicability is demonstrated. The presented numerical results cover a large menu of illustrative test examples of complex plate and doubly curved shell structures, for which linear and nonlinear solutions with a pre- and post-buckling analysis are discussed. In the study altogether sixteen shell elements have been tested. This includes the Lagrange family of 4-, 9- and 16-node displacement-rotation based elements, and 4-node and 9-node elements based on the mixed formulation, on the semi-mixed formulation, and on the assumed strain interpolation.

Where feasible we shall adopt the notation and convention of modern continuum mechanics as well as coordinate free vector and tensor calculus. As a rule we use boldface lower case letters to denote vectors and vector-valued functions. Boldface capital letters will denote tensors and tensor-valued functions, and we write  $\mathbf{u} \cdot \mathbf{v}$ ,  $\mathbf{u} \times \mathbf{v}$  and  $\mathbf{u} \otimes \mathbf{v}$  for the usual inner product, cross product and tensor product of two vectors. Throughout this paper we use standard summation convention that lower-case Greek indices have the range 1,2, lower-case Latin indices the range 1,2,3, and that diagonally repeated indices are summed over their range. If no confusion can arise, we make no distinction between functions and

values of functions. By  $dA$  and  $dL$  we denote surface and line elements of corresponding surface and line integrals.

## Chapter I

# Concepts in finite element analysis of shells

### 1. Formulation of shell finite elements

**1.1 Basic steps in the finite element formulations.** The finite element method was initially developed for structural problems but it has since been extended to numerous field problems. Generally, the finite element method may be formulated and interpreted from two different viewpoints: a physical and a mathematical one. The physical approach is closely related to the original formulation and an extensive application of the method in structural analysis. Mathematically, the finite element method can be considered as an application of the Rayleigh-Ritz method or its more general counterpart, the Bubnov-Galerkin method, together with the use of piecewise polynomials to approximate solutions of boundary value problems. Regardless of the adopted viewpoint and of a problem to be solved, a standard finite element formulation primarily involves the following steps:<sup>1</sup>

1. Definition of the problem and its domain;
2. Discretization (approximation) of the domain;
3. Discretization (approximation) of independent (unknown) variables of the problem.

Each step requires a great deal of different constructions depending on the physical and mathematical nature of the problem. In this work we shall be concerned with the problems of shells.

**1.2 Continuum mechanics formulation.** Shells, whatever shape they have and however thin they could be, are three-dimensional bodies. The deformation of a

---

<sup>1</sup> Since the basic concepts of the finite element method are well-known, e.g. ZIENKIEWICZ AND TAYLOR [1989], we need not go into details here.

shell is thus governed by the basic laws of continuum mechanics. These laws can be stated either as integral balance laws (balance laws of linear and angular momentum) or as integral identities (principle of virtual work of forces and torques). In the finite element analysis the integral identities are usually taken as the point of departure of a formulation. These identities provide also the starting point of the weak formulation of the problem.

Relative to a reference configuration  $B$  the deformation of the body is described by a map  $\chi$ , which assigns to each particle  $X$  its spatial place  $x$  in the current configuration:

$$\mathbf{x} = \chi(\mathbf{X}) = \mathbf{X} + \mathbf{u}(\mathbf{X}), \quad (1.1)$$

where  $\mathbf{u}$  denotes the associated displacement field (Fig. 1).

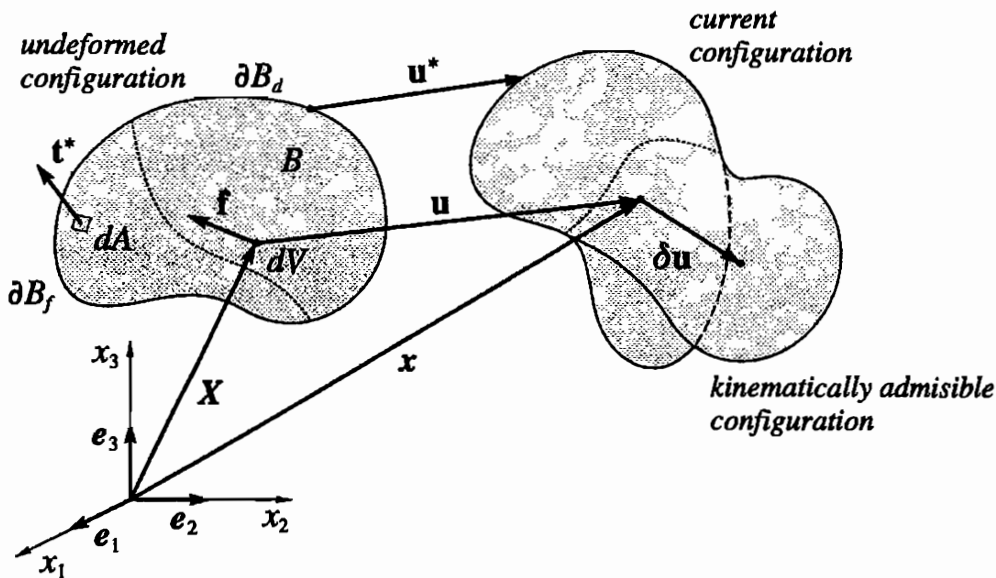


Fig. 1

Under prescribed loading and boundary conditions the principle of virtual work (of forces) asserts that

$$W_{int} - W_{ext} = 0, \quad (1.2)$$

for every kinematically admissible virtual displacement  $\delta \mathbf{u}$ , where the internal and external virtual work are given by

$$\begin{aligned} W_{int} &= \int_B \mathbf{T} \cdot \delta \mathbf{F} dV = \int_B \mathbf{S} \cdot \delta \mathbf{E} dV, \\ W_{ext} &= \int_B \mathbf{f} \cdot \delta \mathbf{u} dV + \int_{\partial B_f} \mathbf{t}^* \cdot \delta \mathbf{u} dA. \end{aligned} \quad (1.3)$$

The following standard notations are used here:

- $\mathbf{T}(X)$  – the first Piola-Kirchhoff stress tensor,
- $\mathbf{S}(X)$  – the second Piola-Kirchhoff stress tensor,
- $\mathbf{F}(X)$  – the deformation gradient,
- $\mathbf{E}(X)$  – the Green strain tensor,
- $\mathbf{f}(X)$  – the body force vector,
- $\mathbf{t}^*(X)$  – the external boundary force vector prescribed on the part  $\partial B_f$  of the boundary,

together with the well-known relations

$$\mathbf{F} = \nabla \boldsymbol{\chi} = \mathbf{1} + \nabla \mathbf{u}, \quad \mathbf{C} = \frac{1}{2}(\nabla \mathbf{u} + \nabla \mathbf{u} + \nabla \mathbf{u}^T \nabla \mathbf{u}), \quad \mathbf{T} = \mathbf{F} \mathbf{S}. \quad (1.4)$$

The variational equation (1.2) remains valid independent of the nature of constitutive equations. When used with appropriate constitutive equations it provides the weak formulation of the problem.

The solution of a nonlinear problem is typically achieved using a suitable iterative procedure, which in turn involves a linearization process. With appropriate assumptions regarding material constitutive behavior and loading, the linearized form of the principle of virtual work (1.2) can be derived in a standard manner.

**1.3 Strategies for shell element formulations.** Basically, in the computational analysis of shells, such as the finite element method, two approximation processes are employed:

- Reduction process – reduction of an otherwise three-dimensional problem of continuum mechanics to one having the coordinates of a certain surface as the only independent variables.
- Discretization process – finite dimensional approximations of an otherwise continuum problem (infinite dimensional problem).

The two processes are essentially independent of each other and they can be applied in either order. In effect, two basic strategies emerge for the development of shell finite elements:

- A. Shell theory based formulation – the classical concept of a shell theory is employed as the starting point of the finite element formulations.
- B. Degenerated shell element concept – the shell elements are derived directly from the basic equations of continuum mechanics simultaneously with the finite element discretization.

Thus these strategies employ the two approximation processes in the inverse order, as it is illustrated in Fig. 2.

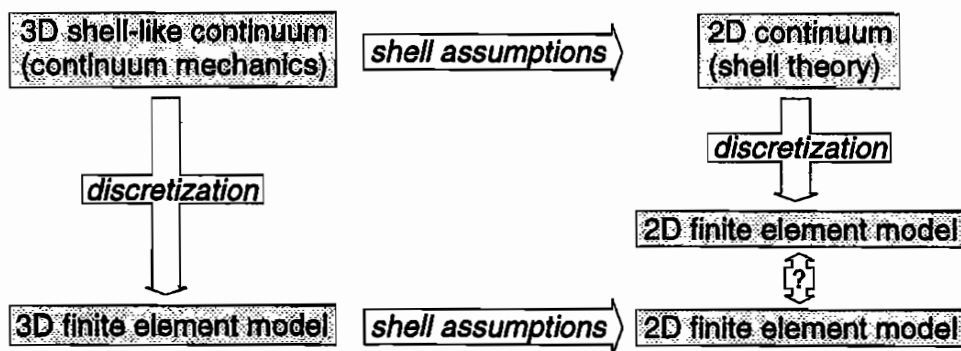


Fig. 2

**1.4 Finite element models.** Mathematical formulation of the finite element method involves two basic aspects:

- A) Weak formulation of the problem,
- B) Selection of the space of trial functions and of test functions (technically, the choice of the number of nodes, the number of nodal variables and the so-called shape functions).

With respect to A) two main classes of finite element formulations can be distinguished:

- A1) Single field finite elements,
- A2) Multi-field finite elements.

An application of the finite element method to the analysis of shells typically starts with the displacement approach based on the principle of stationary total potential energy together with a Lagrangean interpolation scheme. These elements remain still most often used owing to their simplicity, computational efficiency, and the clarity of the formulation. The most typical example of the class A1) are finite

elements based on the displacement (in our case displacement/rotation) formulation having the principle of virtual displacements as the underlying weak formulation of the problem.

As an alternative to the displacement-like models mixed formulations may be employed, in which separate interpolants are used for the displacement and the other fields. Among the finite elements belonging to this class we can mention mixed formulations usually based on a Hellinger-Reissner type variational formulation.

The clear foundation of the method finite element method gives rise to various finite element formulations, which are mainly based on some technical constructions usually having no variational formulation of the problem. Among such formulations the assumed strain techniques appear to be the most often used ones. However, finite elements formulated within these techniques are less reliable, although they can provide a sound solution for many engineering problems.<sup>2</sup>

**1.5 Shell hypotheses.** The conventional procedure for developing shell theories employs the three-dimensional theory as the point of departure, and subsequently, certain simplifying assumptions are introduced to reduce the three dimensional problems of continuum mechanics to be applicable for shells. Classically, three basic groups can be distinguished:

1. Kirchhoff-Love type theory;
2. Mindlin-Reissner type theory;
3. Higher order theories.

Clearly, the resulting shell theory as well as the finite element formulations depend on the nature of the assumed kinematic constraints. The choice, which type of theory one intends to use, depends on several factors; among them are:

1. The regularity factor – the smoothness of the variables and the domain (shell reference surface);
2. The accuracy factor – the accuracy we wish to attain;

---

<sup>2</sup> SIMO AND HUGHES [1986] showed that the assumed strain methods in the linear case can be explained in a variational context by adopting the Hu-Washizu principle. However, this explanation does not seem to be easily extensible to nonlinear case.



3. The cost-efficiency factor – the price we are willing to pay in terms of computational time and effort for the formulation.

**1.6 Requirements on shell elements.** Independent of the type of shell theory used and the type of finite element formulation employed, various requirements have to be set upon the development of shell elements in order to render the elements widely applicable in the engineering analysis. Ideally, quite a few requirements should be satisfied:<sup>3</sup>

1. The element should be reliable and computationally effective.
2. The theoretical formulation of the element should be strongly based on continuum mechanics with assumptions in the finite element discretization, that are physically and mathematically clear and well-founded.
3. The element should be formulated using only the complete set of engineering nodal degrees of freedom – three nodal displacements and three rotations – preferably at corners only.
4. The element formulation should be general, i.e. the element should be applicable to any shell problem including
  - linear and nonlinear problems with finite displacements/rotations and finite strains,
  - thin and thick shells,
  - arbitrary geometry admitting non-smooth shells and multi-shells,
  - the predictive capability of the element should be high and be relatively insensitive to mesh distortions,
5. The element should possess the actual physical rigid body modes and should have no rank deficiency (should not contain spurious zero energy mechanism).
6. The element formulation should provide resultant stress/couples as accurate as displacements/rotations.
7. The element should be connectable with rod elements.

While easily stated, the above criteria are difficult to satisfy and a reasonable compromise is needed in general.

**1.7 Computational issues.** There is a number of purely computational issues that affect the efficiency of finite element solutions of shell problems:

- generation of a mesh,

---

<sup>3</sup> BATHE [1986], FREY [1989].

- element assembly,
- implementation of boundary conditions,
- the selection of numerical techniques to solve the resulting system of linear algebraic equations,
- the evaluation of the accuracy and quality of the solution,
- selection of numerical integration of the stiffness matrix and load vector.

In contrast to solving linear problems, the solution of nonlinear problems may vary considerably depending on the values of the independent and dependent variables. Accordingly, a main problem in the nonlinear analysis is the efficient and complete solution of the resulting system of nonlinear algebraic equations. All techniques used for solving sets of nonlinear algebraic equations involve a sequence of iterations, and most have the drawback that convergence depends on an initial approximation, which should be close to the true solution. Additional difficulties arise in the analysis of buckling problems, which require to locate and determine all singular points (limit points, branch points, etc.). Most techniques used for solving nonlinear problems are based on the continuation method, which has the advantage of producing solutions over a large range of the independent variables.

**1.8 Testing shell elements and error estimations.** The objective of the finite element formulation is to obtain an acceptably accurate and reliable solution of the problem under study. Accordingly, the formulation should provide not only an approximate solution but also some reliable information about its accuracy. In general, the quality of the finite element solutions depends on several key factors such as:

- The regularity (smoothness) of the solutions;
- The highest order derivative appearing in the definition of the functional underlying the finite element formulation;
- The largest degree of complete polynomials in the space spanned by the shape functions.

The problem of accuracy of the finite element formulations has mainly been transformed into the question of how well the energy can be approximate. For linear elliptic problems this question has been extensively studied in the literature. However, the error estimation for shell problems is much more difficult.

## 2. Classical $C^0$ shell elements

**2.1 Isoparametric finite elements.** The standard finite element recipe for handling curvilinear elements (such as shell-like elements) is provided by the isoparametric concept, which have been used successfully for three-dimensional problems. Within this concept the same shape functions are employed to approximate both geometry (domain of a problem) and displacements (independent variables of a problem). This formulation may be well applied for the analysis of shells avoiding the use of shell theories. Within this approach, the geometry of the shell-like finite element  $\Omega_{(e)}$  is described by a set of natural curvilinear coordinates  $(\xi_i) \in [-1, +1]^3$ ,  $i=1,2,3$ , such that a cube  $v_{(e)}$  of bi-unit sides is uniquely mapped onto the shell element (Fig. 3). Then the displacement field (as well as the geometry) within the element is interpolated from its nodal values using a Lagrange interpolation scheme

$$\mathbf{u}(\xi_i) \equiv \begin{Bmatrix} u_1(\xi_i) \\ u_2(\xi_i) \\ u_3(\xi_i) \end{Bmatrix} = \sum_{a=1}^{n_e} L_a(\xi_i) \mathbf{u}_a, \quad \mathbf{u}_a \equiv \begin{Bmatrix} u_1 \\ u_2 \\ u_3 \end{Bmatrix}_a, \quad (2.1)$$

where  $L_a(\xi_i)$ ,  $a=1,2,\dots,n$ , are the so-called shape functions (usually Lagrange polynomials).

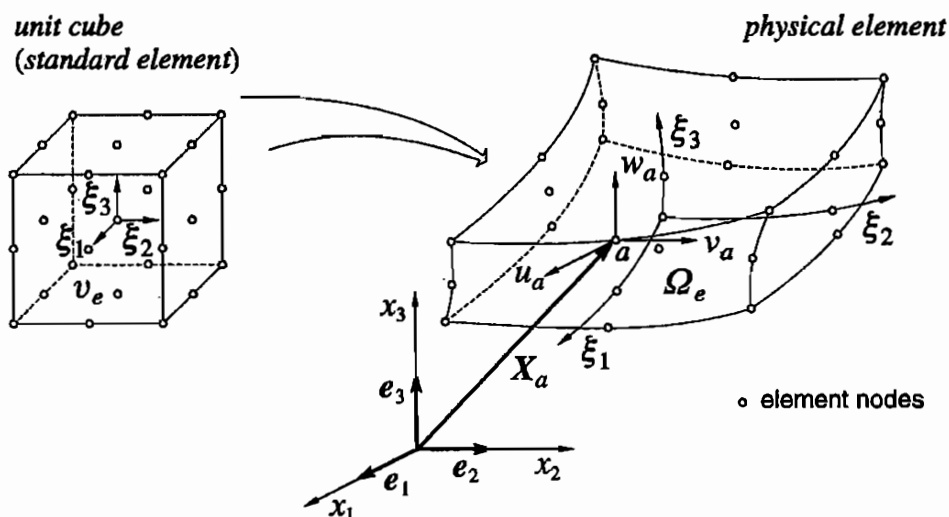


Fig. 3

Introducing the approximation (2.1) into the principle of virtual work (1.2) the discretized finite element equation follows in the standard manner. However, a straightforward application of the isoparametric concept to shell problems meets certain difficulties:<sup>1</sup>

- The use of several nodal points through-the-thickness ignores the well-known fact that for thin shells the through-the-thickness fibres remain nearly straight and preserve their length after deformation. This leads to an element with excessive degrees-of-freedom, which render the element uneconomical.
- The retention of all three nodal displacements at each node leads to large stiffness coefficients for relative displacements along an edge corresponding to the shell thickness. This causes numerical problems and inevitably leads to ill-conditioned equations, when the shell thickness becomes small compared with other dimensions of the element. Thus the element fails at a moderate length to thickness ratio due to displacement locking.

**2.2 Degenerated solid shell element.** The concept of the degenerated solid shell element has been first applied by Ahmad to the linear analysis of shells.<sup>2</sup> Since then, the popularity of this concept has grown enormously. The popularity of this concept is due mainly to its simplicity of formulation.

The degenerated element concept begins by discretizing directly the three-dimensional equations of continuum mechanics applying the isoparametric concept. Thus the three-dimensional formulation is first applied to a three-dimensional shell-like continuum and subsequently degenerated by assuming linear interpolation in the thickness direction, while retaining interpolation of any order in the surface directions. In this sense, the finite element discretization of the three-dimensional shell-like continuum is performed first and subsequent approximations in the thickness direction are imposed. In this way the nodal displacements on the bottom and top surfaces are replaced by the nodal displacement of the reference surface and the nodal vector (Fig. 4). The main advantages of this approach are:

- Conceptual simplicity is inherited from the three-dimensional theory.
- Direct applicability of existing three-dimensional constitutive models is maintained.

---

<sup>1</sup> ZIENKIEWICZ, TAYLOR AND TOO [1971].

<sup>2</sup> See AHMAD, IRONS AND ZIENKIEWICZ [1971].

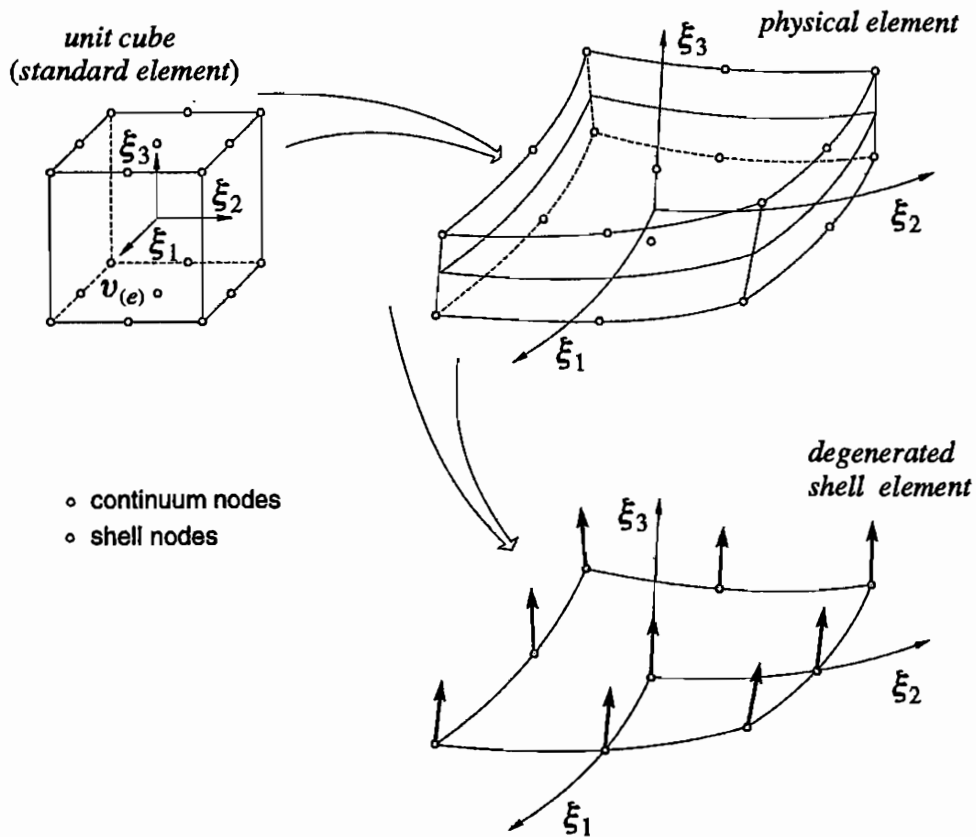


Fig. 4

While the basic concept behind the degenerated shell finite elements is very simple, this approach has its own weak sides. The basic inconveniences are:

- Their range of applicability is severely delimited by the assumption the adopted assumptions, which rules out the deformation along through-the-thickness fibres of the shell and thus excludes finite strain problems.
- The evaluation of the element matrices requires a spatial integration and hence the elements are in general expensive in computation.
- Essential difficulties arise in the analysis of irregular shell structures, since the element has only two rotational degrees of freedom.

**2.3 Mindlin-Reissner hypothesis.** Actually, the basic assumptions employed in the formulation of degenerated shell elements are identical to those used in the classical Mindlin-Reissner shell theory. In this sense the two approaches have much in common. In particular, since both are based on the same kinematical assumption, the either formulation accounts for the primary effects of transverse

shear and thus extend their applicability to moderately thick shells. However, they exclude the transverse normal deformation and thus they are restricted to small strain problems. From the computational point of view the main advantage compared with the Kirchhoff-Love type shell theory is the fact that only  $C^0$  inter element continuity is required, what simplifies considerably the construction of the finite element space.

Let us recall that according to the classical Mindlin-Reissner hypothesis:

1. Through-the-thickness shell fibres remain straight and inextensible during the deformation.
2. The normal stresses can be neglected (plane stress hypothesis).

When employed together with the standard variational procedure these two assumptions directly lead to the two dimensional shell equations, which provide the basis for the finite element discretizations.<sup>3</sup>

Commonly, a shell is regarded as a thin or moderately thin three dimensional body, whose reference configuration  $B$  can be described using curvilinear coordinates  $(\xi^i) \equiv (\xi^\beta, \xi)$  chosen in such a manner that the equation  $\xi = 0$  defines a shell reference surface  $M$ , and the position vector  $X$  of any point in the region  $B$  can be expressed in the form

$$X(\xi^\beta, \xi) = Y(\xi^\beta) + \xi D(\xi^\beta, \xi), \quad \xi \in [-h_0^-(\xi^\beta), +h_0^+(\xi^\beta)], \quad (2.2)$$

where  $Y(\xi^\beta) = X(\xi^\beta, 0)$  denotes the position vector of the reference surface  $M$ , the unit vector  $D$  defines through-the-thickness shell fibres, and the function  $h_0 = h_0^+ + h_0^- > 0$  determines the initial shell thickness. Typically, one takes  $D = A_N$  to be the unit normal vector to the surface  $M$ , which in turn is assumed to be the mid-surface so that  $h_0^+ = h_0^- = h_0 / 2$ .

Now, according to the first Mindlin-Reissner assumption the position vector in the deformed configuration of the shell can be expressed in the form (Fig. 5)

$$x(\xi^\beta, \xi) = y(\xi^\beta) + \xi d(\xi^\beta). \quad (2.3)$$

By virtue of (2.2) and (2.3) the three-dimensional displacement field is obtained in the form

---

<sup>3</sup> See, e.g., SIMO, FOX, AND RIFAI [1990].

$$\mathbf{u}(\xi^\beta, \xi) = \mathbf{u}(\xi^\beta) + \xi \boldsymbol{\beta}(\xi^\beta), \quad (2.4)$$

where

$$\mathbf{u}(\xi^\beta, \xi) = \mathbf{y}(\xi^\beta) - \mathbf{Y}(\xi^\beta), \quad \boldsymbol{\beta}(\xi^\beta) = \mathbf{d}(\xi^\beta) - \mathbf{D}(\xi^\beta), \quad (2.5)$$

are the displacements associated with the reference surface. This leads to the five parameter shell theory consisting, aside from the three components of the displacement field, of two rotational parameters, which may be defined in various manner.

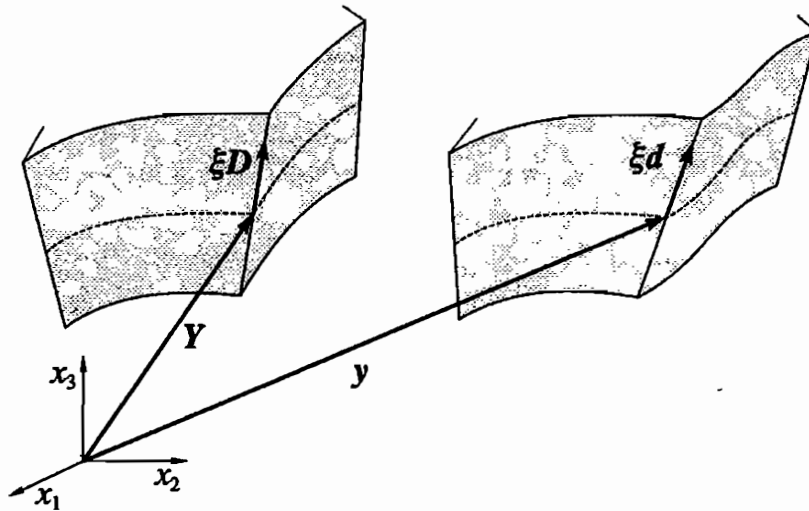


Fig. 5

**2.6 Finite element discretization.** The standard finite element discretization applied to the shell theory based on the Mindlin-Reissner assumptions leads to the finite elements having at each node five degrees of freedom: three displacements ( $u_a, v_a, w_a$ ) and two rotations ( $\theta_{1a}, \theta_{2a}$ ). These are the same degrees-of-freedom, which possess the degenerated shell elements (Fig. 6).

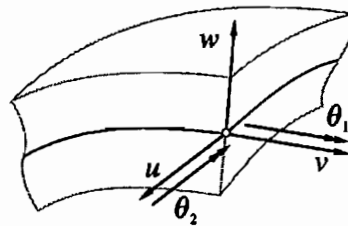


Fig. 6

### 3. Other types of shell finite elements

**3.1 Kirchhoff assumptions.** The earlier shell finite element formulations have been mainly based on the classical Kirchhoff-Love shell theory and the principle of stationary total potential energy.<sup>1</sup> In this theory the displacement field of the reference surface is the only independent kinematical variable. This theory has been widely used in the formulation of curved thin shell elements due to its well-established nature. However, such formulation entails some limitations and difficulties. The Kirchhoff-Love shell theory requires continuity of the normal slope across the inter-element boundaries. The convergence requirements, according to the classical finite element theory, are simple polynomial completeness through second-order and global  $C^1$  continuity. Considerable ingenuity is needed to devise element interpolatory schemes satisfying these conditions. The requirement to ensure the  $C^1$  inter-element continuity leads to a very large finite element basis (high order interpolation polynomials). The difficulties in developing such basis are severe and they become even more acute for non-smooth shells. The excessive continuity needed in these elements may also induce peculiar effects in the analysis of plastic shells. Moreover, the range of applicability is delimited by underlying kinematic assumptions, which in the classical form ignore both the transverse shear and the through-the-thickness deformation.

**3.2 Discrete Kirchhoff assumptions.** The aforementioned limitations and difficulties led to the development of the discrete Kirchhoff theory (DKT) elements, for which the requirement of  $C^1$  continuity is relaxed, but additional techniques are used to incorporate the Kirchhoff hypothesis at a discrete number of points. The discrete Kirchhoff element was originally developed by Wempner et al. in 1968 but the concept has only more recently become popular.<sup>2</sup> Within this approach the formulation starts with the Mindlin-Reissner plate or shell theory and the standard finite element approximations. Subsequently, Kirchhoff hypothesis are enforced at a finite number of discrete points. However, some doubts arise related to the discrete nature of the constraints.

**3.3 Shallow shell elements.** The problems connected with geometric representation are reduced somehow by formulating curved elements in terms of

---

<sup>1</sup> See WEMPNER [1989]. Recent works in this field can be found in VAN KEULEN, BOUT, AND ERNST [1993], VAN KEULEN [1993].

<sup>2</sup> See, e.g., DHATT, MARCOTTE AND MATTE [1986], TALBOT AND DHATT [1987].



the shallow shell theory. This theory allows all the necessary mathematical manipulations to be performed in a base reference plane. In addition, it is sufficient to assume constant geometric curvature over the element. However, this introduces geometric discontinuities in the shell reference surface at adjacent elements, which are part of different parabolic surfaces, and they will not match properly together.

Regardless of whether the shallowness assumption is used or not, a proper description of the rigid body modes in elements based on curvilinear shell theory is only possible with the inclusion of transcendental functions into the displacement expressions. This will violate interelement compatibility and it is more convenient to approximate the rigid body motions with higher order polynomials describing the displacements. This higher order representation of the displacements leads to the introduction of additional degrees-of-freedom, namely the first- and second-order derivatives, which lead to difficulties at shell intersections.

**3.4 Idealization of shells with flat elements.** The simplest and earliest application of the finite element method to the analysis of shells involved the replacement of the curved shape by an assemblage of flat triangular or rectangular elements. By superposing the independent membrane and flexural behavior (plane stress elements and plate bending elements) together with the appropriate spatial transformation, the desired shell elements were developed. However, the success of such analysis was delayed until formulations of plate bending elements became mature. The research to represent the shell behavior by flat elements and to overcome the associated difficulties continues to attract interest.

Among the major attractive features of this modelling of shells are:

- a) It is easy to input data to describe the geometry.
- b) They are simple to formulate.
- c) It is easy to mix with other types of elements.
- d) They are capable of modelling rigid body motions without inducing strains.
- e) The requirement of using a relatively large number of elements provides the advantage of a convenient incorporation of complex loading and boundary conditions.

Their well-known shortcomings are:<sup>1</sup>

- a) They poorly represent the geometry of curved shells. This problem is particularly severe in the analysis of imperfection-sensitive problems.
- b) They exclude at the element level the coupling of stretching and bending behavior so typical for curved shells.
- c) They give rise to the presence of "discontinuous" bending moments, which do not appear in continuously-curved actual shells,
- d) They lead to ill-conditioned or even singular stiffness matrices, whenever elements are coplanar or nearly so.

These deficiencies, which can be surmounted to some extent through various artifices, are particularly severe in the nonlinear and buckling analysis. Nevertheless, due to their simplicity in use, flat and facet shell elements still attract much attention in the literature.

## 4. Folds, junctions and shell intersections

**4.1 Non-smooth and multi shells.** In the engineering analysis it is often necessary to model shell structures composed of various structural elements, containing shell branches, junctions and intersections or the possibility of connecting rod and shell structural elements. When discussing different ways to describe non-smooth shells, intersections and branches of shells, one remark has to be made. In the literature it is occasionally pointed out that the formulation of shell intersections falls out of the realm of shell theory, and one needs a truly three-dimensional description of the problem. Thus suggesting that any attempt in this direction is superfluous. While this observation is true, one must realize that this is equally valid for smooth shells at the boundary layer.

The finite element approximations of irregular shell structures (structures of any kind noted above) requires reliable description of each structural element as well as an appropriate representation of their junctions. The main difficulties that arise in the analysis of these problems are due to the lack of the sixth degree-of-freedom in the standard formulations of shell elements. In effect, this leads to problems in computation and modelling. The difficulties turn out to be even more severe for K-L type and higher order shell theory based elements, which typically lead to nodal

---

<sup>1</sup> Recent works by ALLMAN [1994], CHEN [1992], ORAL AND BARUT [1991] provide a detailed account of the problem.

degrees of freedom with higher order derivatives of the displacements. This fact was recognized since long and various concepts have been considered in order to overcome this restriction.

**4.2 Continuous field of local triads.** Within a direct and simple approach one tries to apply standard shell finite elements with 5 DOF per node to kinked and branching shell structures in either of two ways:<sup>2</sup>

- a) Through the transformation of two local rotations, described in a local coordinate basis associated with the element, into a global coordinate basis, which serves to assemble the elements into the global structure. In this way the number of nodal unknowns increases from five to six due to the appearance of an extra rotation due to the transformation.
- b) Through defining the director field in a continuous manner through non-smooth intersections of different parts of the shell structure. Such triads then serve to assemble the element matrices into the global one.

While both possibilities are often pointed out or even worked out at length in the literature, there is an apparent lack of representative test examples to validate the applicability of these concepts. In fact, most of the works do not present any numerical example at all. In some others they are illustrated by smooth shell problems, in which case neither of the techniques is really needed. It seems that both techniques can be applied with minor reliability of the solutions and only for a limited class of problems. Moreover, it should be noted also that none of such techniques will make it possible to connect rod and shell elements.

**4.3 Transient elements.** Shell intersections and shell-to-solid transitions can be modelled effectively using the so-called transition elements.<sup>3</sup> Such elements have mid-surface nodes to couple with other shell elements and top and bottom nodes to connect with other elements or with the usual three-dimensional isoparametric elements.

**4.4 The sixth degree-of-freedom.** An alternative method of the analysis of irregular shells requires to extend the number of rotational nodal parameters from two to three. Earlier efforts were based on various artificial means such as a fictitious beam along the edges of an element or a fictitious spring (rotational

---

<sup>2</sup> See HUGHES AND LIU [1981], HUANG AND HINTON [1986] and VU-QUOC AND MORA [1989].

<sup>3</sup> See, e.g., BATHE [1982].

stiffness) added to an element stiffness matrix. This was recognized to be of very limited use. The in-plane rotational degree of freedom associated with the shell normal rotation is commonly referred to as drilling degree-of-freedom. This DOF is particularly advantageous in the analysis of shells with the aim of extending the range of applicability of standard shell elements to non-smooth problems. Moreover, in many finite element formulations the absence of the rotation about the shell normal as a degree of freedom can also lead to serious errors and spurious buckling modes for structures having shell segments joined with a discontinuous tangent. In general, the main motivations behind the idea of including the sixth degree-of-freedom into the shell/plate elements are:

- To improve the element performance;
- To provide reliable modelling of connections between plates, shells and beams, as well as the treatment of folds and junctions in shell structures.

Classical attempts to develop plate/shell as well as membrane elements with sixth degree-of-freedom can be viewed as unsuccessful and some authors had dismissed the task as hopeless.<sup>4</sup> A significant progress in this direction began with the independent works by Allman and Bergan and Felippa in the context of plane problems.<sup>5</sup> Along the lines of the "non-conventional interpolation" of Allman and the "free formulation" of Bergan and Felippa and extensive current attempts followed to develop shell finite elements with the drilling rotation. This more recent efforts have shown that the sixth degree-of-freedom, absent in the classical shell elements, can be formulated and built into the element in a widely varying, not equivalent manner. Basically, the two cases can be distinguished:<sup>6</sup>

- the drilling rotation,
- the vertex rotation.

**4.5 The drilling rotation.** Within the two-dimensional linear elasticity the drilling rotation is interpreted as the in-plane rotation  $\Omega_{xy}$  defined by

$$\Omega = \frac{1}{2}(v_{,x} - u_{,y}), \quad (6.1)$$

where  $u, v$  are the in-plane components of the displacement and  $x, y$  are the in-plane coordinates. The possibility to include  $\Omega_{xy}$  as a nodal parameter in the

<sup>4</sup> A compilation of these early efforts is presented in MACNEAL AND HARDER [1976].

<sup>5</sup> See ALLMAN [1994], FELIPPA AND MILITELLO [1992] and references cited therein.

<sup>6</sup> FREY [1989].

formulation of finite elements was suggested already in 1965. At that time, the advantage in using  $\Omega_{xy}$  for shell analysis was understood. However, no application was made.<sup>7</sup> The present trend is to relating the in-plane rotational degrees of freedom to the average in-plane rotation of the shell reference surface as a constraint by the penalty function method could lead to an exact definition of drilling rotation in continuum mechanics.<sup>8</sup> However, strong enforcement of such a constraint can lead to strong locking. This is particularly severe when curved shells are idealized.

**4.6 Vertex rotational DOF.** In 1984 Allman have included three vertex rotations into CST (Constant Strain Triangular) element remarkably improving its performance. In this approach the tangential displacement is taken to be linear, whereas, due to the vertex rotations (additional nodal unknowns) the normal displacement is quadratic:

$$\begin{aligned} u_s &= (1 - s/l_{12})u_{s1} + (s/l_{12})u_{s2}, \\ u_n &= (1 - s/l_{12})u_{n1} + (s/l_{12})u_{n2} + (s/2)(1 - s/l_{12})(\omega_2 - \omega_1). \end{aligned} \quad (6.2)$$

The vertex rotations are then defined by

$$\omega_2 - \omega_1 = u_{n,s}(s=l_{12}) - u_{n,s}(s=0), \quad (6.3)$$

where a comma denotes derivative with respect to  $s$ . Thus, the vertex rotations are related to the derivatives of the displacements computed at the nodes of the element.

This approach has been extended to facet shell element based on DKT (Discrete Kirchhoff Triangular) bending element and to a curved element based on the Marguerre shallow shell theory. While these concepts still lack firm theoretical foundations, they have attracted much attention in the literature with varying degrees of success. The common experience shows that special care must be taken to avoid unexpected solutions by using elements based on this concept. Also it became clear that some ad-hoc devices will be needed to attain satisfactory performance of such elements.

It should be noted that some techniques of including sixth DOF into the standard shell elements make use of a special geometry, and they are not applicable to higher order shell elements. For example, neither Allman's approach nor the free

<sup>7</sup> Details of this preliminary work may be found in IRONS AND AHMAD [1975].

<sup>8</sup> See HUGHES AND BREZZI [1989], FOX AND SIMO [1992].

formulation has ever been applied within nine and sixteen nodes elements, which can represent a complex shell geometry not possible within triangular and quadrilateral elements (they do not accommodate accurately the curvature of the shell geometry).

## Chapter II

# Boundary value problems of irregular shells

### 1. Shell structures and shell theory

**1.1 Preliminary remarks.** A short overview presented in the previous chapter tried to make clear that in the finite element analysis of shells there are primarily three sources of approximations:

1. Shell theory approximation – approximations due to the two-dimensional formulation of an otherwise three-dimensional problem.
2. Structural approximation – approximations due to the impossibility of a two-dimensional description of irregularities of real shell structures.
3. Finite element approximation – approximations due to the discretization of an otherwise continuum problem.

Type as well as source of each approximation are entirely different. Therefore, it seems to be desirable that the formulation of shell finite elements should make a sharp distinction, as far as it is possible, between all three aspects. This is the point of view which we take in this work.

**1.2 Concepts in shell theory.** Generally, the aim of shell theory is to reduce for a shell-like body an otherwise three-dimensional problem of continuum mechanics to one having the coordinates of a certain surface as the only independent spatial variables. Within the shell theory the shell-like body is thus geometrically represented by a distinguished surface, called the shell reference surface, endowed with certain kinematic and dynamic properties, which reflect the dominant features of the body it represents.

In the formulation of shell governing equations special care is needed for a proper modeling of structural irregularities such as folds (non-smoothness of the shell

faces), multiple shell intersections (three or more shell segments intersecting at a common juncture), stiffeners, etc. Structures, which are composed of rod-like and shell-like elements interconnected pointwise at joints and along junctions, are typical examples. In general, the possibilities are so numerous that it is impossible to lay down any general rule for their rigorous characterization.

The shell-like body and the shell reference surface are the basic underlying concept of the shell theory. Intuitively, the concept of a shell-like body might seem to be obvious. However, a rigorous description of its geometry is a quite subtle analytical problem.<sup>1</sup> This is particularly so in the analysis of shell structures, which are characterized by discontinuities in geometry, stiffness and loading.

From the point of view of a general theory of such structures, a few cases need to be considered in detail. Most of them can be grouped into five categories for which we shall use the following names:

- I) Smooth shells,
- II) Folded shells,
- III) Multiple-shell intersections,
- IV) Multi-shell structures,
- V) Rod-shell structures.

We have shown in Part I that the first two categories can be treated at one time. They are based on the concept of a regular shell-like body. The remaining three categories require separate considerations.

**1.3 Regular shell-like body.** Generally, a shell has three basic identifying features: its reference surface, its thickness, and its edges. These features follow from the specific geometry of the shell-like body<sup>2</sup>, whose boundary  $\partial B$  consists of three parts: an upper shell face  $M^+$ , a lower shell face  $M^-$  and a lateral surface (edge)  $\partial B^*$ . We shall assume that the shell faces  $M^\pm$  are piecewise smooth, connected, but not necessarily simply connected, that the lateral surface  $\partial B^*$  is a piecewise smooth surface, not necessarily connected, i.e.  $\partial B^*$  can be a union of some number of piecewise smooth surfaces (Fig. 1).

---

<sup>1</sup> See MAKOWSKI AND STUMPF [1994], hereafter referred to as Part I.

<sup>2</sup> For the purpose of this work there is no loss in generality in identifying a body with a region it occupies in the undeformed configuration.



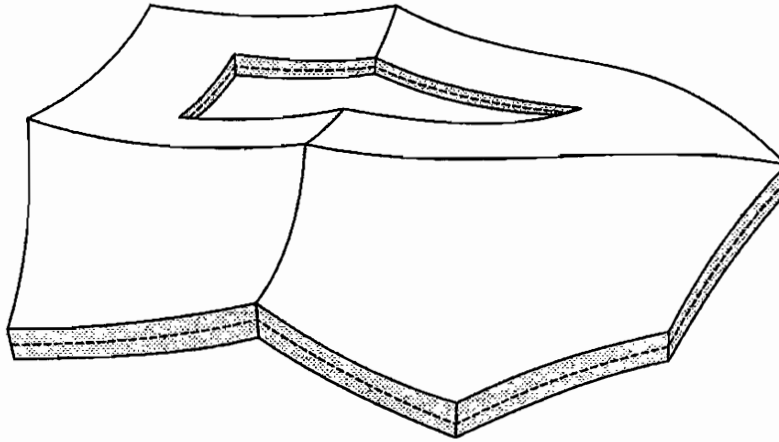


Fig. 1

We shall further assume that the shell reference surface  $M \subset B$  is arbitrarily located within the region  $B$ . Relative to the fixed Cartesian coordinates in space the position vector of a typical point of  $M$  be denoted by  $Y$ . For simplicity, the points of  $M$  and also their position vectors will be denoted by  $Y$  leaving the context to make clear which one is meant. Let us note that even in the case of non-smooth shell faces, the shell reference surface  $M$  can still be defined to be smooth, but such choice of the reference surface need not be the most appropriate one. Therefore, we shall take  $M$  to be an oriental piecewise smooth surface (Fig. 2).

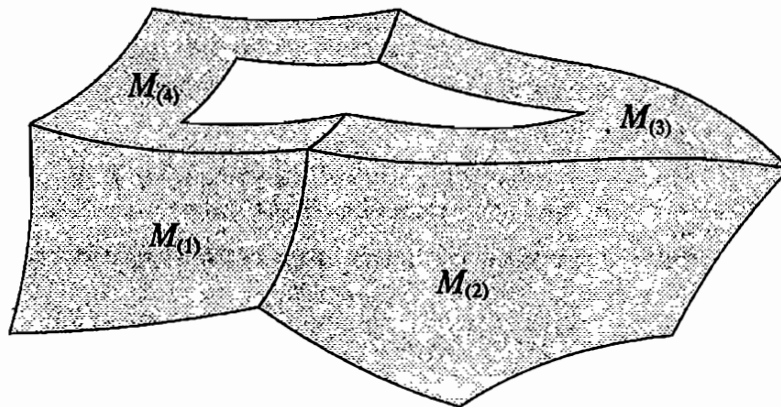


Fig. 2

Let us further assume that at each point of the shell reference surface  $M$  a unit vector  $D$  is defined such that every point in the region  $B$  is uniquely determined by the position vector given in the form

$$X(Y, \xi) = Y + \xi D(Y), \quad \xi \in [-h_0^-(Y), +h_0^+(Y)], \quad (1.1)$$

where  $h_0^\pm$  are given non-negative piecewise smooth functions on  $M$  such that

$$h_0(Y) = h_0^-(Y) + h_0^+(Y) > 0. \quad (1.2)$$

The vector  $D$  is required to be not tangent to  $M$  and it serves to define through-the-thickness fibres. Note that the functions  $h_0^\pm$  define the location of the reference surface relative to the shell faces whose position vectors are given by

$$X^\pm(Y) = Y \pm h_0^\pm(Y) D(Y). \quad (1.3)$$

We shall refer to  $\xi$  as through-the-thickness or "normal" coordinate and we call  $h_0$  the initial shell thickness. It is clear that the thickness of the shell defined in this way depends on the choice of the vector  $D$ . We also note that the field  $D$  on  $M$  can be defined in a continuous manner even if  $M$  is not smooth. Moreover, without loss of generality we can assume that the lateral surface  $\partial B^*$  is a ruled surface, whose generators at each point  $Y \in \partial M$  are defined by (1.1). When these assumptions are satisfied we shall call  $B$  a regular shell-like body.

**1.4 Irregular shells and multi-structures.** The concept of the regular shell-like body applies to a wide class of shell geometries. Nevertheless, there are still many structures of engineering importance which are excluded by this definition. The group III includes all structures, which resemble shells understood in a broader sense, but which are not regular in the sense of the above definition. Generally, structures of this group contain shell branching, i.e. three or more shell segments intersect at a common juncture (Fig. 3). In such cases, the difficulties in a rigorous derivation of the shell governing equations lie in the fact that at the intersection it is not possible to define in a unique way the shell reference surface and the shell thickness. In this sense they are not a regular shell-like body, but rather a union of two or more regular shell-like bodies. Of course, we can simplify the problem ignoring the transition zone, what is the common practice in the engineering approach to the problem.

An example shown in Fig. 4, while similar to the previous one, in essence is quite different. It shows not a single shell-like body but rather two shell-like bodies, which are interconnected along the common boundaries in some technological manner. The kinematical and mechanical properties of the interconnection cannot be derived from the laws of continuum mechanics alone, but they must be

supplemented by some a priori given technological data. Structures of this kind belong to the group IV).

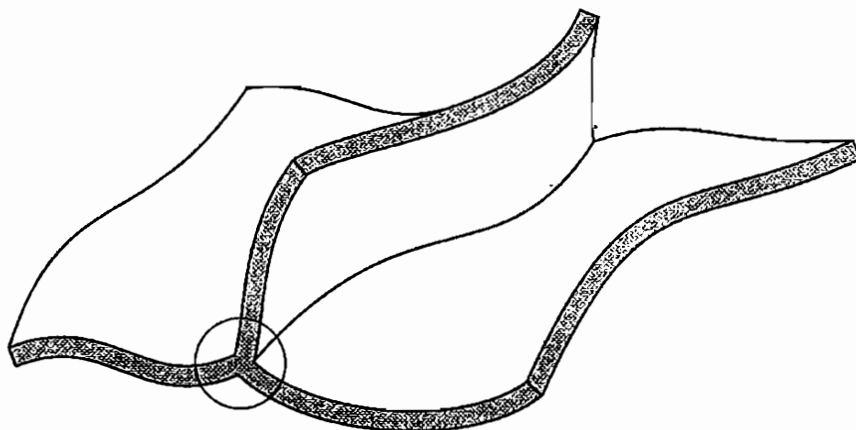


Fig. 3

Shell structures sustained by columns (Fig. 5) belong to the group V). They are easier to handle by theories of structures, except for a small region of the rod-to-shell transition.

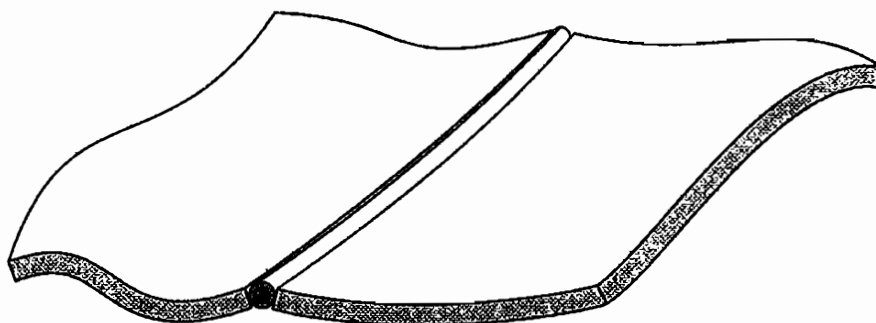


Fig. 4

The structures of all three groups III-V require a special treatment and this was the topic we have considered in Part I.

As we have pointed out, structures of all three groups are not regular shell-like bodies. However, their important feature is the fact that they are the union of such bodies. Therefore, multiple-shell intersections and technological interconnections of regular shell-like bodies can be modelled fairly correctly or even completely rigorously by a union of some number of shells, whose common boundaries are

spatial curves having their own mechanical properties. This approach to irregular shell structures was developed in Part I and it provides the basis for the finite element modelling presented in this paper. Without going into all details of this concept (see Part I) we only note that this implies that irregular shell structures can be viewed as a structured continuum, which is the superposition of two-dimensional continua  $M^{(A)}$  (shells in the conventional sense) and one-dimensional continua  $\Gamma^{(a)}$  being a common boundary for two or more surfaces  $M^{(A)}$  and having some of the properties of the conventional rods.

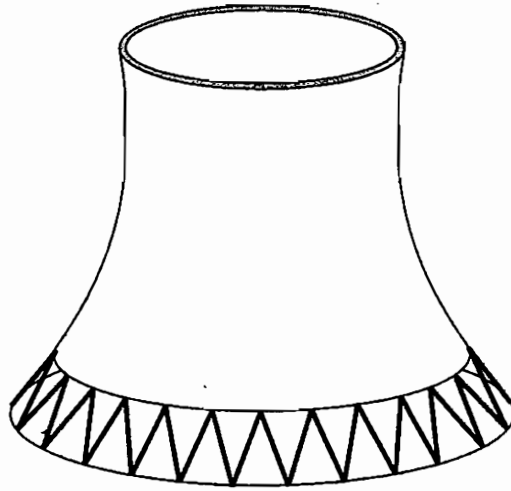


Fig. 5

**1.5 Surface coordinates.** We shall further assume that each smooth part of the reference surface  $M$  is given in parametric form so that the position vector can be expressed as  $Y(\xi^\beta) = Y_i(\xi^\beta)e_i$ , where  $(\xi^\beta)$ ,  $\beta = 1, 2$ , are surface coordinates chosen in any convenient way. Then the natural base vectors and the unit normal vector to  $M$  within the domain of the chosen coordinates, the components of the surface metric and curvature tensors can be expressed in the classical form (Fig. 6)

$$\begin{aligned}
 A_\beta &= Y_{,\beta}, & A^\alpha \cdot A_\beta &= \delta_\beta^\alpha, & A_N &= \frac{1}{2} \epsilon^{\alpha\beta} A_\alpha \times A_\beta, \\
 A_{\alpha\beta} &= A_\alpha \cdot A_\beta, & A^{\alpha\beta} &= A^\alpha \cdot A^\beta, & A &= \det A_{\alpha\beta} > 0, \\
 B_{\alpha\beta} &= A_N \cdot A_{\alpha,\beta} = A_N \cdot Y_{,\alpha\beta}, & B_\beta^\alpha &= A^{\alpha\lambda} B_{\lambda\beta}.
 \end{aligned} \tag{1.4}$$

Here and in the sequel a comma denotes the partial derivatives with respect to the surface coordinates and  $\epsilon^{\alpha\beta}$  denotes the usual surface permutation symbol. From

(1.4) other geometric quantities can be obtained in the usual way. The differential area element of  $M$  is given by

$$dA = \sqrt{A} d\xi^1 d\xi^2, \quad A = \det A_{\alpha\beta} > 0. \quad (1.5)$$

The operation of rising and lowering of the indices for the surface vector and tensor fields is carried out with the help of the metric tensor (1.4)<sub>2</sub>.

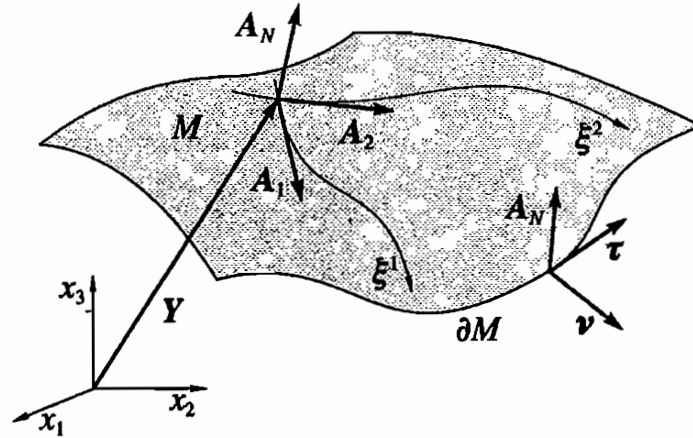


Fig. 6

However, it has to be noted here that for the curvature tensor  $B_{\alpha\beta}$  to exist we have to assume that  $M$  can be partitioned into smooth surface elements such that each  $M_{(k)}$  is of class  $C^2$  or higher. This is the minimal regularity assumption needed within the formulation of shell finite elements based on a Kirchhoff-Love type shell theory. However, it would preclude the possibility to formulate compatible  $C^0$  shell elements, which will be our concern in this work. It will become clear later on that such assumption is not needed and nowhere we shall use the curvature tensor (1.4)<sub>3</sub>. Thus we shall assume that each part  $M_{(k)}$  of  $M$  is only smooth, i.e. of class  $C^1$ .

The boundary of the undeformed shell reference surface  $M$  will be denoted by  $\partial M$ . Since  $M$  need not be simply connected,  $\partial M$  will be in general the union of some number of piecewise smooth curves, each of which can be given in the form  $Y(s) = Y(\xi^\beta(s))$ , where  $s$  denotes the arc length parameter along every smooth part of the boundary curve. Then at each regular point of  $\partial M$  we can define the orthonormal triad  $\{v, \tau, A_N\}$  in standard way

$$\tau = Y' = \tau^\beta A_\beta, \quad v = Y' \times A_N = v_\beta A^\beta, \quad (1.6)$$

where  $\nu$  and  $\tau$  are the tangent vector and the outward normal vector, both lying in the tangent plane to  $M$  at the underlying point. Here a prime denotes the derivative with respect to the arc length parameter.

**1.5 Shell coordinates.** Each regular part of the shell-like body can be described in terms of curvilinear coordinates  $(\xi^i) \equiv (\xi^\beta, \xi)$  chosen in such a way that the equation  $\xi = 0$  defines the reference surface, and any other point in the shell space is determined by the position vector given by

$$X(\xi^\beta, \xi) = Y(\xi^\beta) + \xi D(\xi^\beta), \quad \xi \in [-h_0^-(\xi^\beta), +h_0^+(\xi^\beta)]. \quad (1.7)$$

Then the natural base vectors and components of the metric tensor are defined in the usual way

$$\begin{aligned} G_i &= X_{,i}, & G^i \cdot G_j &= \delta_j^i, \\ G_{ij} &= G_i \cdot G_j, & G^{ij} &= G^i \cdot G^j, & G &= \det G_{ij} > 0. \end{aligned} \quad (1.8)$$

From (1.7) and (1.8) all other geometric relations can be derived in standard manner.

## 2. General theory of irregular shells

**2.1 Deformation of the shell-like body.** In order to reduce in an exact manner the three-dimensional balance laws of continuum mechanics to the two-dimensional form appropriate for the shell, we shall represent the three-dimensional deformation of the shell-like body in the form (Fig. 8)

$$\mathbf{x}(Y, \xi) = \chi(\mathbf{X}(Y, \xi)) = \chi(Y) + \zeta(Y, \xi). \quad (2.1)$$

Here  $\chi: M \rightarrow \mathcal{E}$  with  $\mathbf{y} = \chi(Y)$  is the deformation map of the shell reference surface and  $\zeta$  is an unknown vector-valued function, which defines the location of the particle, whose initial position is measured relative to the corresponding point on the deformed reference surface. It must be stressed that the representation (2.1) is purely formal and imposes no restrictions on the three-dimensional deformation of the shell-like body.

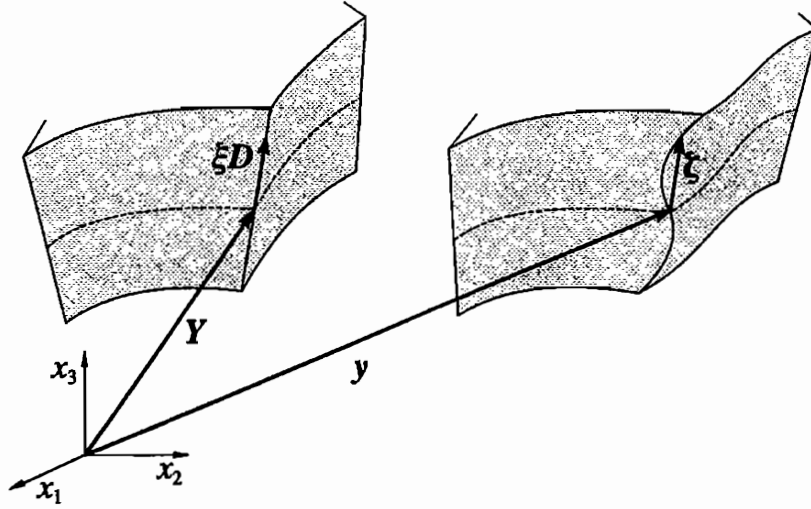


Fig. 8

**2.2 Resultant balance laws.** Within a purely mechanical theory the basic laws governing the deformation of the body are the balance laws of linear and angular momentum. In the quasi-static case they assert that the total force and the total torque acting on each subbody vanish in every equilibrium configuration. With the help of (2.1) the balance laws of continuum mechanics can be specified for any part  $P \subset B$  of the regular shell-like body to give the overall resultant balance laws expressed entirely in terms of through-the-thickness resultant quantities:

$$\begin{aligned} \iint_{\Pi} \mathbf{p} \, dA + \int_{\partial\Pi \cap \partial M_f} \mathbf{n}_\nu \, dL + \int_{\partial\Pi \cap \partial M_f} \mathbf{n}^* \, dL = \mathbf{0}, \\ \iint_{\Pi} (\mathbf{l} + \mathbf{y} \times \mathbf{p}) \, dA + \int_{\partial\Pi \cap \partial M_f} (\mathbf{m}_\nu + \mathbf{y} \times \mathbf{n}_\nu) \, dL + \int_{\partial\Pi \cap \partial M_f} (\mathbf{m}^* + \mathbf{y} \times \mathbf{n}^*) \, dL = \mathbf{0}. \end{aligned} \quad (2.2)$$

Here  $\Pi \subset M$  denotes a part of the shell reference surface which corresponds to the subbody  $P \subset B$ ,  $\mathbf{n}_\nu(\mathbf{Y}, \partial\Pi)$  and  $\mathbf{m}_\nu(\mathbf{Y}, \partial\Pi)$  are the resultant stress and couple vectors, and  $\mathbf{p}(\mathbf{Y})$  and  $\mathbf{l}(\mathbf{Y})$  are the resultant external surface loads and couples, which are statically equivalent to the external body force and surface forces acting on the shell faces (see Part I).

**2.3 Resultant stress and couple tensors.** By virtue of the Cauchy's theorem the stress resultant force vector and the resultant stress couple vector are given by the resultant stress tensor  $N$  and the resultant couple stress tensor  $M$  by

$$\mathbf{n}_\nu(\mathbf{Y}, \partial\Pi) = N(\mathbf{Y})\mathbf{v}(\mathbf{Y}), \quad \mathbf{m}_\nu(\mathbf{Y}, \partial\Pi) = M(\mathbf{Y})\mathbf{v}(\mathbf{Y}). \quad (2.3)$$

In the given parametrization of the reference surface the resultant stress tensor and the resultant couple stress tensor are given by (Fig. 9)

$$N = n^\beta \otimes A_\beta, \quad M = m^\beta \otimes A_\beta, \quad (2.4)$$

where the resultant forces and couples along the coordinate curves on the shell reference surface are defined by

$$n^\beta = \int_-^+ t^\beta \mu d\xi, \quad m^\beta = \int_-^+ \xi \times t^\beta \mu d\xi. \quad (2.5)$$

Here  $t^\beta$  are the nominal stress vectors so that the first Piola-Kirchhoff stress tensor is given in the form  $\mathbf{T} = t^\beta \otimes G_\beta + t^3 \otimes G_3$ .

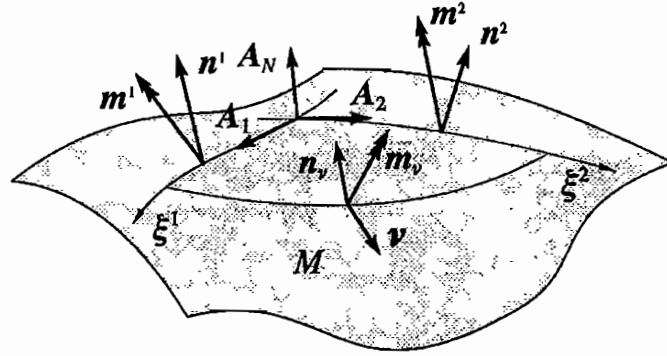


Fig. 9

**2.4 Irregular shells.** In the most general case which we shall consider here, the shell reference surface  $M$  is defined as union  $M = \bigcup_{A=1}^K M^{(A)}$  of some number of smooth or piecewise smooth surfaces  $M^{(A)}$ . Two or more surfaces  $M^{(A)}$  may have in common a piecewise smooth curve and we shall denote by  $\Gamma$  the union of all such curves. In general,  $\Gamma$  will represent kinks of the shell (non-smoothness of the shell faces), multiple shell intersections or curves on  $M$  along which external line forces and couples can be applied. In our subsequent considerations we shall refer to  $M$  and  $\Gamma$  as surface and curve, respectively. Let us note, however, that neither  $M$  is a surface nor  $\Gamma$  is a curve in a strict mathematical sense, but they are the union of surfaces and curves, respectively (see Part I for all details). We shall assume that  $M$  can be partitioned into smooth surface elements  $M = \bigcup_{k=1}^N M_{(k)}$ . In order to account for possible rod-to-shell interactions we can still enrich our model by admitting concentrated forces and couples acting at distinct points of the shell reference surface including the curves of intersection. Then the resultant mechanical laws take the form (Fig. 10)



$$\begin{aligned}
& \iint_{\Pi \cap \Gamma} \mathbf{p} \, dA + \int_{\partial \Pi \cap \partial M_f} \mathbf{n}_v \, dL + \int_{\partial \Pi \cap \partial M_f} \mathbf{n}^* \, dL \\
& \qquad \qquad \qquad + \int_{\Gamma} \mathbf{p}_r \, dL + \sum_{\alpha=1}^n \mathbf{f}_\alpha = \mathbf{0}, \\
& \iint_{\Pi \cap \Gamma} (\mathbf{l} + \mathbf{y} \times \mathbf{p}) \, dA + \int_{\partial \Pi \cap \partial M_f} (\mathbf{m}_v + \mathbf{y} \times \mathbf{n}_v) \, dL + \int_{\partial \Pi \cap \partial M_f} (\mathbf{m}^* + \mathbf{y} \times \mathbf{n}^*) \, dL \\
& \qquad \qquad \qquad + \int_{\Gamma} (\mathbf{l}_r + \mathbf{y}_r \times \mathbf{p}_r) \, dL + \sum_{\alpha=1}^n (\mathbf{c}_\alpha + \mathbf{y}_\alpha \times \mathbf{f}_\alpha) = \mathbf{0}.
\end{aligned} \tag{2.6}$$

Here  $\mathbf{n}_v$  and  $\mathbf{m}_v$  as well as  $\mathbf{p}$  and  $\mathbf{l}$  are defined exactly in the same way as for regular shell-like bodies. The physical meaning of the line force  $\mathbf{p}_r$  and couple  $\mathbf{l}_r$  and of the concentrated forces and couples  $\mathbf{f}_\alpha$  and  $\mathbf{c}_\alpha$  acting at distinct points  $Y_\alpha \in M$  may vary substantially depending on the intended application of the theory. They need to be specified for each problem separately.

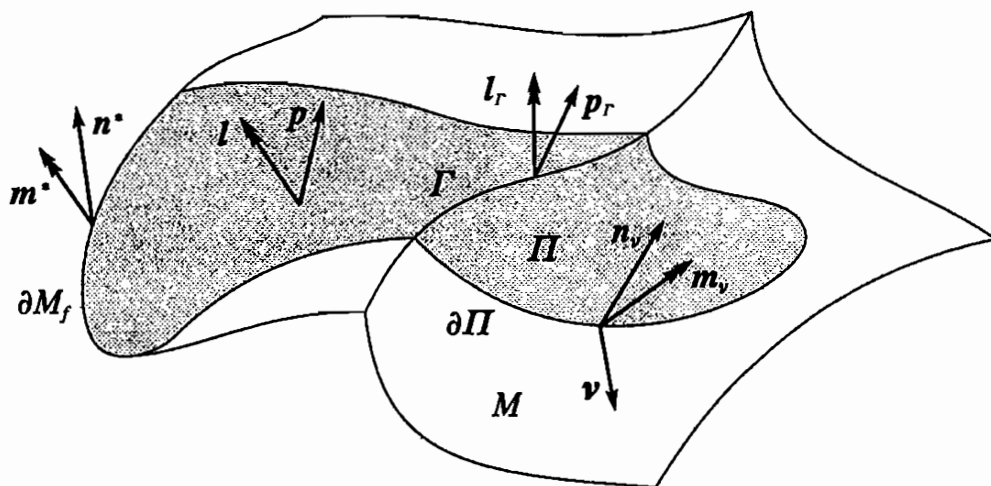


Fig. 10

**2.5 Virtual work identity.** The next step towards the formulation of a complete shell theory requires the introduction of suitable kinematic variables. Within the approach developed in Part I the kinematics of the shell, like the static equations and side conditions, are the outcome of the analysis and not the basic postulate of the theory. The basic idea is quite simple. Let  $\mathbf{v}(Y)$  and  $\mathbf{w}(Y)$  be any two vector fields, which are defined over the shell reference surface except possibly at the curve  $\Gamma$ , and let  $\mathbf{v}_r(Y)$  and  $\mathbf{w}_r(Y)$  be any two vector fields defined along  $\Gamma$ . In the special case, we may regard  $(\mathbf{v}_r, \mathbf{w}_r)$  as the restriction of  $(\mathbf{v}, \mathbf{w})$  to  $\Gamma$ . We shall also assume that the fields  $\mathbf{v}$  and  $\mathbf{w}$  are of class  $C^n$ ,  $n \geq 1$ , within the interior of each

smooth part  $M_{(k)}$  of the reference surface and that they have finite limits  $\mathbf{v}^{(k)}(Y)$  and  $\mathbf{w}^{(k)}(Y)$  at every point  $Y \in \Gamma$  taken along paths in  $M_{(k)}$ :

$$\mathbf{v}^{(k)}(Y) = \lim_{Z \rightarrow Y} \mathbf{v}(Z), \quad \mathbf{w}^{(k)}(Y) = \lim_{Z \rightarrow Y} \mathbf{w}(Z), \quad Z \in M_{(k)}. \quad (2.7)$$

Under these assumptions we have the following integral identity

$$\begin{aligned} \iint_{M \setminus \Gamma} \mathbf{w} dA + \int_{\Gamma} \mathbf{w}_r dL = \iint_{M \setminus \Gamma} (\mathbf{f} \cdot \mathbf{v} + \mathbf{c} \cdot \mathbf{w}) dA \\ + \int_{\partial M_f} (\mathbf{n}^* \cdot \mathbf{v} + \mathbf{m}^* \cdot \mathbf{w}) dL + \int_{\partial M_d} (N\mathbf{v} \cdot \mathbf{v} + M\mathbf{v} \cdot \mathbf{w}) dL, \end{aligned} \quad (2.8)$$

where

$$\mathbf{w} = \mathbf{n}^\beta \cdot (\mathbf{v}_{,\beta} + \mathbf{y}_{,\beta} \times \mathbf{w}) + \mathbf{m}^\beta \cdot \mathbf{w}_{,\beta}, \quad (2.9)$$

and

$$\mathbf{w}_r = \llbracket \mathbf{n}_\nu \cdot (\mathbf{v}_r - \mathbf{v} + (\mathbf{y}_r - \mathbf{y}) \times \mathbf{w}_r) \rrbracket + \llbracket \mathbf{m}_\nu \cdot (\mathbf{w}_r - \mathbf{w}) \rrbracket - \mathbf{p}_r \cdot \mathbf{v}_r + \mathbf{l}_r \cdot \mathbf{w}_r. \quad (2.10)$$

In effect, the integral identity (2.8) expresses the principle of virtual work with (2.9) and (2.10) being the internal virtual work density and the virtual work density of all forces and couples acting at the curve  $\Gamma$ . In this sense the vector fields  $\mathbf{v}(Y)$ ,  $\mathbf{w}(Y)$ ,  $\mathbf{v}_r(Y)$  and  $\mathbf{w}_r(Y)$  can be called the generalized virtual displacements or test functions.

### 3. Field equations and side conditions

**3.1 Deformation of the shell.** Referring to Part I for all details, we summarize in this chapter the complete set of shell governing equations and we shall point out those concepts, which play an essential role in the subsequent development of shell finite elements.

The undeformed configuration of the shell is represented by the shell reference surface  $M$  and the triad of linearly independent vectors  $\{\mathbf{D}_i(Y)\}$  assigned to each point  $Y \in M$ . We then define the reciprocal triad  $\{\mathbf{D}^i(Y)\}$  in the usual way, i.e.  $\mathbf{D}^i \cdot \mathbf{D}_j = \delta^i_j$ . The deformation of the shell is completely described by the (weighted or real) deformation  $\chi: M \rightarrow \mathcal{E}$  of the reference surface and the field of rotation tensors  $\mathbf{Q}: M \rightarrow SO(3)$ , which specifies an independent mean deformation of the shell cross sections. Here  $SO(3)$  denotes the rotation group. The map

$\chi: M \rightarrow \mathcal{E}$  assigns to every surface particle  $Y$  its spatial place  $y$  it occupies in the current configuration,

$$y = \chi(Y) = Y + u(Y), \quad (3.1)$$

where  $u$  denotes the associated displacement field of the reference surface. The independent mean deformation of the shell cross sections specified by the rotation of the triad  $\{D_i(Y)\}$  into its spatial counterpart  $\{d_i(y)\}$  is given by

$$d_i(Y) = Q(Y)D_i(Y), \quad d^i(Y) = Q(Y)D^i(Y), \quad (3.2)$$

where  $\{d_i(y)\}$  is the reciprocal triad in the deformed configuration, and we write  $d_i(Y) = d_i(\chi(Y))$ .

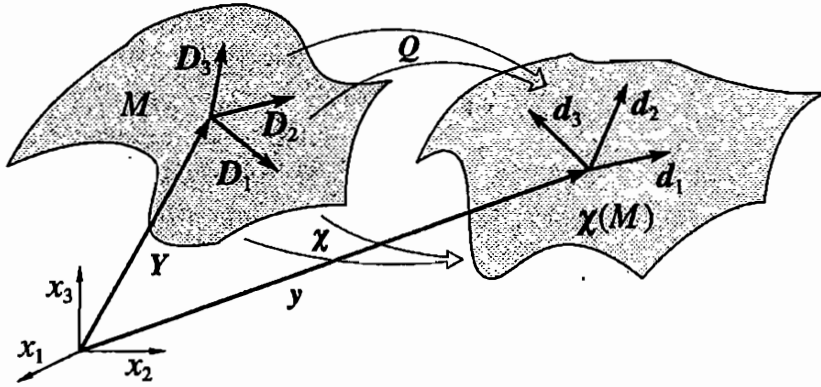


Fig. 12

Generally, we shall assume that (3.1) is a continuous function over each regular surface element  $M_{(k)}$  and differentiable of class  $C^n$ ,  $n \geq 1$ , in the interior  $\text{int } M_{(k)}$  of each smooth surface element. Under this assumption the deformation gradient  $F(Y) = \nabla_Y \chi(Y)$  exists at every point  $Y \in \text{int } M_{(k)}$  and it can be expressed in the form

$$F(\xi^\alpha) = y_{,\beta} \otimes A^\beta, \quad (3.3)$$

for any choice of the local surface coordinates. We shall not assume a priori that the deformation  $\chi: M \rightarrow \mathcal{E}$  is continuous across the singular curve  $\Gamma$  or some parts thereof. Accordingly, we regard (3.1) as being defined for all  $Y \in M \setminus \Gamma$ , i.e.  $\chi: M \setminus \Gamma \rightarrow \mathcal{E}$ , and it has a finite limit at every point  $Y \in \Gamma$ ,

$$\chi^{(k)}(Y) = \lim_{Z \rightarrow Y} \chi(Z) = Y + \lim_{Z \rightarrow Y} u(Z), \quad Z \in \Pi_{(k)}, \quad (3.4)$$

whenever  $\Gamma$  is a part of the boundary  $\partial M_{(k)}$ .

Thus in the most general case the complete description of the deformation of the shell requires to introduce two sets of kinematical variables. The first set consists of the deformation function  $\chi$  of the shell reference surface and the rotation tensor  $Q$  representing the mean rotation of the shell cross sections. Both being defined at all points of the undeformed reference surface  $M$  except possibly at a singular curve  $\Gamma$ . The deformation of the curve  $\Gamma$  itself is specified by the second set consisting of the deformation function  $\chi_r$  and the rotation tensor  $Q_r$ . Thus we can admit that the singular curve may follow its own deformation

$$y_r = \chi_r(Y) = Y + u_r(Y), \quad Q_r = Q_r(Y), \quad (3.5)$$

where  $\chi_r: \Gamma \rightarrow \mathcal{E}$  and  $Q_r: \Gamma \rightarrow SO(3)$  are continuous maps defined only along the singular curve. In the special case, when the deformation of the shell is assumed to be smooth,  $\chi_r$  and  $Q_r$  will denote the restrictions of  $\chi$  and  $Q$  to the curve  $\Gamma$ .

In this work we shall assume that both fields  $u(Y)$  and  $Q(Y)$  are continuous over the whole surface  $M$ , they are smoothly differentiable (i.e. of class  $C^1$ ) in the interior of each smooth part  $M_{(k)}$  of  $M$ , and their first surface gradients have continuous and bounded extensions to the boundary of  $M_{(k)}$ . Then we shall denote by  $u_r(Y)$  and  $Q_r(Y)$  the restrictions of these fields to the curve  $\Gamma$ . Let us note that we do not assume that the first surface gradients of the fields  $u(Y)$  and  $Q(Y)$  are continuous over the whole surface  $M$  but solely bounded. The important implication of these assumptions is the fact that multiple-shell intersections are rigid and the jump conditions are satisfied identically in the weak form. Let us also note that the regularity assumptions, adopted here while fairly weak, are much stronger than those considered in Part I.

**3.5 Strain measures.** Similar arguments, which led us from the generalized virtual displacements to their real counterparts (see Part I), can also be used in order to show that the work-conjugate strain measures consist of the stretching and bending tensors, which in the given parametrization of the reference surface can be expressed in the form

$$E(Y) = \varepsilon_\beta(Y) \otimes A^\beta(Y), \quad K(Y) = \kappa_\beta(Y) \otimes A^\beta(Y), \quad (3.6)$$

where the stretching vectors and the bending vectors are defined by

$$\boldsymbol{\varepsilon}_\beta = \mathbf{u}_{,\beta} - (\mathbf{Q} - \mathbf{1})\mathbf{Y}_{,\beta}, \quad \boldsymbol{\kappa}_\beta = a d^{-1} \mathbf{K}_\beta, \quad \mathbf{K}_\beta = \mathbf{Q}_{,\beta} \mathbf{Q}^T. \quad (3.7)$$

The equivalent strain measures referred to the undeformed configuration are obtained as:

$$\mathbf{E}(\mathbf{Y}) = \boldsymbol{\varepsilon}_\beta(\mathbf{Y}) \otimes A^\beta(\mathbf{Y}), \quad \mathbf{K}(\mathbf{Y}) = \boldsymbol{\kappa}_\beta(\mathbf{Y}) \otimes A^\beta(\mathbf{Y}), \quad (3.8)$$

where the stretching vectors and the bending vectors are defined by

$$\boldsymbol{\varepsilon}_\beta = \mathbf{Q}^T \mathbf{u}_{,\beta} - (\mathbf{1} - \mathbf{Q}^T)\mathbf{Y}_{,\beta}, \quad \boldsymbol{\kappa}_\beta = a d^{-1} \mathbf{K}_\beta, \quad \mathbf{K}_\beta = \mathbf{Q}^T \mathbf{Q}_{,\beta}. \quad (3.9)$$

The two sets of strains are related one to the other by the pull-back/push forward formulae

$$\begin{aligned} \mathbf{E} &= \mathbf{Q}\mathbf{E}, & \mathbf{K} &= \mathbf{Q}\mathbf{K}, \\ \boldsymbol{\varepsilon}_\beta &= \mathbf{Q}\boldsymbol{\varepsilon}_\beta, & \boldsymbol{\kappa}_\beta &= \mathbf{Q}\boldsymbol{\kappa}_\beta, & \mathbf{K}_\beta &= \mathbf{Q}\mathbf{K}_\beta\mathbf{Q}^T. \end{aligned} \quad (3.10)$$

**3.3 Equilibrium equations and static side conditions.** We shall also assume that the resultant stress tensor  $\mathbf{N}$  and the resultant couple stress tensor  $\mathbf{M}$  are of class  $C^n$ ,  $n \geq 1$ , in the interior  $\text{int } M_{(k)}$  of each smooth surface element and that they have finite limits

$$\mathbf{N}^{(k)}(\mathbf{Y}) = \lim_{\mathbf{Z} \rightarrow \mathbf{Y}} \mathbf{N}(\mathbf{Z}), \quad \mathbf{M}^{(k)}(\mathbf{Y}) = \lim_{\mathbf{Z} \rightarrow \mathbf{Y}} \mathbf{M}(\mathbf{Z}), \quad \mathbf{Z} \in \Pi_{(k)}, \quad (3.11)$$

at every point  $\mathbf{Y} \in \Gamma$  taken along any path in  $M_{(k)}$ . Under the assumptions stated above, the boundary integrals in the integral balance laws containing  $\mathbf{N}$  and  $\mathbf{M}$  can be transformed into surface integrals using the generalized surface divergence theorem considered in details in Part I. In this way we can obtain the local equilibrium equations at each regular point of  $M$ , which in a given (local) parametrization of the reference surface  $M$  take the form

$$\mathbf{n}^\beta|_\beta + \mathbf{p} = \mathbf{0}, \quad \mathbf{m}^\beta|_\beta + \mathbf{y}_{,\beta} \times \mathbf{n}^\beta + \mathbf{l} = \mathbf{0}. \quad (3.12)$$

Here the vertical stroke denotes the covariant derivative in the metric of the reference surface  $M$ .

The equivalent resultant stress and couple vectors referred to the undeformed configuration are defined by

$$\mathbf{N}(\mathbf{Y}) = \mathbf{n}^\beta(\mathbf{Y}) \otimes A_\beta(\mathbf{Y}), \quad \mathbf{M}(\mathbf{Y}) = \mathbf{m}^\beta(\mathbf{Y}) \otimes A_\beta(\mathbf{Y}), \quad (3.13)$$

and

$$\begin{aligned} N &= QE, & M &= QK, \\ \mathbf{n}^\beta &= Q\mathbf{n}^\beta, & \mathbf{m}^\beta &= Q\mathbf{m}^\beta. \end{aligned} \quad (3.14)$$

In the same way, the remaining static quantities are defined.

The equilibrium equations in terms of these variables take the form

$$\mathbf{n}^\beta|_\beta + \boldsymbol{\kappa}_\beta \times \mathbf{n}^\beta + \mathbf{p} = \mathbf{0}, \quad \mathbf{m}^\beta|_\beta + \boldsymbol{\kappa}_\beta \times \mathbf{m}^\beta + (\mathbf{A}_\beta + \boldsymbol{\varepsilon}_\beta) \times \mathbf{n}^\beta + \mathbf{l} = \mathbf{0}. \quad (3.15)$$

The formal similarity of the equilibrium equations (3.12) with those known in the literature should not conceal the richness of their content and the manner they have been obtained here. But we postpone the discussion of this point to the next chapter. This is evident in two ways, from the structure of the static equations and from the structure of the associated virtual work expressions. Recalling the definitions of the resultant stress vector and the resultant couple stress vector, it becomes obvious that both have all three components with respect to any basis (typically, two tangential components and one normal component). Thus in the scalar form the equilibrium equations (3.12) constitute a system of six independent equations involving six resultant forces and six resultant couples.

**3.4 Static boundary conditions.** We shall further assume that the boundary  $\partial M$  of the reference surface is the disjoint union of two parts  $\partial M_f$  and  $\partial M_d$ , along which the static boundary conditions and the kinematic boundary conditions, respectively, are prescribed:

$$N\mathbf{v} = \mathbf{n}^*, \quad M\mathbf{v} = \mathbf{m}^*, \quad \text{along } \partial M_f, \quad (3.16)$$

where an asterisk indicates prescribed quantities. Let us note that we do not exclude the dependency of the surface, line and boundary forces and couples on the deformation. In general, they need not be even conservative.

**3.5 Static jump conditions.** In general, along the singular curve  $\Gamma$  the following jump conditions hold

$$\begin{aligned} \mathbf{p}_r - \llbracket \mathbf{n}_v \rrbracket &= \mathbf{0}, \\ \mathbf{l}_r - \llbracket \mathbf{m}_v \rrbracket + \llbracket (\mathbf{u}_r - \mathbf{u}) \times \mathbf{n}_v \rrbracket &= \mathbf{0}. \end{aligned} \quad (3.17)$$

The static jump conditions (3.17) and the static boundary conditions (3.16), when expressed in component form, constitute a system of six scalar equations. For the

shell reference surface to support these static equations extra kinematical variables are needed besides the deformation of the reference surface.

**3.6 Elastic shells.** The field equations consisting of the equilibrium equations, the kinematic relations, boundary conditions and the jump conditions, when supplemented by suitable constitutive equations, provide the complete description of shell problems with any kind of irregularities. In overall, the shell theory formulated in this way is both geometrically and statically exact. There is no single assumption about the three-dimensional deformation of the shell-like body, there are no restrictions of the magnitude of displacements, rotations and strains, there is even no thickness assumption. Moreover, this approach clearly distinguishes the general equations valid for all shells and undergoing whatsoever deformation (possibly unelastic) from specific constitutive relations defining particular classes of materials the shell is made of.

The mechanical properties of the shell are specified by suitable constitutive equations. In the case of elastic shells their most general form is

$$\begin{aligned} N &= \tilde{N}(E, K; Y), & M &= \tilde{M}(E, K; Y), \\ \mathbf{N} &= \tilde{\mathbf{N}}(\mathbf{E}, \mathbf{K}; Y), & \mathbf{M} &= \tilde{\mathbf{M}}(\mathbf{E}, \mathbf{K}; Y), \end{aligned} \quad (3.18)$$

or, equivalently,

$$\begin{aligned} n^\beta &= \tilde{n}^\beta(\varepsilon_\alpha, \kappa_\alpha; Y), & m^\beta &= \tilde{m}^\beta(\varepsilon_\alpha, \kappa_\alpha; Y), \\ \mathbf{n}^\beta &= \tilde{\mathbf{n}}^\beta(\boldsymbol{\varepsilon}_\alpha, \boldsymbol{\kappa}_\alpha; Y), & \mathbf{m}^\beta &= \tilde{\mathbf{m}}^\beta(\boldsymbol{\varepsilon}_\alpha, \boldsymbol{\kappa}_\alpha; Y). \end{aligned} \quad (3.19)$$

The response functions specify particular elastic properties. Their explicit dependence on  $Y$  signifies that the mechanical response of the shell includes not only the material properties but also the local geometry of the reference state through the curvature tensor of  $M$  and other parameters like variable shell thickness.

The shell is defined to be hyperelastic, if there exists a strain energy function

$$\begin{aligned} \Phi &= \Phi(E, K; Y) = \Phi(\varepsilon_\beta, \kappa_\beta; Y) \\ &= \Phi(\mathbf{E}, \mathbf{K}; Y) = \Phi(\boldsymbol{\varepsilon}_\beta, \boldsymbol{\kappa}_\beta; Y), \end{aligned} \quad (3.20)$$

such that

$$\tilde{N}(E, K; Y) = \partial_E \Phi(E, K; Y), \quad \tilde{M}(E, K; Y) = \partial_K \Phi(E, K; Y), \quad (3.21)$$

or, equivalently,

$$\tilde{\mathbf{n}}^\beta(\boldsymbol{\varepsilon}_\alpha, \boldsymbol{\kappa}_\alpha; \mathbf{Y}) = \frac{\partial \Phi(\boldsymbol{\varepsilon}_\alpha, \boldsymbol{\kappa}_\alpha; \mathbf{Y})}{\partial \boldsymbol{\varepsilon}_\beta}, \quad \tilde{\mathbf{m}}^\beta(\boldsymbol{\varepsilon}_\alpha, \boldsymbol{\kappa}_\alpha; \mathbf{Y}) = \frac{\partial \Phi(\boldsymbol{\varepsilon}_\alpha, \boldsymbol{\kappa}_\alpha; \mathbf{Y})}{\partial \boldsymbol{\kappa}_\alpha}. \quad (3.22)$$

In general, the response functions as well as the strain energy must satisfy the principle of frame-indifference in a form carefully examined in Part I. Let us note only that this principle can be satisfied identically whenever the constitutive relations are written in component form. In general, the constitutive equations are also delimited by suitable constitutive restrictions and possible material symmetries, but for the time being this need not be our concern here.

## 4. Weak form of the momentum balance laws

**4.1 Configuration space.** Within the considered theory each configuration of the shell is determined by the displacement field  $\mathbf{u} : M \rightarrow E$  of the reference surface and the field of rotation tensors  $\mathbf{Q} : M \rightarrow SO(3)$ . Thus the ordered pair  $\mathbb{w} \equiv (\mathbf{u}, \mathbf{Q})$  of two fields determines completely any other configuration of the shell, whenever the undeformed configuration is fixed. Using the terminology of the theory of dynamical systems, the set of all configurations can be called the configuration space of the shell and it can be defined as the set

$$\mathcal{U} \equiv \mathcal{C}(M, E \times SO(3)) = \{ \mathbb{w} = (\mathbf{u}, \mathbf{Q}) \mid \mathbb{w} : M \rightarrow E \times SO(3) \}. \quad (4.1)$$

The basic fact to be noted here is that the configuration space (4.1) lacks any vector space structure, because it involves the rotation group  $SO(3)$ . This fact has many important implications for the solution of nonlinear shell problems.

Under some rather mild regularity assumptions, it can be shown that the configuration space carrying the topology of uniform convergence is an infinite dimensional manifold. Moreover, with the usual group operation defined pointwise by

$$(\mathbb{w}_1 + \mathbb{w}_2)(\mathbf{Y}) = (\mathbf{u}_1(\mathbf{Y}) + \mathbf{u}_2(\mathbf{Y}), \mathbf{Q}_2(\mathbf{Y})\mathbf{Q}_1(\mathbf{Y})), \quad \forall \mathbf{Y} \in M \quad (4.2)$$



for all  $\mathfrak{u}_1, \mathfrak{u}_2 \in \mathcal{U}$ , the configuration space (4.1) becomes an infinite dimensional (Banach) Lie group.<sup>1</sup> Using this fact the shell problem can be formulated within a differential-geometric setting.

**4.1 Virtual displacements and rotations.** The (global) virtual states of the shell are defined as elements of the tangent bundle  $T\mathcal{U}$ , which in turn is defined as the pairwise disjoint union  $T\mathcal{U} = \bigcup_{\mathfrak{u} \in \mathcal{U}} T_{\mathfrak{u}}\mathcal{U}$  of the tangent spaces  $T_{\mathfrak{u}}\mathcal{U}$  to the configuration space  $\mathcal{U}$  at all points  $\mathfrak{u} \in \mathcal{U}$ . Obviously, each tangent space  $T_{\mathfrak{u}}\mathcal{U}$  carries the linear space structure. Moreover, by the theorems on manifolds of maps  $TC(M, N)$  is isomorphic with  $C(M, TN)$  for two manifolds  $M$  and  $N$ . By this arguments we can identify the space of virtual displacements with the space

$$T_{\mathfrak{u}}\mathcal{U} = C(M, T(E \times SO(3))), \quad (4.3)$$

where  $T(E \times SO(3))$  denotes the tangent bundle of the six-dimensional Lie group (direct product group)  $E \times SO(3)$ . Here we are using the standard differential-geometric notion, but perhaps it needs to be explained that the tangent space  $T_{\mathfrak{u}}\mathcal{U}$  given by (4.3) is the vector space of maps defined as follows: for any configuration  $\mathfrak{u} \in \mathcal{U}$  of the shell the associated virtual displacement  $\mathfrak{v} \in T_{\mathfrak{u}}\mathcal{U}$  is defined as the map

$$\mathfrak{v}: M \rightarrow T_{\mathfrak{u}(\mathfrak{Y})}(E \times SO(3)), \quad \forall \mathfrak{Y} \in M. \quad (4.4)$$

In other words, the tangent bundle  $T\mathcal{U}$  is the vector space (obviously infinite dimensional) of maps of the shell reference surface  $M$  into tangent spaces to the group  $E \times SO(3)$ . Taking further into account that the tangent space to the rotation group at any point is isomorphic with the vector space  $E \wedge E$  of skew-symmetric tensors, which in turn is isomorphic with the Euclidean vector space  $E$ , we have the sequence of isomorphisms:  $E \rightarrow so(3) \rightarrow T_Q SO(3)$  by  $\mathfrak{w} \rightarrow W \rightarrow \delta Q$  for every rotation tensor  $Q$ , where  $W$  denotes the skew-symmetric tensor, whose axial vector is  $\mathfrak{w}$ ,  $W = ad\mathfrak{w}$ . By virtue of these facts the virtual displacement  $\mathfrak{v} \in T_{\mathfrak{u}}\mathcal{U}$  for every  $\mathfrak{u} \in \mathcal{U}$  can be identified with the ordered pair of fields:

$$\mathfrak{v} = (\mathfrak{v}, W): M \rightarrow E \times (E \wedge E) \quad \text{or} \quad \mathfrak{v} = (\mathfrak{v}, \mathfrak{w}): M \rightarrow E \times E. \quad (4.5)$$

Thus we can define the space of virtual displacements as

$$\mathcal{V} \equiv C(M, E \times E) = \{ \mathfrak{v} = (\mathfrak{u}, \mathfrak{w}) \mid \mathfrak{v}: M \rightarrow E \times E \}. \quad (4.6)$$

<sup>1</sup>This follows from the general theorems on manifolds of maps, see Part I and the references cited therein.

We can arrive at this result quite formally (see Part I).

**4.2 Matrix-operator description.** For an appropriate formulation of shell finite elements, it will be convenient to introduce a matrix-operator description. To this end we shall write the virtual displacement  $\mathbb{v} = (\mathbf{v}, \mathbf{w})$  and the external surface force  $\mathbb{p} = (\mathbf{p}, \mathbf{l})$  and boundary force  $\mathbf{s}^* = (\mathbf{n}^*, \mathbf{m}^*)$  in vector form

$$\mathbb{v} = \begin{Bmatrix} \mathbf{v} \\ \mathbf{w} \end{Bmatrix}, \quad \mathbb{p} = \begin{Bmatrix} \mathbf{p} \\ \mathbf{l} \end{Bmatrix}, \quad \mathbf{s}^* = \begin{Bmatrix} \mathbf{n}^* \\ \mathbf{m}^* \end{Bmatrix}. \quad (4.7)$$

Here and subsequently we use the term displacement, force, strain and stresses in a generalized sense. Using the notation (4.7) the virtual work densities of the external loads can be written as

$$\mathbb{v}^T \mathbb{p} = \mathbf{p} \cdot \mathbf{v} + \mathbf{l} \cdot \mathbf{w}, \quad \mathbb{v}^T \mathbf{s}^* = \mathbf{n}^* \cdot \mathbf{v} + \mathbf{m}^* \cdot \mathbf{w}. \quad (4.8)$$

Using the notation for the generalized line force  $\mathbb{p}_r = (\mathbf{p}_r, \mathbf{l}_r)$  measured per unit length of the curve  $\Gamma$  and the generalized concentrated forces  $\mathbb{f}_a = (\mathbf{f}_a, \mathbf{c}_a)$  acting at distinct points of the reference surface we write

$$\mathbb{v}_r^T \mathbb{p}_r = \mathbf{p}_r \cdot \mathbf{v}_r + \mathbf{l}_r \cdot \mathbf{w}_r, \quad \mathbb{v}_a^T \mathbb{f}_a = \mathbf{f}_a \cdot \mathbf{v}_a + \mathbf{c}_a \cdot \mathbf{w}_a. \quad (4.9)$$

The generalized strain and stresses are the ordered pairs  $\boldsymbol{\varepsilon} = (\mathbf{E}, \mathbf{K})$  and  $\mathbf{s} = (\mathbf{N}, \mathbf{M})$ , respectively, and they can be defined as four-tuples consisting of the associated strain and stress vectors  $\boldsymbol{\varepsilon} = (\boldsymbol{\varepsilon}_\beta, \boldsymbol{\kappa}_\beta)$  and  $\mathbf{s} = (\mathbf{n}^\beta, \mathbf{m}^\beta)$ :

$$\boldsymbol{\varepsilon} = \begin{Bmatrix} \mathbf{E} \\ \mathbf{K} \end{Bmatrix} = \begin{Bmatrix} \boldsymbol{\varepsilon}_1 \\ \boldsymbol{\varepsilon}_2 \\ \boldsymbol{\kappa}_1 \\ \boldsymbol{\kappa}_2 \end{Bmatrix}, \quad \mathbf{s} = \begin{Bmatrix} \mathbf{N} \\ \mathbf{M} \end{Bmatrix} = \begin{Bmatrix} \mathbf{n}^1 \\ \mathbf{n}^2 \\ \mathbf{m}^1 \\ \mathbf{m}^2 \end{Bmatrix}, \quad (4.10)$$

so that the internal virtual work density (2.13) can be written in the form

$$\begin{aligned} \mathbf{s}^T \delta \mathbf{e} &= \mathbf{N} \cdot \delta \mathbf{E} + \mathbf{M} \cdot \delta \mathbf{K} = \mathbf{n}^\beta \cdot \delta \boldsymbol{\varepsilon}_\beta + \mathbf{m}^\beta \cdot \delta \boldsymbol{\kappa}_\beta \\ &= \mathbf{N} \cdot \delta \mathbf{E} + \mathbf{M} \cdot \delta \mathbf{K} = \mathbf{n}^\beta \cdot \delta \boldsymbol{\varepsilon}_\beta + \mathbf{m}^\beta \cdot \delta \boldsymbol{\kappa}_\beta. \end{aligned} \quad (4.11)$$

Similarly, the strain-displacement relations (3.7) can be represented as

$$\boldsymbol{\varepsilon} = \hat{\boldsymbol{\varepsilon}}(\boldsymbol{\omega}) = \begin{Bmatrix} \hat{\boldsymbol{E}}(\boldsymbol{\omega}) \\ \hat{\boldsymbol{K}}(\boldsymbol{\omega}) \end{Bmatrix} = \begin{Bmatrix} \hat{\boldsymbol{\varepsilon}}_1(\boldsymbol{\omega}) \\ \hat{\boldsymbol{\varepsilon}}_2(\boldsymbol{\omega}) \\ \hat{\boldsymbol{\kappa}}_1(\boldsymbol{\omega}) \\ \hat{\boldsymbol{\kappa}}_2(\boldsymbol{\omega}) \end{Bmatrix}, \quad (4.12)$$

while the virtual changes of strains take the form

$$\delta\boldsymbol{\varepsilon}(\boldsymbol{\omega}) = \mathbb{B}(\boldsymbol{\omega})\boldsymbol{v}. \quad (4.13)$$

Here the differential matrix-operator is defined by

$$\mathbb{B}(\boldsymbol{\omega}) = \begin{bmatrix} \mathbf{1}(\cdot)_{,1} & (\mathbf{A}_1 + \mathbf{u}_{,1}) \times (\cdot) \\ \mathbf{1}(\cdot)_{,2} & (\mathbf{A}_2 + \mathbf{u}_{,2}) \times (\cdot) \\ \mathbf{0} & \mathbf{1}(\cdot)_{,1} \\ \mathbf{0} & \mathbf{1}(\cdot)_{,2} \end{bmatrix}. \quad (4.14)$$

For elastic shells the constitutive equations (3.18) can be written as  $\mathbf{s} = \tilde{\mathbf{s}}(\boldsymbol{\varepsilon})$ .

**3.3 Principle of virtual displacements.** We shall denote by  $\mathcal{U}_A \subset \mathcal{U}$  the set of all kinematically admissible displacement fields (trial fields), i.e. the fields  $\boldsymbol{\omega} = (\mathbf{u}, \mathbf{Q})$  satisfying the kinematic boundary conditions along  $\partial M_d$ :

$$\mathcal{U}_A \equiv \{ \boldsymbol{\omega} \in \mathcal{U} \mid \boldsymbol{\omega} = \boldsymbol{\omega}^* \text{ along } \partial M_d \}. \quad (4.15)$$

Consistently, we denote by  $\mathcal{V}_A \subset \mathcal{V}$  the set of all kinematically admissible virtual fields (test fields), i.e. fields  $\boldsymbol{v} = (\mathbf{v}, \boldsymbol{w})$  satisfying homogeneous kinematic boundary conditions  $\boldsymbol{v} = \mathbf{0}$  along  $\partial M_d$ :

$$\mathcal{V}_A \equiv \{ \boldsymbol{v} \in \mathcal{V} \mid \boldsymbol{v} = \mathbf{0} \text{ along } \partial M_d \}. \quad (4.16)$$

The fields  $\boldsymbol{\omega}$  and  $\boldsymbol{v}$  must satisfy the regularity assumptions stated in the previous chapter and we shall denote by  $\boldsymbol{\omega}_\Gamma$  and  $\boldsymbol{v}_\Gamma$ , respectively, the restriction of these fields to the curve  $\Gamma$ .

For elastic shells with the strain-displacement relations  $\boldsymbol{\varepsilon} = \hat{\boldsymbol{\varepsilon}}(\boldsymbol{\omega})$  and the constitutive equations  $\mathbf{s} = \tilde{\mathbf{s}}(\boldsymbol{\varepsilon})$  as subsidiary conditions, and with  $\boldsymbol{\omega} \in \mathcal{U}_A$  and  $\boldsymbol{v} \in \mathcal{V}_A$  we can define the functional

$$G[\boldsymbol{\omega}; \boldsymbol{v}] \equiv G_{int}[\boldsymbol{\omega}; \boldsymbol{v}] - G_{ext}[\boldsymbol{\omega}; \boldsymbol{v}], \quad (4.17)$$

where

$$\begin{aligned} G_{int}[\mathbb{w}; \mathbb{v}] &= \iint_{M \setminus \Gamma} (\mathbb{B}(\mathbb{w})\mathbb{v})^T \tilde{\mathfrak{s}}(\mathbb{w}) dA, \\ G_{ext}[\mathbb{w}; \mathbb{v}] &= \iint_{M \setminus \Gamma} \mathbb{v}^T \mathbb{p} dA + \int_{\partial M_f} \mathbb{v}^T \mathfrak{s}_i^* dS + \int_{\Gamma} \mathbb{v}_r^T \mathbb{p}_r dS + \sum_{\alpha} \mathbb{v}_a^T \mathfrak{f}_\alpha \end{aligned} \quad (4.18)$$

are the internal and external virtual work, respectively.

Now as an obvious implication of the virtual work identity (2.8) we find that  $\mathbb{w} \in \mathcal{U}_A$  is a weak solution of the shell boundary value problem if and only if

$$G[\mathbb{w}; \mathbb{v}] \equiv G_{int}[\mathbb{w}; \mathbb{v}] - G_{ext}[\mathbb{w}; \mathbb{v}] = 0, \quad (4.19)$$

for all  $\mathbb{v} \in \mathcal{V}_A$ . The variational statement (4.19) is nothing else but the principle of virtual displacements. A weak or generalized solution borrows its name from the fact that the admissible class of  $\mathbb{w}$  is larger than that required in the classical formulation. Indeed, (4.19) provides the integral representations of the problem instead of the differential one, which requires that the differential equilibrium equations are satisfied at each point of the shell reference surface.

## 5. Iterative solutions of nonlinear problems

**5.1 Linearized equations.** The solution of nonlinear shell problems, like any other nonlinear problem, typically requires to employ a suitable iterative procedure. All such procedures involve successive approximations of a nonlinear problem by a sequence of linearized problems. Thus a correctly formulated linearized problem is the main point of the approximation procedure. The linearized form of the principle of virtual displacements (4.19) about a trial solution  $\mathbb{w} = (\mathbf{u}, \mathbf{Q}) \in \mathcal{U}_A$  can be derived as follows. Let us consider a one-parameter family  $\mathbb{w}(\eta) = (\mathbf{u}(\eta), \mathbf{Q}(\eta))$  of the deformation in the form

$$\mathbf{u}(\eta) = \mathbf{u} + \eta \Delta \mathbf{v}, \quad \mathbf{Q}(\eta) = \exp(\eta \Delta \mathbf{W}) \mathbf{Q}, \quad (5.1)$$

where  $\mathbb{v} = (\Delta \mathbf{v}, \Delta \mathbf{w}) \in \mathcal{U}_A$  denotes any kinematical admissible virtual displacement field. As usual we denote by  $\Delta \mathbf{w}$  the axial vector of the skew-symmetric tensor  $\Delta \mathbf{W}$ . The directional derivative of the functional (4.17) at the point  $\mathbb{w}$  and in the direction  $\Delta \mathbb{w}$  is defined by

$$\begin{aligned} \delta G[\mathbb{w}; \Delta \mathbb{v}, \mathbb{v}] &= \frac{d}{d\eta} G[\mathbb{w}(\eta); \mathbb{v}]_{\eta=0} \\ &= \delta G_{int}[\mathbb{w}; \Delta \mathbb{v}, \mathbb{v}] - \delta G_{ext}[\mathbb{w}; \Delta \mathbb{v}, \mathbb{v}]. \end{aligned} \quad (5.2)$$

A not very difficult calculation yields the following form of the linearized internal virtual work expression<sup>1</sup>

$$\delta G_{int}[\mathbb{w}; \Delta \mathbf{v}, \mathbf{v}] = \iint_{M \setminus \Gamma} ((\mathbb{B}\mathbf{v})^T \mathbb{C}(\mathbb{B}\Delta \mathbf{v}) + (\mathbb{D}\mathbf{v})^T \mathbb{G}(\mathbb{D}\Delta \mathbf{v})) dA. \quad (5.3)$$

Here  $\mathbb{B}$  is the differential operator given by (4.14),  $\mathbb{C}$  denotes the constitutive matrix defined by

$$\mathbb{C}(\boldsymbol{\varepsilon}) = \partial_{\boldsymbol{\varepsilon}} \mathbf{s}(\boldsymbol{\varepsilon}) = \begin{bmatrix} \partial_E N(\mathbf{E}, \mathbf{K}) & \partial_K N(\mathbf{E}, \mathbf{K}) \\ \partial_E \mathbf{M}(\mathbf{E}, \mathbf{K}) & \partial_K \mathbf{M}(\mathbf{E}, \mathbf{K}) \end{bmatrix} \quad (5.4)$$

and  $\mathbb{G}$ ,  $\mathbb{D}$  are matrix-operators being defined by

$$\mathbb{D} = \begin{bmatrix} (\cdot)_{,1} \mathbf{1} & \mathbf{0} \\ (\cdot)_{,2} \mathbf{1} & \mathbf{0} \\ \mathbf{0} & (\cdot)_{,1} \mathbf{1} \\ \mathbf{0} & (\cdot)_{,2} \mathbf{1} \\ \mathbf{0} & \mathbf{1} \end{bmatrix}, \quad (5.5)$$

$$\mathbb{G}(\mathbb{w}) = \begin{bmatrix} \mathbf{0} & \mathbf{0} & \mathbf{0} & \mathbf{0} & -\mathbf{n}^1 \times (\cdot) \\ \mathbf{0} & \mathbf{0} & \mathbf{0} & \mathbf{0} & -\mathbf{n}^2 \times (\cdot) \\ \mathbf{0} & \mathbf{0} & \mathbf{0} & \mathbf{0} & -\mathbf{m}^1 \times (\cdot) \\ \mathbf{0} & \mathbf{0} & \mathbf{0} & \mathbf{0} & -\mathbf{m}^2 \times (\cdot) \\ \mathbf{n}^1 \times (\cdot) & \mathbf{n}^1 \times (\cdot) & \mathbf{0} & \mathbf{0} & \mathbf{H} \end{bmatrix}, \quad (5.6)$$

where we have introduced the following notation

$$\mathbf{H}(\mathbb{w}) = \mathbf{n}^\beta \otimes (\mathbf{A}_\beta + \mathbf{u}_{,\beta}) + (\mathbf{n}^\beta \bullet (\mathbf{A}_\beta + \mathbf{u}_{,\beta})) \mathbf{1}. \quad (5.7)$$

In (5.6) it is understood that all entries of this matrix are functions of the generalized displacement through constitutive equations and strain-displacement relations.

Admitting that external loads acting on the shell can be configuration dependent, we denote by

$$\mathbb{F}(\mathbb{w}) = \partial_{\mathbf{u}} \mathbb{p}(\mathbb{w}), \quad \mathbb{F}_r(\mathbb{w}) = \partial_{\mathbf{u}} \mathbb{p}_r(\mathbb{w}), \quad \mathbb{F}^*(\mathbb{w}) = \partial_{\mathbf{u}} \mathbf{s}_v^*(\mathbb{w}) \quad (5.8)$$

<sup>1</sup> See MAKOWSKI AND STUMPF [1988,1990].

their derivatives. Then the linearized external virtual work expression can be written in the form

$$\delta G_{ext}[\mathbb{w}; \Delta \mathbb{v}, \mathbb{v}] = \iint_{M \setminus \Gamma} \mathbb{v}^T (\mathbb{F} \Delta \mathbb{v}) dA + \int_{\Gamma} \mathbb{v}_r^T (\mathbb{F}_r \Delta \mathbb{v}_r) dS + \int_{\partial M_f} \mathbb{v}^T (\mathbb{F} \Delta \mathbb{v}) dS. \quad (5.9)$$

**5.2 Successive linearizations.** Let us assume that the load acting on the shell is specified by a single parameter  $\lambda$ . For smoothly varying  $\lambda$  in some range, the regular solutions of the shell boundary value problem form a curve (one-dimensional solution manifold)  $\mathbb{w}(\lambda) \in \mathcal{U}_A$  on the configuration space, called an equilibrium path. By virtue of the principle of virtual displacements (4.19),  $\mathbb{w}(\lambda) \in \mathcal{U}_A$  is a weak solution of the boundary value problem if

$$G[\mathbb{w}(\lambda); \mathbb{v}] \equiv G_{int}[\mathbb{w}(\lambda); \mathbb{v}] - G_{ext}[\mathbb{w}(\lambda); \mathbb{v}] = 0 \quad (5.10)$$

for all kinematically admissible virtual displacements  $\mathbb{v} \in \mathcal{V}_A$ . The iterative procedure of tracing an equilibrium path may be formulated in the following way. We seek solutions for a finite number of discrete values  $\lambda_0, \lambda_1, \dots, \lambda_n, \dots$  of the load parameter. Let  $\mathbb{w}_n = \mathbb{w}(\lambda_n)$  be a solution we are looking for, and let  $\mathbb{w}_n^{(i)}$  denote the  $i$ -th approximation to the solution  $\mathbb{w}_n$ . It has to be noted that  $\mathbb{w}_n^{(i)}$  need not belong to the equilibrium path. We then need suitable linearized equations, which would allow us to calculate a correction  $\Delta \mathbb{v}_n^{(i+1)}$ , determining together with  $\mathbb{w}_n^{(i)}$  uniquely a successive approximation  $\mathbb{w}_n^{(i+1)}$  to the solution  $\mathbb{w}_n$ . The most efficient method to construct such approximations is based on successive linearizations of equation (5.10). Suppose that the approximation  $\mathbb{w}_n^{(i)}$  has been found. To calculate the next approximation  $\mathbb{w}_n^{(i+1)}$  we replace equation (5.10) by an equation which is linearized at  $\mathbb{w}_n^{(i)}$ :

$$\delta G[\mathbb{w}_n^{(i+1)}; \Delta \mathbb{v}_n^{(i+1)}, \mathbb{v}] + G[\mathbb{w}_n^{(i)}; \mathbb{v}] = 0. \quad (5.11)$$

The method defined by (5.11) is known as the Newton or Newton - Kantorovich method. The physical meaning of equation (5.11) is standard. The second term represents the unbalanced force at the configuration  $\mathbb{w}_n^{(i)}$  and the first term being linear in the unknown correction  $\Delta \mathbb{v}_n^{(i+1)}$  yields the so-called tangent stiffness matrix.

A typical iterative solution procedure consists of three basic steps:

- 1) Given the  $i$ -th approximation  $\mathbb{w}^{(i)} = (\mathbf{u}^{(i)}, \mathbf{Q}^{(i)})$  to the exact solution  $\mathbb{w} = (\mathbf{u}, \mathbf{Q})$  we calculate all entries of the linearized equation (5.11),

- 2) The equation (5.11) is then solved for the next correction to the solution we are looking for,
- 3) Through the update procedure the next approximation  $\mathbb{w}^{(i+1)} = (\mathbf{u}^{(i+1)}, \mathbf{Q}^{(i+1)})$  to the exact solution is calculated.

This process is continued until the calculated successive approximation is close, in the defined sense, to the exact one.

**5.3 Exact update procedure.** The central issue concerns the update procedure of the rotation field, because the displacement field takes its values in the vector space  $E$  and is subjected to a standard accumulation procedure. Let  $\mathbb{w}^{(i)} = (\mathbf{u}^{(i)}, \mathbf{Q}^{(i)})$  denote the known  $i$ -th approximation to the true solution. Assume next that the correction  $\Delta \mathbf{v}_n^{(i+1)}$  has been obtained from the solution of the linearized problem (5.11). Then the successive approximation  $\mathbb{w}^{(i+1)} = (\mathbf{u}^{(i+1)}, \mathbf{Q}^{(i+1)})$  has to be calculated according to the rule

$$\begin{aligned} \mathbf{u}^{(i+1)} &= \mathbf{u}^{(i)} + \Delta \mathbf{v}^{(i+1)}, \\ \mathbf{Q}^{(i+1)} &= (\exp \Delta \mathbf{W}^{(i+1)}) \mathbf{Q}^{(i)}, \quad \Delta \mathbf{W}^{(i+1)} = ad(\Delta \mathbf{w}^{(i+1)}). \end{aligned} \quad (5.12)$$

The exponential function entering (5.12) is effectively calculated using the well-known formula

$$\begin{aligned} \exp \Psi &= 1 + \Psi + \frac{1}{2} \Psi^2 + \dots \\ &= 1 + \frac{\sin \psi}{\psi} \Psi + \frac{1 - \cos \psi}{\psi^2} \Psi^2, \\ \psi &= -\frac{1}{2} tr \Psi^2, \end{aligned} \quad (5.13)$$

for every skew tensor  $\Psi$ , being the straightforward implication of the Cayley - Hamilton theorem applied to the definition of the exponential function. Once the successive approximation  $\mathbb{w}^{(i+1)}$  has been calculated the associated strains  $\boldsymbol{\varepsilon}^{(i+1)}$  can be obtained easily from the kinematical relations. Then the corresponding stresses  $\boldsymbol{\mathfrak{s}}^{(i+1)}$  have to be calculated using the constitutive equations.

**5.4 Tracing equilibrium paths.** In the nonlinear analysis of shells we are typically interested in finding not only a single solution but a solution manifold for smoothly varying control (usually load) parameters. In the case of loads proportional to a single scalar parameter the tracing of a one-dimensional solution manifold is obtained by the continuation methods, in engineering literature better known as incremental methods. There exists a comprehensive literature on the

subject and the basic concept is by now well developed. Nevertheless, an effective computer realization of the method requires some ingenuity. The main points of the problem are:

- 1) Specification of a maximum and minimum step size.
- 2) Devising a simple rule for determining the incremental size in advancing a step.
- 3) Specification of means to recognize non-convergence of the iterative process, as opposed to slow convergence, and then deciding to terminate the process or redefine the increment.
- 4) Specification of a criterion for terminating the iterative process, when convergence is obtained.
- 5) Choice of suitable measures (norms) for the unknowns of the problem.

## 6. Parametrization of rotations

**6.1 Global parametrizations.** So far we have considered the complete set of the shell governing equations regarding the displacement field  $\mathbf{u}$  and the rotation tensor  $\mathbf{Q}$  as the primary unknown fields. In this way we exposed the differential-geometrical structure of the theory without resorting to a particular parametrization of the rotation group  $SO(3)$ . A choice of parametrization of the rotation group is a central issue to analytical or numerical solutions of the boundary value problems. The familiar Euler (or Bryant) angles, Cayley-Klein parameters or quaternions are examples of possible representations of rotations, none of which has a clear advantage over others. In evaluating the usefulness of a particular parametrization the following factors must be considered: 1) The number of parameters needed and possible singularities, 2) The complexity of the resulting equations, 3) The susceptibility to numerical errors in the computer implementation of the shell equations, 4) Difficulties in the formulation of kinematical boundary conditions.

As it is known, it is impossible to have a global singular free representation of rotational degrees of freedom in terms of less than five parameters. In turn, only three parameters are independent and any more than three-dimensional parametrization results in redundant parameters which must satisfy suitable constraints. This leads to an extended system of field equations with corresponding Lagrange multipliers as additional unknown fields of the problem.



Thus from the numerical point of view such approach is of less importance and hence we shall consider only three-dimensional parametrizations.

**6.2 Local parametrizations.** A local singular free parametrization of rotations means no more no less but a choice of a particular coordinate system on the rotation group. This makes sense, since  $SO(3)$  is the Lie group and hence it is first of all a differentiable manifold. Let  $U \subset SO(3)$  be an open neighborhood of  $Q \in SO(3)$ , where  $Q$  is a fixed but otherwise arbitrary rotation tensor. Then any diffeomorphism of  $U$  onto an open set of the real space  $\mathbb{R}^3$ . In short notation, we can simply write

$$Q = Q(\vartheta), \quad \vartheta = (\vartheta_k) = (\vartheta_1, \vartheta_2, \vartheta_3), \quad (6.1)$$

where the triple  $(\vartheta_k)$  of real numbers are local coordinates of the rotation tensor  $Q$ .

The virtual rotation is then obtained in the form

$$W(\vartheta) = \delta Q(\vartheta) Q(\vartheta)^T = \sum_{k=1}^3 W^{(k)}(\vartheta) \delta \vartheta_k, \quad (6.2)$$

where

$$W^{(k)}(\vartheta) = Q^{(k)}(\vartheta) Q^T(\vartheta), \quad Q^{(k)}(\vartheta) \equiv \frac{\partial Q(\vartheta)}{\partial \vartheta_k}. \quad (6.3)$$

The tensors  $W^{(k)}$  are necessarily skew-symmetric, so we can compute their axial vectors  $w^{(k)}$ . In this manner we obtain

$$w(\vartheta) = ad^{-1} W(\vartheta) = \sum_{k=1}^3 w^{(k)}(\vartheta) \delta \vartheta_k, \quad w^{(k)}(\vartheta) = ad^{-1} W^{(k)}(\vartheta). \quad (6.4)$$

We can write this relation in matrix form

$$w(\vartheta) = \Xi(\vartheta) \vartheta, \quad \vartheta = \begin{Bmatrix} \vartheta_1 \\ \vartheta_2 \\ \vartheta_3 \end{Bmatrix}. \quad (6.5)$$

**6.3 Kinematical relations.** This approach applies, when we consider not a fixed rotation tensor but a field of rotation tensors. In this case (6.1) must be understood as

$$Q(Y) = Q(\vartheta(Y)). \quad (6.6)$$

If  $M$  is given locally in the parametric form, then the partial derivatives of (6.6) with respect to the surface coordinates are given by

$$\mathcal{Q}_{,\beta}(\vartheta) = \frac{\partial \mathcal{Q}(\vartheta)}{\partial \xi^{\beta}} = \sum_{k=1}^3 \frac{\partial \mathcal{Q}(\vartheta)}{\partial \vartheta_k} \frac{\partial \vartheta_k}{\partial \xi^{\beta}} = \sum_{k=1}^3 \mathcal{Q}^{(k)}(\vartheta) \vartheta_{k,\beta}, \quad (6.7)$$

where

$$\mathcal{Q}^{(k)}(\vartheta) = \frac{\partial \mathcal{Q}(\vartheta)}{\partial \vartheta_k}, \quad k = 1, 2, 3. \quad (6.8)$$

Now the skew tensor defined by (3.7)<sub>3</sub> can be expressed in the form

$$\mathbf{K}_{\beta}^{(k)}(\vartheta) \equiv \mathcal{Q}_{,\beta}(\vartheta) \mathcal{Q}^{(k)}(\vartheta) = \kappa_{\beta}^{(k)}(\vartheta). \quad (6.9)$$

and the strain-displacement relations (3.7) expressed in terms of the displacement field and rotational parameters read

$$\varepsilon_{\beta}(\mathbf{u}, \vartheta) = \mathbf{u}_{,\beta} - (\mathcal{Q}(\vartheta) - \mathbf{1}) \mathbf{A}_{\beta}, \quad \kappa_{\beta}(\vartheta) = \sum_{k=1}^3 \kappa_{\beta}^{(k)}(\vartheta) \vartheta_{k,\beta}. \quad (6.10)$$

Combining these results with the results of the previous section the virtual changes of strains can be written as

$$\delta \varepsilon_{\beta} = \mathbf{v}_{,\beta} + (\mathbf{A}_{\beta} + \varepsilon_{\beta}) \times \mathbf{w}(\vartheta), \quad \delta \kappa_{\beta} = \sum_{k=1}^3 \mathbf{w}_{\beta}^{(k)}(\vartheta) \delta \vartheta_{k,\beta}. \quad (6.11)$$

**5.4 Finite rotation vectors.** Among various possible parametrizations of the rotation group of special interest are the so-called finite rotation vectors. In general, let  $\boldsymbol{\psi}$  be any vector and let  $\boldsymbol{\Psi} = \text{ad}\boldsymbol{\psi}$  be the associated skew-symmetric tensor, whose axial vector is  $\boldsymbol{\psi}$ . Then

$$\mathcal{Q} = \exp \boldsymbol{\Psi} \quad (6.12)$$

is necessarily a uniquely defined proper orthogonal tensor (rotation tensor). Geometrically,  $\mathcal{Q}$  represents the rotation about a unit vector  $\mathbf{e}$  in the positive sense through the angle  $\psi$ , where  $\boldsymbol{\psi} = \psi \mathbf{e}$ . Now let  $\lambda = \lambda(\psi)$  be any monotonously increasing function such that  $\lambda(0) = 0$ . Then the generalized finite rotation vector and the associated skew tensor can be defined as

$$\boldsymbol{\lambda} = \lambda(\psi) \mathbf{e}, \quad \mathbf{A} = \lambda(\psi) \mathbf{E}, \quad \mathbf{E} = \text{ad} \mathbf{e}. \quad (6.13)$$

The assumption about the function  $\lambda(\psi)$  ensures that there exists the unique inverse function  $\psi = \psi(\lambda)$ , and hence the rotation tensor  $\mathcal{Q}$  given by (6.12) can be regarded as function of the finite rotation vector  $\lambda$  alone. Thus the three components of  $\lambda$  provide a local singular free parametrization of the rotation group.

## Chapter III

# Finite element approximations

### 1. Preliminaries

**1.1 Finite element models.** The finite element method may be formulated and interpreted from two different viewpoints: a physical and a mathematical one. The physical approach is closely related to the original formulation and extensive application of the method in structural analysis. The basic concept is that every structure may be considered to be fabricated as or approximated by an assemblage of individual structural components or "finite elements". The elements are interconnected at a finite number of "node points". Mathematically, the finite element method can be considered as an application of the Rayleigh-Ritz method or its more general counterpart, the Bubnov-Galerkin method, together with the use of piecewise polynomials to approximate solutions of boundary value problems. As such it involves two basic aspects:

- A) Weak formulation of the problem,
- B) Selection of the space of trial functions and of the space of test functions (technically, the choice of the number of nodes, the number of nodal variables, and the so-called shape functions).

With respect to A) two main classes of finite element formulations can be distinguished:

- A1) Single field finite elements,
- A2) Multi-field finite elements.

The most typical example of the class A1) are finite elements based on the displacement (in our case displacement/rotation) formulation having the principle of virtual displacements as the underlying weak formulation of the problem.

Among the finite elements belonging to the class A2) we can mention mixed formulations usually based on a Hellinger-Reissner type variational formulation.

There exist also finite element formulations, which are mainly based on some technical constructions usually having no variational formulation of the problem. Among such formulations the assumed strain techniques appear to be the most often used ones. However, finite elements formulated within these techniques are less reliable, although they can provide a sound solution for many engineering problems.

In this chapter we shall present the formulation of shell finite elements on the basis of the theory summarized in the previous chapter within all three classes. From the computational point of view the following features of this shell theory are worth to be noted:

- a) Only  $C^0$  continuity of the independent kinematic variable  $\mathfrak{w} = (\mathbf{u}, \mathbf{Q})$  and  $C^{-1}$  (piecewise) continuity of the resultant stress  $\mathfrak{s} = (\mathbf{n}^\beta, \mathbf{m}^\beta)$  and strain  $\boldsymbol{\varepsilon} = (\boldsymbol{\varepsilon}_\beta, \boldsymbol{\kappa}_\beta)$  need to be ensured across the element edges. In this respect the underlying shell theory has the same properties as the shell finite elements formulated within the degenerated concept.
- b) The formulation itself eliminates the costs associated with the through-the-thickness integration even for thick shells undergoing finite strain deformation with highly nonlinear through-the-thickness deformation. This is an essential advantage of our formulation compared with the degenerated shell concept.
- c) The theory incorporates all three rotational parameters as independent kinematical variables, and hence the finite elements with six degrees of freedom per node can be constructed in the usual way with no special techniques or ad hoc devices. This completely solves the problem of modeling irregular shells containing kinks and multi-shell intersections.
- d) The construction of various finite elements is performed here according to the usual procedure, which is independent on whether the shell is thin or thick, isotropic or not, undergoing small or finite strain deformation. The distinction appears only through the choice of specific constitutive relations, whose general structure is only needed in the formulation of shell elements. The explicit form of the constitutive equations is required only for the solution of the specific problem under consideration.

It is also worth to be noted that the basic concepts of the finite element method are entirely independent of a particular problem to be considered. Thus the

development of shell finite elements is essentially based on the same concepts as in the formulation of three-dimensional finite elements, etc. However, there is one essential point, which distinguishes the shell finite elements to be formulated in this paper from the classical elements. This distinguishing feature is due to the lack of a convenient vector space structure of the underlying configuration space.

Independent of a particular class of finite elements, an effective solution of nonlinear problems requires:

- C) A suitable iterative procedure involving a correct formulation of the linearized equations,
- D) Development of a procedure enabling to trace a complete equilibrium path together with detecting all singular points (bifurcation and snap-through points).

However, these two additional aspects are not a part of the finite element method, and they do not influence the accuracy of the obtained solution. We have considered both aspects within a continuum formulation of the shell problems, and they will be used to solve discrete problems resulting from the finite element discretization.

**1.2 Physical coordinates.** In the previous chapter we have used an arbitrary local parametrization of the undeformed reference surface  $M$  and we have admitted the triad  $\{D_i\}$  assigned to every point of  $M$  to be chosen in any convenient form. This generality yields components of static and kinematic variables of the theory, which have no physical dimension. In the solution of the specific problems and in the development of shell finite elements, it is preferable to use physical components of the variables. This can be achieved quite easily in the following way.

Let us assume that the undeformed shell reference surface  $M$  is locally parametrized by orthogonal coordinates  $(\xi^\beta) = (\xi^1, \xi^2)$ , i.e. they are assumed to form an orthogonal net on  $M$ . Especially, they can be principal coordinates, but this is not required here. Let us further denote by  $s = (s_1, s_2)$  the arc length parameter along the coordinates  $(\xi^\beta) = (\xi^1, \xi^2)$ , so that we have

$$ds_\beta = \alpha_\beta d\xi^\beta, \quad \alpha_\beta = \sqrt{Y_{,\beta} \cdot Y_{,\beta}}, \quad \beta = 1, 2 \quad (\text{not summed}). \quad (1.1)$$

In effect, we can assume that locally  $M$  is parametrized by coordinates  $s = (s_1, s_2)$  being arc length parameters (Fig. 1). Then the associated natural base vectors and the unit normal vector are given by

$$A_{\langle\beta\rangle} = \frac{\partial \mathbf{Y}}{\partial s_\beta}, \quad \beta=1,2 \quad (\text{not summed}), \quad A_{\langle 3 \rangle} = A_{\langle 1 \rangle} \times A_{\langle 2 \rangle}, \quad (1.2)$$

and they form an orthonormal triad at every point of the reference surface.

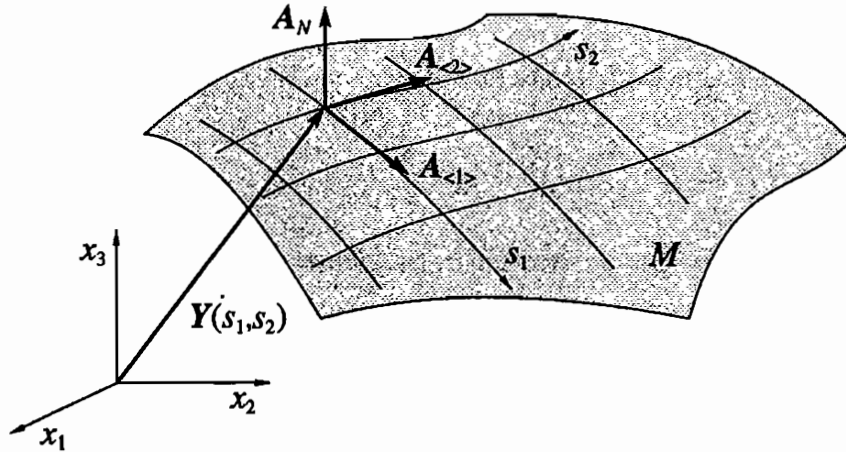


Fig. 1

Within the considered shell theory the geometry of the undeformed shell configuration is specified not only by the position vector  $\mathbf{Y}$ , which from now on is regarded as being given in the form  $\mathbf{Y} = \mathbf{Y}(s_\beta)$ , but also by the field of the triads  $\{\mathbf{D}_i(\mathbf{Y})\}$ . In the context of the finite element formulation, we take  $\{\mathbf{D}_i\}$  to be an orthonormal triad, i.e.

$$\mathbf{D}_i \cdot \mathbf{D}_j = \delta_{ij}, \quad \mathbf{D}^i = \mathbf{D}_i, \quad \mathbf{D} \equiv \mathbf{D}_3 = \mathbf{D}_1 \times \mathbf{D}_2. \quad (1.3)$$

In this case the triad  $\{\mathbf{D}_i\}$  can be defined at each point of  $M$  by a proper orthogonal transformation (Fig. 2)

$$\mathbf{D}_i(\mathbf{Y}) = \mathbf{T}(\mathbf{Y})\mathbf{e}_i, \quad i=1,2,3, \quad (1.4)$$

where  $\mathbf{T}$  is a given field of rotation tensors. From (1.4) and (II.3.2) we have then

$$\mathbf{d}_i(\mathbf{Y}) = \mathbf{Q}(\mathbf{Y})\mathbf{D}_i(\mathbf{Y}) = \mathbf{Q}(\mathbf{Y})\mathbf{T}(\mathbf{Y})\mathbf{e}_i(\mathbf{Y}). \quad (1.5)$$

Since  $\mathbf{T}$  must be given as part of the data, we may take  $\mathbf{QT}$  instead of the rotation tensor  $\mathbf{Q}$  as independent rotational variable.

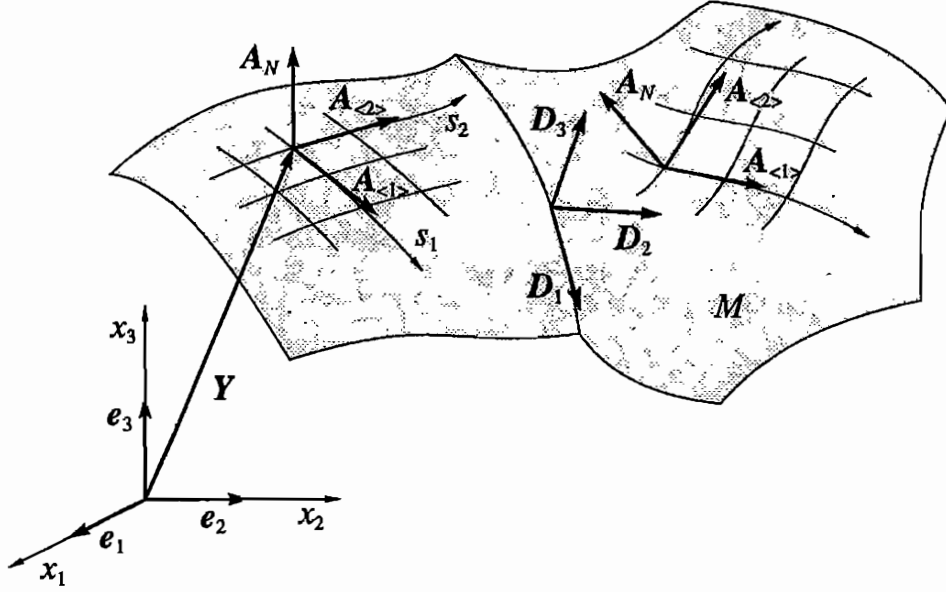


Fig. 2

**2.3 Physical components.** When the shell reference surface  $M$  is parametrized by the arc length parameters  $s = (s_1, s_2)$ , then all kinematic and static quantities and relations have a physical dimension. Assuming that this is the case, all relations summarized in the previous chapter can be used for the subsequent considerations without any additional rederivation. Let us note that this is not an essential restriction, because finally we shall not need these coordinates. The point of view which we adopt here is just a convenient way to get physical components for all variables without extra effort.

Having in mind that  $\{D_i\}$  is an orthonormal triad, the physical components of the resultant stress and the resultant couple vectors are defined by (Fig. 3)

$$\begin{aligned} \mathbf{n}^{(1)} &= N^{(11)}D_1 + N^{(21)}D_2 + Q^{(1)}D, & \mathbf{n}^{(2)} &= N^{(12)}D_1 + N^{(22)}D_2 + Q^{(2)}D, \\ \mathbf{m}^{(1)} &= -M^{(12)}D_1 + M^{(11)}D_2 + M^{(1)}D, & \mathbf{m}^{(2)} &= -M^{(22)}D_1 + M^{(21)}D_2 + M^{(2)}D. \end{aligned} \quad (1.6)$$

In the same way are also defined physical components of strain vectors as well as all static and kinematic variables entering the shell governing equations.

$$\begin{aligned} \boldsymbol{\varepsilon}_{(1)} &= \varepsilon_{(11)}D_1 + \varepsilon_{(12)}D_2 + \varepsilon_{(1)}D, & \boldsymbol{\varepsilon}_{(2)} &= \varepsilon_{(21)}D_1 + \varepsilon_{(22)}D_2 + \varepsilon_{(2)}D, \\ \boldsymbol{\kappa}_{(1)} &= -\kappa_{(12)}D_1 + \kappa_{(11)}D_2 + \kappa_{(1)}D, & \boldsymbol{\kappa}_{(2)} &= -\kappa_{(22)}D_1 + \kappa_{(21)}D_2 + \kappa_{(2)}D. \end{aligned} \quad (1.7)$$



By virtue of (1.5) it then follows that the physical components of stresses ( $\mathbf{n}^\beta, \mathbf{m}^\beta$ ) and strains ( $\boldsymbol{\varepsilon}_\beta, \boldsymbol{\kappa}_\beta$ ) with respect to the rotated triad coincide with the components of the stresses ( $\mathbf{n}^\beta, \mathbf{m}^\beta$ ) and strains ( $\boldsymbol{\varepsilon}_\beta, \boldsymbol{\kappa}_\beta$ ) defined by (1.6) and (1.7). Consequently, both sets of stresses and strains can equally well be taken in the finite element formulations.

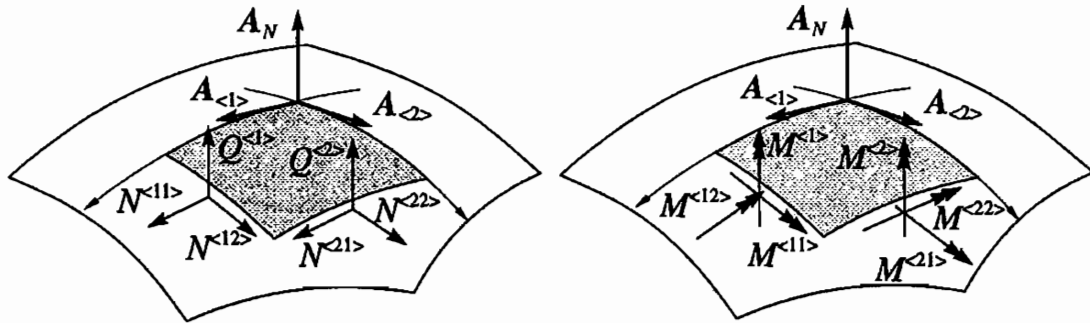


Fig. 3

## 2. Discretization of the undeformed configuration

**2.1 Typical finite element.** In the finite element analysis of shells not only the unknowns of the problem need to be approximated but also the domain of the unknowns, i.e. the undeformed reference surface  $M$ . Moreover, within the shell theory under consideration the complete description of the undeformed configuration of the shell requires to specify the reference surface  $M$  and the triad  $\{\mathbf{D}_i\}$  at each point of  $M$ .

According to the standard finite element procedure, the reference surface  $M$  is represented as the union  $M = \bigcup_{e \in N_e} \Pi_{(e)}$  of subdomains (finite elements)  $\Pi_{(e)}$  as illustrated in Fig. 4. According to the isoparametric concept, a typical finite element  $\Pi_{(e)}$  is defined as a smooth image of the standard element  $\pi_{(e)} \subset \mathbb{R}^2$  referred to the natural coordinates

$$\boldsymbol{\xi} \equiv (\xi_1, \xi_2) \in [-1, +1] \times [-1, +1] \subset \mathbb{R}^2. \quad (2.1)$$

Usually, the standard element  $\pi_{(e)}$  is defined as a triangular or rectangular domain with  $n$  nodes defined by the values of the natural coordinates:

$$\xi_1, \xi_2, \dots, \xi_a, \dots, \xi_n, \quad \boldsymbol{\xi}_a = (\xi_{1a}, \xi_{2a}) \in \pi_{(e)} \subset \mathbb{R}^2. \quad (2.2)$$

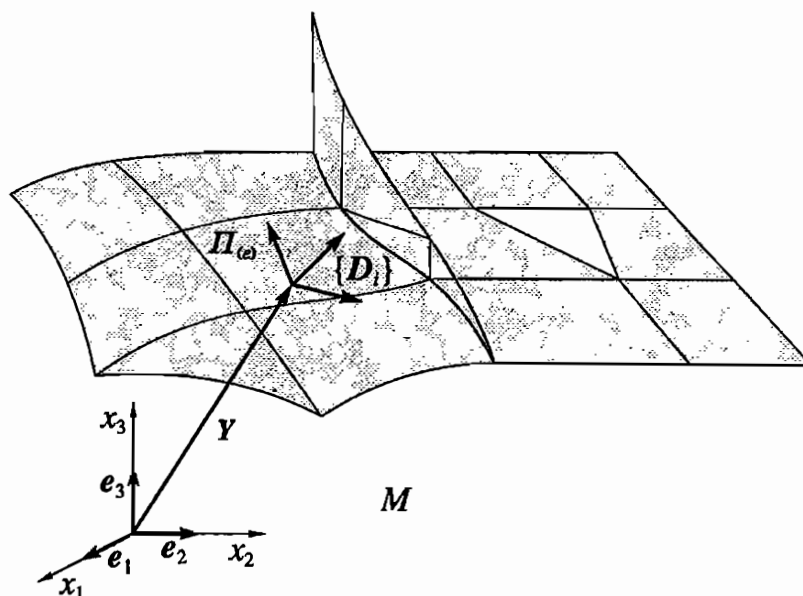


Fig. 4

The nodes of a typical element  $\Pi_{(e)}$  are determined by their position vectors  $\mathbf{Y}_a$ ,  $a=1,2,\dots,n$ . The orthonormal triad  $\{\mathbf{D}_i\}_a \equiv \{\mathbf{D}_i(\mathbf{Y}_a)\}$  at every node is next defined by the proper orthogonal transformation according to (1.4), i.e.

$$\mathbf{D}_i(\mathbf{Y}_a) = \mathbf{T}_a \mathbf{e}_i, \quad i=1,2,3, \quad a=1,2,\dots,n. \quad (2.3)$$

In this way a typical  $n$ -node finite element is completely defined by the ordered pairs  $(\mathbf{Y}_a, \mathbf{T}_a)$ ,  $a=1,2,\dots,n$ , (Fig. 5). Then the position vector  $\mathbf{Y}(\boldsymbol{\xi})$  and the rotation tensor  $\mathbf{T}(\boldsymbol{\xi})$  at every point within the element are interpolated from the nodal values.

**2.2 Shape functions.** The position vector  $\mathbf{Y}$  at any point of the typical element is given by the standard interpolating formula

$$\mathbf{Y}(\boldsymbol{\xi}) = \sum_{k=1}^n L_k(\boldsymbol{\xi}) \mathbf{Y}_k, \quad (2.4)$$

where  $L_a(\boldsymbol{\xi})$  are the so-called shape functions having the property  $L_a(\boldsymbol{\xi}_b) = \delta_{ab}$ ,  $a,b=1,2,\dots,n$ . In the case of rectangular (standard) elements the shape functions are usually taken in the form of Lagrange interpolating polynomials (Fig. 6).

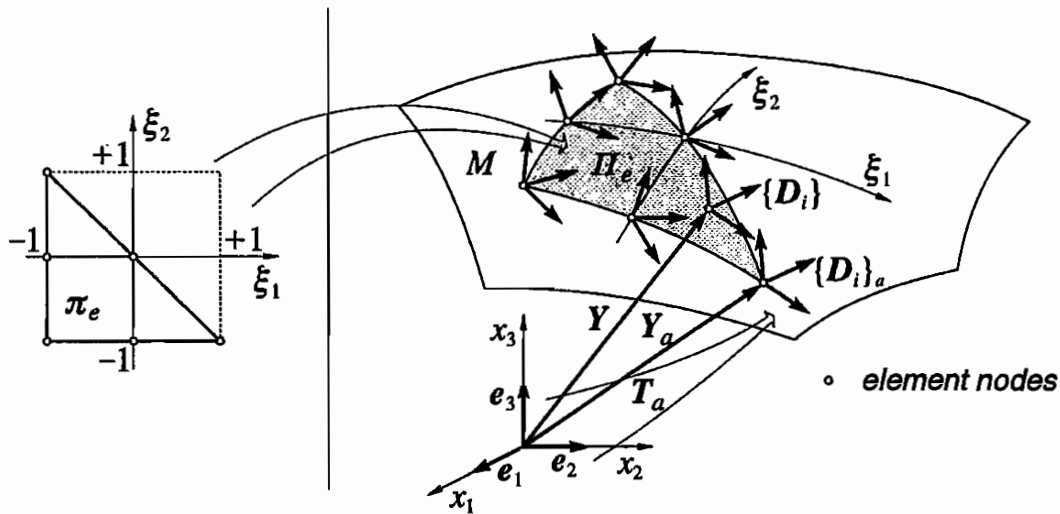


Fig. 5

**2.3 Interpolation of rotations.** Within the considered shell theory the basic difficulty inherent in devising interpolating functions lies in the fact that the rotation group lacks a linear space structure. This problem can be overcome using a local singular free parametrization of the rotation group in the following way. Given a parametrization of  $SO(3)$ , the tensor  $T$  is (locally) represented by three rotational parameters  $\vartheta = (\vartheta_1, \vartheta_2, \vartheta_3)$  in the way described in Chapt. II.5. We then calculate the nodal values  $\vartheta_a$  of the rotational parameters from the given rotation tensors  $T_a$ . The rotational parameters  $\vartheta(\xi)$  at any point within the element are interpolated from the nodal values using the formula (2.4), and subsequently the rotation tensor  $T(\xi)$  is computed according to the chosen parametrization of the rotation group:

$$T(\xi) = T(\vartheta(\xi)), \quad \vartheta(\xi) = \sum_{a=1}^n L_a(\xi) \vartheta_a. \quad (2.5)$$

**2.4 Transformation formulae.** A typical finite element  $\Pi_{(e)}$ , as it is defined above, is parametrized by the natural coordinates  $\xi = (\xi_1, \xi_2)$ . On the other hand the shell governing equations summarized in Chapt. II contain partial derivatives with respect to the surface (arc length) coordinates  $s = (s_1, s_2)$ . We then need the corresponding transformation rules allowing to express the partial derivatives with respect to the coordinates  $s = (s_1, s_2)$  in terms of the partial derivatives with respect to the natural coordinates  $\xi = (\xi_1, \xi_2)$ . Since the position vector  $Y$  can be regarded as given function of either coordinates,  $Y(s_\beta) = Y(\xi_\alpha(s_\beta))$ , from the chain rule we have

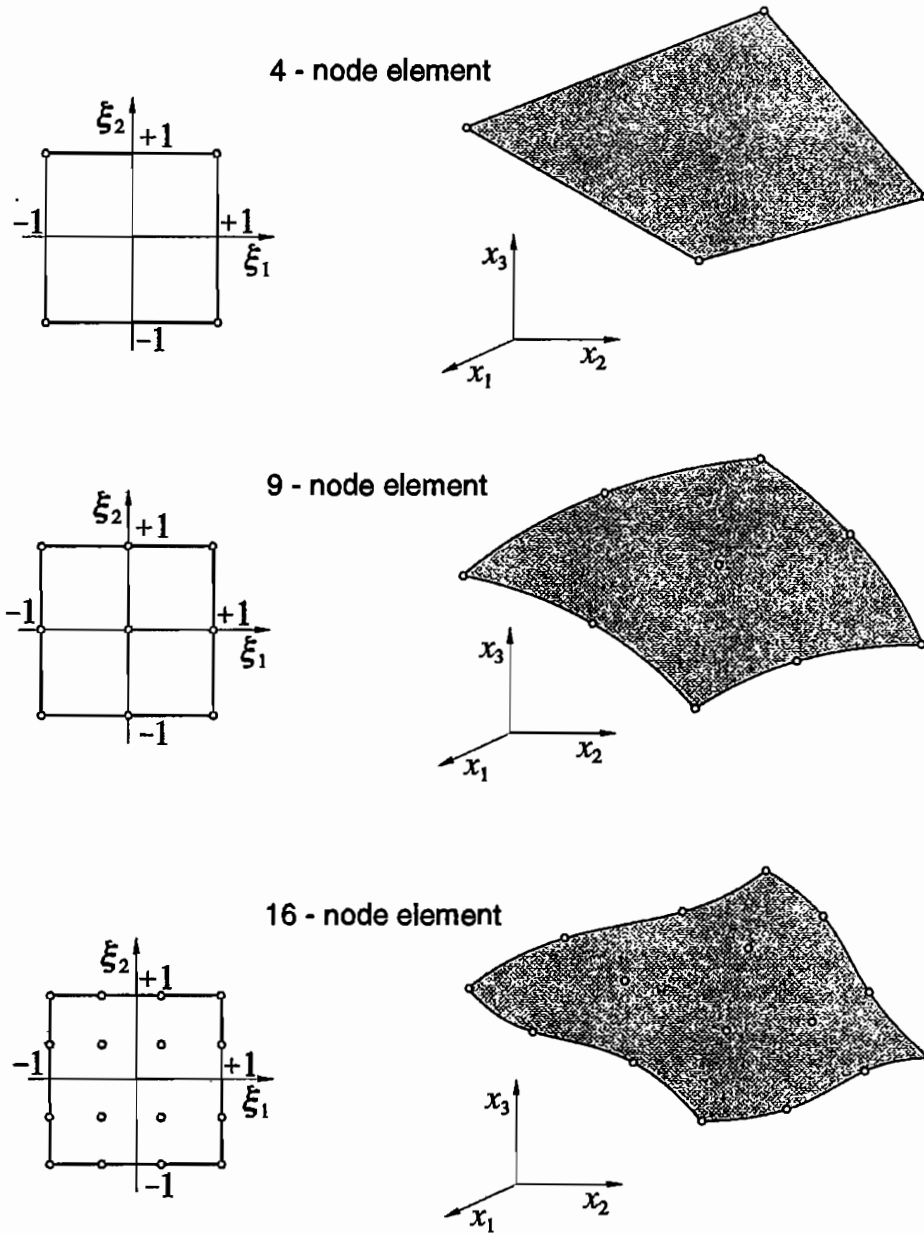


Fig. 6

$$A_{(\beta)} = \frac{\partial Y}{\partial s_\beta} = \sum_{\alpha=1}^2 \frac{\partial Y}{\partial \xi_\alpha} \frac{\partial \xi_\alpha}{\partial s_\beta}, \quad \beta=1,2 \text{ (not summed)}. \quad (2.6)$$

This formula applies to any variable entering shell equations such as the displacement field  $\mathbf{u}$  or the rotation tensor  $\mathbf{Q}$ . Moreover, taking  $\{D_i\} = \{A_{(\beta)}, A_N\}$  together with the interpolating formula (2.5) we obtain

$$\frac{\partial \xi_\alpha}{\partial s_\beta}(\xi) = \frac{\partial Y(\xi)}{\partial \xi_\alpha} \cdot A_{\langle \beta \rangle}(\xi) = \frac{\partial Y(\xi)}{\partial \xi_\alpha} \cdot T(\xi) e_\beta, \quad \alpha, \beta = 1, 2. \quad (2.7)$$

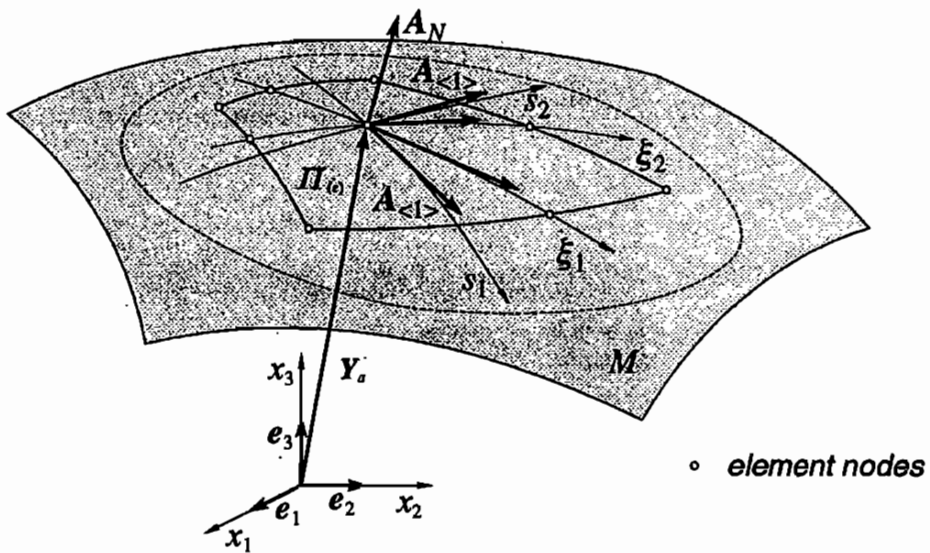
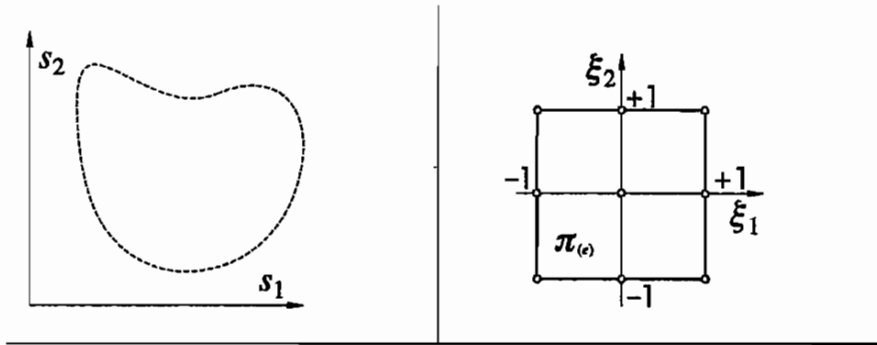


Fig. 7

Moreover, the area element is now given by

$$dA = ds_1 ds_2 = \alpha d\xi_1 d\xi_2, \quad \alpha(\xi) = \det \left( \frac{ds_\alpha}{d\xi_\beta} \right). \quad (2.8)$$

### 3. Displacement/rotation based shell elements

**3.1 Finite element discretization.** Our formulation of the finite elements starts with the displacement/rotation approach rigorously based on the weak formulation in the form of the principle of virtual displacements: find the displacement  $\mathbb{w} = (\mathbf{u}, \mathbf{Q}) \in \mathcal{U}_A$  such that (see Chapt. II.4)

$$G[\mathbb{w}; \mathbf{v}] \equiv G_{int}[\mathbb{w}; \mathbf{v}] + G_{ext}[\mathbb{w}; \mathbf{v}] = 0, \quad \forall \mathbf{v} = (\mathbf{v}, \mathbf{w}) \in \mathcal{V}_A. \quad (3.1)$$

The linearized version of the variational problem (3.1) is then formulated as in Chapt. II.5.

The construction of the finite element discretization is essentially equivalent to the determination of an approximating solution  $\mathbb{w}^h = (\mathbf{u}, \mathbf{Q}) \in \mathcal{U}_A^h$  in the finite dimensional subspace (precisely, submanifold)  $\mathcal{U}_A^h \subset \mathcal{U}_A$  of trial functions such that

$$G[\mathbb{w}^h; \mathbf{v}^h] \equiv G_{int}[\mathbb{w}^h; \mathbf{v}^h] + G_{ext}[\mathbb{w}^h; \mathbf{v}^h] = 0, \quad \forall \mathbf{v}^h = (\mathbf{v}^h, \mathbf{w}^h) \in \mathcal{V}_A^h, \quad (3.2)$$

where  $\mathcal{V}_A^h \subset \mathcal{V}_A$  denotes the finite dimensional subspace of test functions, and  $h$  is a characteristic parameter such that  $\mathbb{w}^h \rightarrow \mathbb{w}$  as  $h \rightarrow 0$  in a defined sense.

The basic idea underlying the finite element method crucially relies on the interpolation concept of constructing approximating functions. Assuming that the adopted interpolation scheme assures  $C^0$  continuity across inter-element boundaries the functional defined by (II.4.17), (II.4.18) and (II.5.2) can be written as sum over the finite element domains:

$$G[\mathbb{w}; \mathbf{v}] = \sum_{e \in N_e} G^{(e)}[\mathbb{w}; \mathbf{v}], \quad \delta G[\mathbb{w}; \mathbf{v}, \Delta \mathbf{v}] = \sum_{e \in N_e} \delta G^{(e)}[\mathbb{w}; \mathbf{v}, \Delta \mathbf{v}]. \quad (3.3)$$

Consequently, the linearized variational problem (II.5.11) takes the form

$$\sum_{e \in N_e} (\delta G^{(e)}[\mathbb{w}; \mathbf{v}, \Delta \mathbf{v}] + G^{(e)}[\mathbb{w}; \mathbf{v}]) = 0. \quad (3.4)$$

In this way we can restrict our considerations to a single typical finite element.

**3.2 Nodal degrees-of-freedom.** Given a parametrization of the rotation group, the tensor  $\mathbf{Q}$  is (locally) represented by three rotational parameters  $\mathfrak{d} = (\mathfrak{d}_1, \mathfrak{d}_2, \mathfrak{d}_3)$ ,

$Q = Q(\vartheta)$ , in the way described in Chapt. II.5. We then define the nodal parameters of a typical  $n$ -node finite element by

$$q_{(e)} = \begin{Bmatrix} q_1 \\ q_2 \\ \vdots \\ q_n \end{Bmatrix}, \quad q_a = \begin{Bmatrix} u_a \\ \vartheta_a \end{Bmatrix} = \begin{Bmatrix} u(\xi_a) \\ \vartheta(\xi_a) \end{Bmatrix}. \quad (3.5)$$

In the context of the finite element formulation, (3.5) will denote column vectors consisting of a consistent sequential arrangement of the (physical) components of the displacement vector and the rotation parameters, respectively.

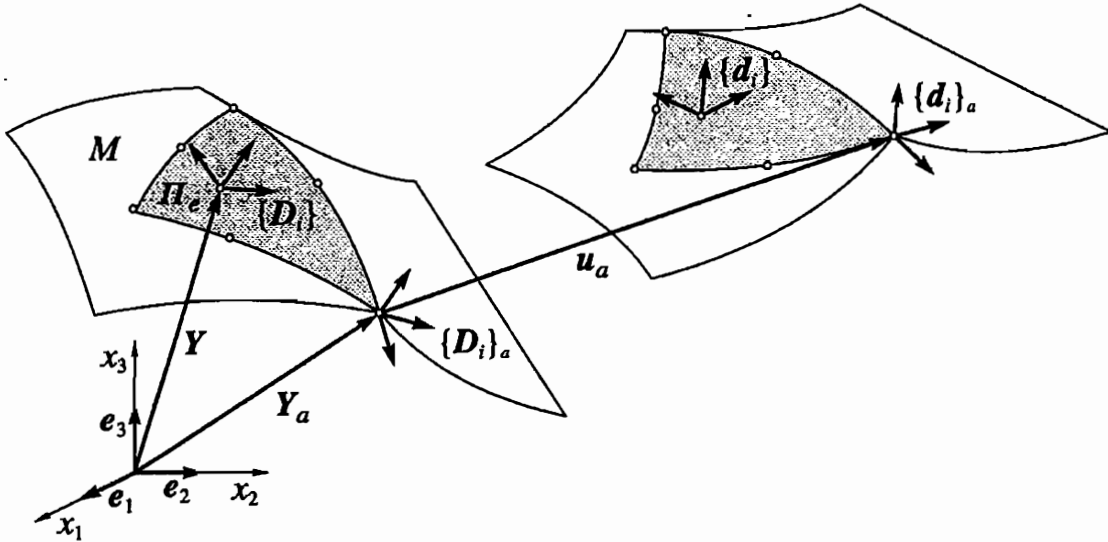


Fig. 8

Now the unknowns of the problem are interpolated from their nodal values. The displacements and rotations within the element are interpolated from the nodal parameters by

$$\begin{Bmatrix} u(\xi) \\ \vartheta(\xi) \end{Bmatrix} = \mathbb{L}(\xi) q_{(e)}, \quad (3.6)$$

where  $\mathbb{L}$  is the matrix consisting of the interpolating functions (the so-called shape functions). Then from (3.6) and the inverse relation for the chosen parametrization of the rotation group we calculate the interpolated rotation tensor  $Q(\xi) = Q(\vartheta(\xi))$ .

The resulting finite element has all six degrees of freedom at each node, three translations and three of rotational type. However, while the former have a clear geometric interpretation, the geometric interpretation of the latter depends on the specific choice of the parametrization of the rotation group. A convenient parametrization of rotations is obtained by introducing the finite rotation vector  $\psi$  such that  $Q = \exp \Psi$ , where  $\Psi = \text{ad } \psi$  denotes the skew-symmetric tensor whose axial vector is  $\psi$ . In this parametrization the nodal parameters consist of three components of  $u$  (translational variables) and three components of  $\psi$ .

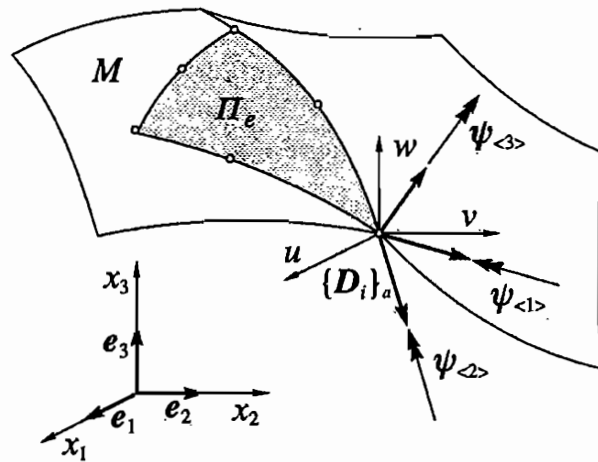


Fig. 9

The interpolation (3.6) is also used for the virtual displacements and virtual rotation parameters:

$$\begin{Bmatrix} \Delta v(\xi) \\ \Delta \vartheta(\xi) \end{Bmatrix} = \bar{\mathbb{L}}(\xi) \Delta q_{(e)}. \quad (3.7)$$

With the help of formula (II.6.5) the generalized virtual displacement is given by

$$\Delta v(\xi) = \begin{Bmatrix} \Delta v(\xi) \\ \Delta w(\xi) \end{Bmatrix} = \begin{bmatrix} \mathbf{1} & \mathbf{0} \\ \mathbf{0} & \Xi(\xi) \end{bmatrix} \begin{Bmatrix} \Delta v(\xi) \\ \Delta \vartheta(\xi) \end{Bmatrix}, \quad (3.8)$$

where the matrix  $\Xi(\xi)$  is a function of the rotational parameters  $\vartheta(\xi)$ , and it is calculated by using the interpolating formula (3.6). Substituting (3.7) into (3.8) we have

$$\Delta v(\xi) = \mathbb{L}(\xi) \Delta q_{(e)}, \quad \mathbb{L}(\xi) = \begin{bmatrix} \mathbf{1} & \mathbf{0} \\ \mathbf{0} & \Xi(\xi) \end{bmatrix} \bar{\mathbb{L}}(\xi). \quad (3.9)$$



Since the space of virtual rotations has the linear space structure the interpolation of virtual rotations may also be carried out directly. This can be treated as a special case of (3.9) by taking  $\mathbf{\Xi} = \mathbf{1}$  to be the identity matrix. Therefore we shall not consider this case separately. Moreover, it may be noted here that the nodal virtual rotations belong to different tangent spaces and in this sense such interpolation is not fully correct.

**3.3 Element matrices and vectors.** Substituting the interpolation formula (3.9) into the expression (II.5.3) we obtain

$$\delta G_{(e)} = \delta \mathbf{q}_{(e)}^T (\mathbb{K}_M^{(e)} + \mathbb{K}_G^{(e)}) \Delta \mathbf{q}_{(e)}, \quad (3.10)$$

where the material and the geometric element matrices are given by

$$\mathbb{K}_M^{(e)} = \iint_{\Pi(e)} (\mathbb{B}\mathbb{L})^T \mathbb{C}(\mathbb{B}\mathbb{L}) dA, \quad \mathbb{K}_G^{(e)} = \iint_{\Pi(e)} (\mathbb{D}\mathbb{L})^T \mathbb{G}(\mathbb{D}\mathbb{L}) dA. \quad (3.11)$$

In the case of configuration dependent loads the external forces lead also to a load matrix resulting from the linearization of the external virtual work expression. The distributed loads acting over the element are accommodated in the external virtual work (I.4.9)<sub>1</sub>, which for the single element with the use of the interpolation (3.9) yields

$$\delta G_{ext}^{(e)} = \delta \mathbf{q}_{(e)}^T \mathbb{K}_L^{(e)} \Delta \mathbf{q}_{(e)}, \quad \mathbb{K}_L^{(e)} = \iint_{\Pi(e)} \mathbb{L}^T \mathbb{F} \mathbb{L} dA, \quad (3.12)$$

where the so-called load matrix is given by

$$\mathbb{K}_L = \iint_{\Pi(e)} \mathbb{L}^T \mathbb{F} \mathbb{L} dA. \quad (3.13)$$

This matrix has to be computed for every specific type of configuration dependent loads.

The internal residual force vector is the discrete counterpart of the unbalanced force. From (II.4.18)<sub>1</sub> and (3.9) we have

$$\mathbf{G}_{int}^{(e)} = \delta \mathbf{q}_{(e)}^T \mathbb{R}_{(e)}, \quad \mathbb{R}_{(e)} = \iint_{\Pi(e)} (\mathbb{B}\mathbb{L})^T \tilde{\mathbf{s}}(\mathbf{w}) dA. \quad (3.14)$$

The concentrated external forces and couples acting on the shell have to be applied at nodal points and they are included directly in the global force vector.

It has to be noted here that these operators contain the derivatives of the shape functions with respect to the arc length parameters. Their effective evaluation is carried out using the transformation rule presented below.

**3.4 Lagrange elements.** According to the standard isoparametric concept the unknowns of the problem are interpolated from their nodal values in uncoupled form, in which case (3.7) takes the form

$$\begin{Bmatrix} \Delta v(\xi) \\ \Delta \vartheta(\xi) \end{Bmatrix} = \sum_{a=1}^n L_a(\xi) \begin{Bmatrix} \Delta v_a \\ \Delta \vartheta_a \end{Bmatrix} = \sum_{k=1}^n L_a(\xi) \Delta q_a, \quad (3.15)$$

and the interpolating matrix reads

$$\bar{\mathbb{L}}(\xi) = [\bar{\mathbb{L}}_1(\xi) \quad \bar{\mathbb{L}}_2(\xi) \quad \dots \quad \bar{\mathbb{L}}_n(\xi)], \quad \bar{\mathbb{L}}_a(\xi) = \begin{bmatrix} L_a(\xi) \mathbf{1} & \mathbf{0} \\ \mathbf{0} & L_a(\xi) \mathbf{1} \end{bmatrix}, \quad (3.16)$$

where  $L_a(\xi)$  are the standard Lagrange interpolating polynomials. In this case the discrete operators are obtained in the form

$$\begin{aligned} \mathbb{B}(\xi) &= [\mathbb{B}_1(\xi) \quad \mathbb{B}_2(\xi) \quad \dots \quad \mathbb{B}_n(\xi)], \\ \mathbb{D}(\xi) &= [\mathbb{D}_1(\xi) \quad \mathbb{D}_2(\xi) \quad \dots \quad \mathbb{D}_n(\xi)]. \end{aligned} \quad (3.17)$$

Substituting now (3.17) into (3.11) the element matrices and vectors take the form

$$\mathbb{K}_M = \begin{bmatrix} \mathbb{k}_{11}^M & \dots & \mathbb{k}_{1n}^M \\ \vdots & \ddots & \vdots \\ \mathbb{k}_{n1}^M & \dots & \mathbb{k}_{nn}^M \end{bmatrix}, \quad \mathbb{K}_G = \begin{bmatrix} \mathbb{k}_{11}^G & \dots & \mathbb{k}_{1n}^G \\ \vdots & \ddots & \vdots \\ \mathbb{k}_{n1}^G & \dots & \mathbb{k}_{nn}^G \end{bmatrix}, \quad \mathbb{R} = \begin{Bmatrix} \mathbb{R}_1 \\ \vdots \\ \mathbb{R}_n \end{Bmatrix}, \quad (3.18)$$

where

$$\mathbb{k}_{ab}^M = \iint_{\Pi(e)} \mathbb{B}_a^T \mathbb{C} \mathbb{B}_b \, dA, \quad \mathbb{k}_{ab}^G = \iint_{\Pi(e)} \mathbb{D}_a^T \mathbb{G} \mathbb{D}_b \, dA. \quad (3.19)$$

**3.5 Numerical integration.** In the evaluation of element matrices we need to compute integrals of the form

$$\mathbb{K} = \iint_{\Pi(e)} \mathbb{k}(\xi) \, dA = \iint_{\pi(e)} \mathbb{k}(\xi) \alpha(\xi) \, d\xi_1 d\xi_2, \quad \xi \equiv (\xi_1, \xi_2), \quad (3.20)$$

where  $\alpha$  is defined by (2.8). In practice, this is carried out applying some numerical integration method of the form

$$\mathbb{K} = \sum_{k=1}^p w_p \mathbb{K}(\xi_p), \quad \xi_p \equiv (\xi_1, \xi_2). \quad (3.21)$$

The most common choice, and the most efficient one, is the Gauss-Legendre quadrature, which is known for its high accuracy and the ease, with which it can be implemented in computer codes.

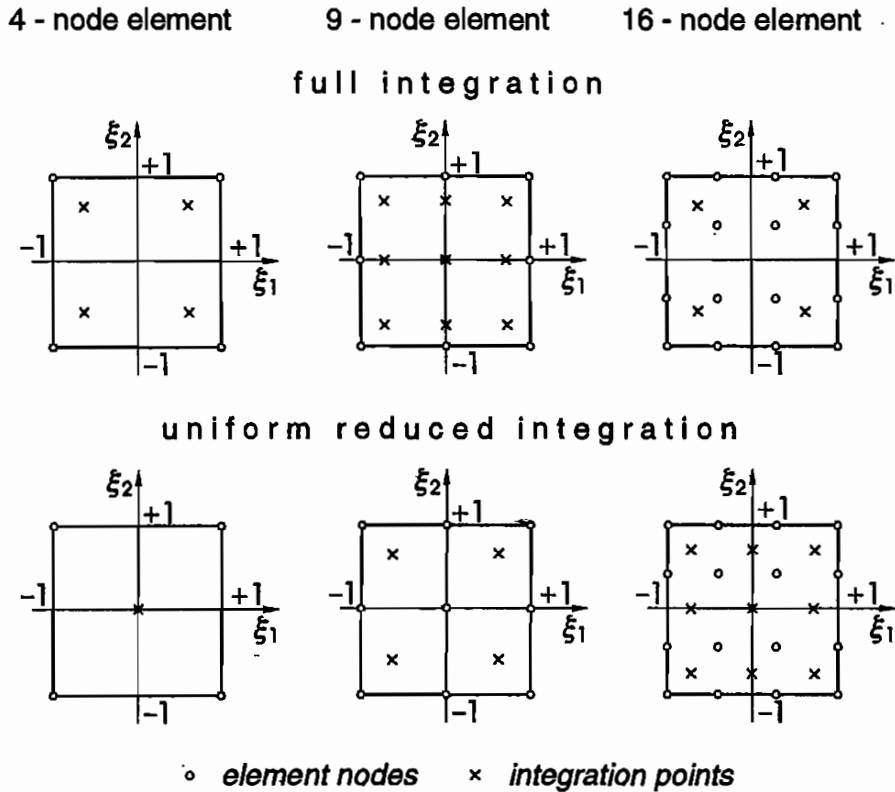


Fig. 10

In the practice of numerical integration, to evaluate element matrices and vectors two questions arise: which kind of integration scheme to use and which order to select. From the point of view of the cost of the analysis the Gauss-Legendre quadrature is very efficient and commonly used. For the element matrices and the vectors to be integrated without error the order of the numerical integration must be high enough, because it influences the solutions. Numerical experimentations show that in the case of a Lagrange family of elements the required order of numerical integration is  $n$  for the one-dimensional element  $n$ -node. Correspondingly, the required order of the numerical integration is  $n \times n$  for the two-dimensional  $(n \times n)$ -node quadrilateral elements. In the finite element literature this is known as full integration scheme.

**3.6 Locking effect.** The simplicity and the clarity of the displacement/rotation based formulations together with the use of standard Lagrange interpolation are the main features of this class of shell elements. They also exhibit a reliable performance in the analysis of moderately thick shells. However, the following difficulties are encountered:

- 1) The finite element solutions appear to be far more sensitive to the shell thickness than the true solutions and they may grossly underestimate the displacements of the shell. As a result the performance of this class of elements degenerates rapidly in the thin shell limit. This became known as locking effect.
- 2) Inextensional or nearly inextensional deformations may be poorly represented by these elements.
- 3) The accuracy of the membrane and transverse shear stress resultants evaluated at nodes of these elements is generally low.

These shortcomings are particularly severe for lower order elements (e.g. the standard four node quadrilateral element) and they diminish substantially for higher order elements (e.g. the sixteen node quadrilateral element).

The third difficulty can, to some extent, be circumvented by calculating stress resultants at the quadrature points rather than at the nodal points. This is the usual practice, but the problem remains and it is particularly severe in the analysis of elastic-plastic shells.

Of the three difficulties the locking effect is the major obstacle with the use of the displacement/rotation based Lagrange elements. The root of this effect is well recognized. Thin shells derive their characteristic behavior from the intricate interaction between the membrane action and the relatively small shear and bending stiffness. Hence, for shell elements even in the linear case it is difficult to ensure that the bending deformation is not accompanied by spurious membrane and shear deformation. There is a voluminous literature devoted to the locking phenomenon. Nevertheless, the problem still misses a complete understanding. A common viewpoint is that the locking effect arises because of the inability of elements to achieve a deformed state, in which the transverse shear and membrane strains vanish throughout the element. The consequences of this shortcoming are severe, particularly in the thin shell limit, when small membrane or shear strains will cause the membrane or shear energy to overshadow the bending energy.

Various techniques were proposed to remove the locking effect of the standard displacement/rotation based elements. The most simple one is known as the uniform reduced integration (URI) technique, which relies on the underintegration of the element matrices. Unfortunately, it is accompanied by spurious solutions (zero energy modes), which can be reduced by a stabilization procedure. A more reliable approach to the locking problem is based on a modified variational formulation.

**3.7 Stabilization procedures.** The reduced integration concept is commonly adopted in the one-dimensional case (plane or spatial rod finite elements). In the two-dimensional case, however, it was recognized that the reduced integration rule may lead to mesh instability often known as hourglassing. This phenomenon is associated with spurious zero-energy modes and, in the static case, it may lead for certain boundary conditions to singularities of the global stiffness matrix. Various techniques have been devised to alleviate singularities associated with the spurious zero energy modes in the case of the reduced integration rule. Unfortunately, the proposed procedures appear to be of more heuristic type, or they are just numerical tricks than fully mathematically sound.

The basic motivation of the stabilization procedures is to take advantage of the rapid convergence of the underintegrated elements. The stabilization approach consists of starting with an underintegrated element and then adding additional stiffnesses so that the spurious singular modes are suppressed.

Most of these techniques are based on the representation of the tangent stiffness matrix (in the same way the residual force vector) as a sum

$$\mathbb{K} = \mathbb{K}^{URI} + \gamma \mathbb{K}^S, \quad (3.22)$$

where  $\mathbb{K}^{URI}$  denotes the underintegrated matrix (evaluated by applying the reduced integration scheme),  $\mathbb{K}^S$  is the so-called stabilization matrix, and  $\gamma$  is the so-called perturbation coefficient (typically,  $\gamma = 10^6$ ). In our developed elements, the stabilization matrix  $\mathbb{K}^S$  has been constructed following the approach presented in our earlier papers.

**3.8 Family of CAM elements.** Our formulation is not restricted to a special class of elements and this is one of its basic feature. Different types of elements are specified by the geometry of the domain (quadrilaterals or triangles), the number of nodes and the location of the nodes. The corresponding shape functions are

constructed by the interpolation method. The Lagrange family of 4-, 9- and 16-node displacement/rotation based elements formulated in a standard way will be included in the numerical analysis presented in the following chapters.

## 4. Stress resultant mixed shell elements

**4.1 Remarks on mixed shell models.** Mixed methods can be formulated directly from the local differential equations using a weighted residual approach or, equivalently, using a variational based approach. Various multi-field functionals can be constructed by regarding, besides displacements and rotations  $\mathbb{w} = (\mathbf{u}, \mathbf{Q})$ , the strains  $\boldsymbol{\varepsilon} = (\mathbf{E}, \mathbf{K})$  or the stresses  $\mathbf{s} = (\mathbf{N}, \mathbf{M})$  or both as additional independent variables, and by introducing the corresponding relations into the functional of total potential energy through Lagrange multipliers. Thus the principle of stationary total potential energy provides the starting point for the formulation of mixed variational principles.

**4.2 Principle of stationary total potential energy.** Let us assume that the external loads acting on the shell are conservative, i.e. that there exists a functional  $V : \mathcal{U} \rightarrow \mathbb{R}$  such that

$$\delta V[\mathbb{w}; \mathbf{v}] = -G_{ext}[\mathbb{w}; \mathbf{v}]. \quad (4.1)$$

If in addition the shell is hyperelastic with the strain energy function

$$\Phi(\boldsymbol{\varepsilon}) = \Phi(\mathbf{E}, \mathbf{K}) = \Phi(\boldsymbol{\varepsilon}_\alpha, \boldsymbol{\kappa}_\alpha), \quad (4.2)$$

then the constitutive relation is given by

$$\mathbf{s} = \begin{Bmatrix} \mathbf{n}^\beta \\ \mathbf{m}^\beta \end{Bmatrix} = \partial_{\boldsymbol{\varepsilon}} \Phi(\boldsymbol{\varepsilon}) = \begin{Bmatrix} \frac{\partial \Phi(\boldsymbol{\varepsilon}_\alpha, \boldsymbol{\kappa}_\alpha)}{\partial \boldsymbol{\varepsilon}_\beta} \\ \frac{\partial \Phi(\boldsymbol{\varepsilon}_\alpha, \boldsymbol{\kappa}_\alpha)}{\partial \boldsymbol{\kappa}_\beta} \end{Bmatrix}. \quad (4.3)$$

The functional of total potential energy  $J : \mathcal{U} \rightarrow \mathbb{R}$  having the displacement  $\mathbb{w} \in \mathcal{U}$  as the only independent variable is defined by

$$J(\mathbb{w}) = \iint_M \Phi(\boldsymbol{\varepsilon}(\mathbb{w})) dA + V(\mathbb{w}). \quad (4.4)$$

The first differential of (4.2) takes exactly the form (3.1) for every kinematical admissible displacement field

$$\delta J[\mathbb{u}; \mathbb{v}] = G[\mathbb{u}; \mathbb{v}] = 0. \quad (4.5)$$

In this form it asserts that among all kinematically admissible displacement fields only those make the functional  $J(\mathbb{u})$  stationary, which satisfy the equilibrium equations and the static boundary conditions. The functional of total potential energy (4.2) is defined on the space of kinematically admissible displacement fields. The strains  $\mathfrak{e}$  and the stresses  $\mathfrak{s}$  are derived quantities through the strain-displacement relations and the constitutive equations.

**4.2 Two-field variational principle.** In the case of linear elastic shells, the usual constitutive restrictions ensure that the constitutive matrix is invertible, which enables one to express the constitutive relation in the inverse form. In general, let us assume that the constitutive relations  $\mathfrak{s} = \tilde{\mathfrak{s}}(\mathfrak{e})$  can be inverted locally to give

$$\mathfrak{e} \equiv \begin{Bmatrix} \mathbf{E} \\ \mathbf{K} \end{Bmatrix} = \tilde{\mathfrak{e}}(\mathfrak{s}) = \begin{Bmatrix} \tilde{\mathbf{E}}(N, M) \\ \tilde{\mathbf{K}}(N, M) \end{Bmatrix}. \quad (4.6)$$

Then through the Legendre transformation we can define the complementary energy density by

$$\begin{aligned} \Psi(\mathfrak{s}) &= \mathfrak{s}^T \mathfrak{e}(\mathfrak{s}) - \Phi(\mathfrak{e}(\mathfrak{s})) \\ &= \mathbf{N} \cdot \mathbf{E}(N, M) + \mathbf{M} \cdot \mathbf{K}(N, M) - \Phi(\mathbf{E}(N, M), \mathbf{K}(N, M)). \end{aligned} \quad (4.7)$$

Upon introducing (4.7) into the functional of total potential energy (4.4) with the use of the strain-displacement relations we obtain a new functional with  $\mathbb{u} = (\mathbf{u}, \mathbf{Q})$  and  $\mathfrak{s} = (N, M)$  as the independent fields

$$\begin{aligned} H(\mathbb{u}, \mathfrak{s}) &= \iint_{M \cup \Gamma} (\mathfrak{s}^T \hat{\mathfrak{e}}(\mathbb{u}) - \Psi(\mathfrak{s})) dA + V(\mathbb{u}) \\ &= \iint_{M \cup \Gamma} (\mathbf{N} \cdot \mathbf{E}(\mathbb{u}) + \mathbf{M} \cdot \mathbf{K}(\mathbb{u}) - \Psi(N, M)) dA + V(\mathbb{u}). \end{aligned} \quad (4.8)$$

The first differential of this functional is given by

$$\delta H[\mathbb{u}, \mathfrak{s}; \mathbb{v}, \delta \mathfrak{s}] = \iint_{M \cup \Gamma} (\mathfrak{s}^T (\mathbb{B}\mathbb{v}) + \delta \mathfrak{s}^T (\hat{\mathfrak{e}}(\mathbb{u}) - \partial_{\mathfrak{s}} \Psi)) dA + \delta V[\mathbb{u}; \mathbb{v}], \quad (4.9)$$

where

$$\begin{aligned} \mathfrak{s}^T (\mathbb{B}\mathbb{v}) &= \mathbf{N} \cdot \delta \mathbf{E}[\mathbb{u}; \mathbb{v}] + \mathbf{M} \cdot \delta \mathbf{K}[\mathbb{u}; \mathbb{v}], \\ \delta \mathfrak{s}^T (\hat{\mathfrak{e}}(\mathbb{u}) - \partial_{\mathfrak{s}} \Psi) &= \delta \mathbf{N} \cdot (\mathbf{E}(\mathbb{u}) - \partial_{\mathbf{E}} \Psi) + \delta \mathbf{M} \cdot (\mathbf{K}(\mathbb{u}) - \partial_{\mathbf{K}} \Psi). \end{aligned} \quad (4.10)$$

Since  $\mathbb{v}$  and  $\mathfrak{s}$  are independent fields we find that

$$\delta H[\mathbb{w}, \mathbf{s}; \mathbf{v}, \Delta \mathbf{s}] = 0, \quad (4.11)$$

for all kinematically admissible virtual displacements  $\mathbf{v}$  and arbitrary  $\delta \mathbf{s}$  if and only if the equilibrium equations, the constitutive equations and the static boundary conditions are satisfied. These are the Euler equations of the Hellinger-Reissner type variational principle (4.11), which provides the basis to formulate mixed finite elements. It should be noted that  $\mathbb{w}$  must be kinematically admissible, while  $\mathbf{s}$  is subject to no constraints except to be smooth enough for the integral in (4.8) to exist. Thus  $\mathbf{s}$  may be piecewise continuous.

**4.3 Linearized equation.** As within the displacement/rotation based formulation, the solution of the nonlinear problem defined above is achieved through an iterative procedure based on a successive linearization of the functional (4.8). The corresponding linearized equation takes the form

$$\delta^2 H[\mathbb{w}, \mathbf{s}; \mathbf{v}, \delta \mathbf{s}, \Delta \mathbf{v}, \Delta \mathbf{s}] + \delta H[\mathbb{w}, \mathbf{s}; \mathbf{v}, \delta \mathbf{s}] = 0, \quad (4.12)$$

where the first differential is given by (4.9). To obtain the second differential of the functional (4.8) we need to compute the first differential of (4.9). We proceed here like in the case of the displacement/rotation formulation

$$\delta^2 H = \iint_{M_V} (\Delta \mathbf{v}^T \mathbb{G} \mathbf{v} + \Delta \mathbf{s}^T (\mathbb{B} \mathbf{v}) + \delta \mathbf{s}^T \mathbb{B} \Delta \mathbf{v} - \delta \mathbf{s}^T \mathbb{H} \Delta \mathbf{s}) dA + \delta^2 V, \quad (4.13)$$

where the operators  $\mathbb{B}$  and  $\mathbb{G}$  are given in the same form as for the displacement/rotation formulation, and the matrix

$$\mathbb{H}(\mathbf{s}) = \frac{\partial^2 \Psi(\mathbf{s})}{\partial^2 \mathbf{s}} = \begin{bmatrix} \frac{\partial^2 \Psi(\mathbf{s})}{\partial n^\alpha \partial n^\beta} & \frac{\partial^2 \Psi(\mathbf{s})}{\partial n^\alpha \partial m^\beta} \\ \frac{\partial^2 \Psi(\mathbf{s})}{\partial m^\alpha \partial n^\beta} & \frac{\partial^2 \Psi(\mathbf{s})}{\partial m^\alpha \partial m^\beta} \end{bmatrix} \quad (4.14)$$

contains second derivatives of the complementary energy density with respect to the generalized stresses. This matrix is just the inverse of the elasticity matrix:

$$\mathbb{H}(\mathbf{s})^{-1} = \mathbb{C}(\tilde{\boldsymbol{\varepsilon}}(\mathbf{s})). \quad (4.15)$$

The second differential of the potential of external loads is just the first differential of the external virtual work expression,

$$\delta^2 V[\mathbb{w}, \Delta \mathbf{v}, \mathbf{v}] = -\delta G_{ext}[\mathbb{w}, \Delta \mathbf{v}, \mathbf{v}], \quad (4.16)$$



which is given by (II.4.18).

**4.5 Finite element approximations.** According to the standard finite element procedure, the shell reference surface  $M$  is represented as the union  $M = \bigcup_{e \in N_e} \Pi_{(e)}$  of subdomains  $\Pi_{(e)}$  (finite elements). Then the unknowns of the problem are interpolated from their nodal values. The interpolation assures the  $C^0$  continuity enabling to express the functional (4.8) in the form

$$H(\mathbb{U}, \mathfrak{s}) = \sum_{e \in N_e} H^{(e)}(\mathbb{U}, \mathfrak{s}). \quad (4.17)$$

The linearized variational problem takes the form

$$\sum_{e \in N_e} (\delta^2 H^{(e)}[\mathbb{U}, \mathfrak{s}; \mathbf{v}, \delta \mathfrak{s}, \Delta \mathbf{v}, \Delta \mathfrak{s}] + \delta H^{(e)}[\mathbb{U}, \mathfrak{s}; \mathbf{v}, \delta \mathfrak{s}]) = 0. \quad (4.18)$$

The kinematical variables are interpolated within the finite element in the same way as in the case of Lagrange elements.

The stress vector consists of the six components of the stress resultant vectors and the six components of the stress couple vectors. In the finite element approximation, the stress  $\mathfrak{s}$  within an element is interpolated in terms of stress parameters as

$$\mathfrak{s}(\xi) = \mathbb{P}(\xi) \mathfrak{s}. \quad (4.19)$$

Substituting (4.19) and (3.9) into the linearized form of the mixed functional we obtain

$$\begin{aligned} \delta^2 H^{(e)} &= \Delta \mathbf{q}^T \mathbb{K}_G \delta \mathbf{q} + \Delta \mathfrak{s}^T \mathbb{K}_G \delta \mathbf{q} \\ &\quad + \Delta \mathbf{v}^T \mathbb{K}_m^T \delta \mathfrak{s} - \Delta \mathfrak{s}^T \mathbb{K}_H \delta \mathfrak{s} + \delta^2 V, \end{aligned} \quad (4.20)$$

where the matrices  $\mathbb{K}_m$  and  $\mathbb{K}_H$  are defined by

$$\mathbb{K}_m = \iint_{\Pi_{(e)}} \mathbb{P}^T (\mathbb{B} \mathbb{L}) dA, \quad \mathbb{K}_H = \iint_{\Pi_{(e)}} \mathbb{P}^T \mathbb{H} \mathbb{P} dA, \quad (4.21)$$

and the matrix  $\mathbb{K}_G$  is given in the same form as for the displacement/rotation formulation. In the same manner we obtain

$$\delta H^{(e)} = \delta \mathbf{q}^T \mathbb{R}_d + \delta \mathfrak{s}^T \mathbb{R}_m + \delta V, \quad (4.22)$$

where

$$\mathbb{R}_d = \iint_{\Pi(e)} \mathbf{s}^T (\mathbb{B}\mathbb{L}) dA, \quad \mathbb{R}_m = \iint_{\Pi(e)} \mathbb{P}^T (\mathbf{e}(\mathbf{u}) - \partial_s \Psi(\mathbf{s})) dA. \quad (4.23)$$

Taking further into account (3.14) the linearized equation for the single element reads

$$\begin{aligned} 0 = \delta \mathbf{q}^T & ((\mathbb{K}_G - \mathbb{K}_L) \Delta \mathbf{q} - \mathbb{R}_m) \\ & + \delta \mathbf{s}^T ((\mathbb{K}_m + \mathbb{K}_m^T) \Delta \mathbf{q} - \mathbb{K}_H \Delta \mathbf{s} - \mathbb{R}_m), \end{aligned} \quad (4.24)$$

so that the resulting system of equations takes the form

$$\begin{aligned} (\mathbb{K}_G - \mathbb{K}_L) \Delta \mathbf{q} + \mathbb{K}_m \Delta \mathbf{s} &= \mathbb{R}_d, \\ \mathbb{K}_m^T \Delta \mathbf{q} - \mathbb{K}_H \Delta \mathbf{s} &= \mathbb{R}_m. \end{aligned} \quad (4.25)$$

Since the stresses are required to be only piecewise continuous, they are interpolated locally within an element and subsequently condensed at the element level:

$$\Delta \mathbf{s} = -\mathbb{K}_H^{-1} \mathbb{K}_m^T \Delta \mathbf{q} + \mathbb{R}_m, \quad (4.26)$$

so that

$$(\mathbb{K}_G - \mathbb{K}_L - \mathbb{K}_m \mathbb{K}_H^{-1} \mathbb{K}_m^T) \Delta \mathbf{q} = \mathbb{R}_d - \mathbb{K} \mathbb{R}_m. \quad (4.27)$$

In effect, the derivation of the element stiffness matrix requires an inversion of the flexibility matrix  $\mathbb{K}_H$  being the main disadvantage of the mixed formulation. From this point of view more effective finite element approximations can be constructed on the basis of a variational principle considered in the following section. Let us further note that since the stress parameters are eliminated at the element level, the resulting shell finite elements have the same nodal degrees-of-freedom as the displacement/rotation based elements.

**4.4 MIX elements.** The crucial point of the mixed formulation concerns the judicious selection of shape functions in the stress approximation, i.e. entries in the matrix  $\mathbb{P}$ .<sup>1</sup> Adhering to the guidelines set forth in the literature, we have developed 4-node and 9-node elements constructed by using a stress based mixed formulation with the stress resultants  $\mathfrak{m} = (\mathbf{n}^1, \mathbf{n}^2)$  and the stress couples  $\mathfrak{m} = (\mathbf{m}^1, \mathbf{m}^2)$  besides  $\mathbf{u} = (\mathbf{u}, \mathbf{Q})$  as the independent variables.<sup>2</sup> Moreover,  $\mathfrak{m}$  and  $\mathfrak{m}$

<sup>1</sup> See, e.g., PIAN AND SUMIHARA [1984], PIAN AND WU [1988], SALEEB, CHANG, GRAF, AND YINGYBUNYONG [1989].

<sup>2</sup> CHRÓŚCIBIEWSKI [1995].

are interpolated independently within the typical element. Thus the formula (4.19) read

$$\mathfrak{s}(\xi) = \begin{Bmatrix} \mathfrak{m}(\xi) \\ \mathfrak{mm}(\xi) \end{Bmatrix} = \begin{bmatrix} \mathbb{P}(\xi) & 0 \\ 0 & \mathbb{P}(\xi) \end{bmatrix} \begin{Bmatrix} \mathfrak{m}_{(e)} \\ \mathfrak{mm}_{(e)} \end{Bmatrix} = \mathbb{P}(\xi) \mathfrak{s}_{(e)}. \quad (4.28)$$

## 5. Stress resultant semi-mixed shell elements

**5.1 General remarks.** The mixed finite element models considered in the previous chapter have been based on the two-field variational principle having the generalized displacement  $\mathfrak{w} = (\mathbf{u}, \mathbf{Q})$  and the generalized stress  $\mathfrak{s} = (\mathbf{N}, \mathbf{M})$  as the independent field variables. Within the finite element method these fields are independently interpolated in terms of generalized nodal displacements  $\mathfrak{q}_{(e)}$  and stress parameters  $\mathfrak{s}_{(e)}$ , respectively. Since the underlying variational principle does not require continuity of the stress field  $\mathfrak{s} = (\mathbf{N}, \mathbf{M})$  at interelement boundaries, the stress parameters  $\mathfrak{s}_{(e)}$  are eliminated on the element level.

**5.2 Modified two-field variational principle.** Within the considered shell theory the space of stresses can be expressed as the direct sum of the space of the stress resultants  $\mathfrak{m}$  and of the space of the stress couples  $\mathfrak{mm}$ . Analogously, we can represent the space of strains as the direct sum of the space of the stretching  $\mathfrak{e}$  and of the space of the bending strains  $\mathfrak{k}$ . In matrix-operator description we can simply write

$$\mathfrak{s} = \begin{Bmatrix} \mathfrak{m} \\ \mathfrak{mm} \end{Bmatrix} = \begin{Bmatrix} \mathbf{n}^1 \\ \mathbf{n}^2 \\ \mathbf{m}^1 \\ \mathbf{m}^2 \end{Bmatrix}, \quad \mathfrak{e} = \begin{Bmatrix} \mathfrak{e} \\ \mathfrak{k} \end{Bmatrix} = \begin{Bmatrix} \boldsymbol{\varepsilon}_1 \\ \boldsymbol{\varepsilon}_2 \\ \boldsymbol{\kappa}_1 \\ \boldsymbol{\kappa}_2 \end{Bmatrix}. \quad (5.1)$$

Corresponding to this splitting we write the constitutive relations in an extended form

$$\mathfrak{s}(\mathfrak{e}, \mathfrak{k}) = \begin{Bmatrix} \mathfrak{m}(\mathfrak{e}, \mathfrak{k}) \\ \mathfrak{mm}(\mathfrak{e}, \mathfrak{k}) \end{Bmatrix} = \begin{Bmatrix} \partial_{\mathfrak{e}} \Phi(\mathfrak{e}, \mathfrak{k}) \\ \partial_{\mathfrak{k}} \Phi(\mathfrak{e}, \mathfrak{k}) \end{Bmatrix}. \quad (5.2)$$

We assume now that the first of the constitutive relations (5.2) can be partially inverted to express the stretching vector in terms of the stress vector and bending vector

$$\mathbf{e} = \mathbf{e}(\mathbf{m}, \mathbf{k}). \quad (5.3)$$

We may then define the mixed energy function through the Legendre transformation

$$\begin{aligned} \Sigma(\mathbf{N}, \mathbf{K}) &= \mathbf{m}^T \boldsymbol{\varepsilon}(\mathbf{e}, \mathbf{k}) - \Phi(\boldsymbol{\varepsilon}(\mathbf{e}, \mathbf{k}), \mathbf{k}) \\ &= \mathbf{N} \cdot \mathbf{E}(\mathbf{N}, \mathbf{K}) - \Phi(\mathbf{E}(\mathbf{N}, \mathbf{K}), \mathbf{K}). \end{aligned} \quad (5.4)$$

With the help of (5.4) and the strain-displacement relations we define a new functional with  $\mathbf{w}$  and  $\mathbf{m}$  as independent variables

$$\begin{aligned} H(\mathbf{w}, \mathbf{m}) &= \iint_{M \cup \Gamma} (\mathbf{m}^T \boldsymbol{\varepsilon}(\mathbf{w}) - \Sigma(\mathbf{m}, \mathbf{k}(\mathbf{w}))) dA + V(\mathbf{w}) \\ &= \iint_{M \cup \Gamma} (\mathbf{N} \cdot \mathbf{E}(\mathbf{w}) - \Psi(\mathbf{N}, \mathbf{K}(\mathbf{w}))) dA + V(\mathbf{w}). \end{aligned} \quad (5.5)$$

We thus arrive at a variational principle

$$H[\mathbf{w}, \mathbf{m}; \mathbf{v}, \delta \mathbf{m}] = 0, \quad (5.6)$$

for all kinematically admissible virtual displacements  $\mathbf{v} \in \mathcal{V}_A$  and arbitrary virtual stress resultants  $\delta \mathbf{m}$ .

**5.2 Semi-mixed shell elements.** The formulation of the shell finite elements on the basis of the principle (5.6) follows exactly in the same way as the mixed elements with the flexibility matrix  $\mathbb{K}_H$  being of twice order lower. This essentially reduces the time of computation.

We have developed 4-node and 9-node elements designated by SEMe4 and SEMe9, respectively. In all examined problems, a very good coincidence between the solutions obtained with the use of MIX and SEM elements was observed. Of these two families SEM elements are simpler and may be regarded as more suitable for engineering computations.

## 6. Assumed strain shell elements

**6.1 Preliminary remarks.** There exist also finite element formulations, which are mainly based on some technical constructions not necessarily having underlying variational formulation of the problem. Among such formulations the assumed strain techniques, discrete Kirchhoff constraints, natural mode techniques or penalty-parameter modifications are the most often used ones. The finite elements formulated within such techniques are less reliable (from the mathematical point of view), although they can provide a sound solution for many engineering problems.

The natural mode method is based on the decomposition of the shell element deformation into rigid-body and pure strain modes.<sup>1</sup> Using this decomposition, which substantially simplifies the formulation, a number of simple shell finite elements, including transverse shear deformation, has been developed and successfully applied to linear and nonlinear problems.

The so-called assumed strain methods are currently regarded as a most promising way to overcome both locking effects and zero-energy modes. While these methods in one-dimension (plane and spatial rods) is remarkably straightforward, the extension to two-dimensions (plates and shells) appears to be challenging and cannot be considered as completely resolved and mathematically justified. It should be also noted that the assumed strain methods encompass a variety of finite element procedures, quite often developed on some technical constructions without formal mathematical justifications.<sup>2</sup>

**6.2 Basic concepts.** Generally, the starting point of the assumed strain technique is based on the classical displacement (in our case displacement/rotation) formulation together with an application of the standard Lagrange interpolations as described in Chapt. III.3. As it is known, the major difficulty within this formulation is due to locking effect, whenever the full integration rule is applied to evaluate the element matrices. By numerical experimentation it has been found that the locking effect can be substantially reduced or even completely eliminated through an independent interpolation of the strain field  $\varepsilon(\xi)$  within an element in

---

<sup>1</sup> See ARGYRIS AND SCHARPF [1971], ARGYRIS AND TENEK [1994] and the references cited therein.

<sup>2</sup> See SIMO AND HUGHES [1986], SIMO AND RIFAI [1990], SIMO AND ARMERO [1992].

terms of the undetermined strain parameters. This interpolation can be written in the form

$$\boldsymbol{\varepsilon}(\boldsymbol{\xi}) = \mathbb{E}(\boldsymbol{\xi})\boldsymbol{\varepsilon}_{(e)}, \quad (6.1)$$

where  $\boldsymbol{\varepsilon}_{(e)}$  denotes a vector of undetermined strain parameters and  $\mathbb{E}(\boldsymbol{\xi})$  is an interpolation matrix. In the analysis of nonlinear problems the same scheme is applied for the incremental (virtual) strains

$$\Delta\boldsymbol{\varepsilon}(\boldsymbol{\xi}) = \mathbb{E}(\boldsymbol{\xi})\Delta\boldsymbol{\varepsilon}_{(e)}, \quad (6.2)$$

what directly leads to the discrete differential operator given in the form

$$\overline{\mathbb{B}}_{(e)} = \mathbb{B}\mathbb{E}(\boldsymbol{\xi}). \quad (6.3)$$

Here we use the overbar for the discrete operator in order to distinguish it from the operator  $\mathbb{B}_{(e)}$ , which is computed in the classical way (Chapt. III.3). The whole subsequent formulation of element matrices and vectors proceeds exactly in the same way as within the standard displacement (displacement/rotation) based formulation with the discrete operator  $\mathbb{B}_{(e)}$  replaced by the operator (6.3). Of course, in this case element matrices and vectors are evaluated applying the full integration rule.

Then it becomes clear that the choice of strain parameters  $\boldsymbol{\varepsilon}_{(e)}$  and of an interpolating matrix  $\mathbb{E}(\boldsymbol{\xi})$  are the crucial points of the whole concept. There is also a little help which could be taken as a guideline in their choice, since the concept is lacking a firm mathematical foundation.

In the existing literature on the subject, strain parameters  $\boldsymbol{\varepsilon}_{(e)}$  are usually defined as the values of the strain field  $\boldsymbol{\varepsilon}(\boldsymbol{\xi})$  computed within an element from the standard displacement interpolation scheme at selected points. Such points are called sampling points, and they are specified by the values of the natural coordinates  $\boldsymbol{\xi} = (\xi_1, \xi_2) \in [-1, +1] \times [-1, +1]$ . Let us denote by

$$\boldsymbol{\xi}_{(i,j)} = (\xi_{1(i)}, \xi_{2(j)}) \in [-1, +1] \times [-1, +1], \quad i = 1, 2, \dots, L_1, \quad j = 1, 2, \dots, L_2, \quad (6.4)$$

the natural coordinates of the sampling points. Then the vector  $\boldsymbol{\varepsilon}_{(e)}$  is defined as suitable arrangement of the strain values calculated according to

$$\Delta\boldsymbol{\varepsilon}_{(i,j)} = \Delta\boldsymbol{\varepsilon}(\boldsymbol{\xi}_{(i,j)}) = \mathbb{B}(\boldsymbol{\xi}_{(i,j)})\Delta\boldsymbol{q}_{(e)}, \quad (6.5)$$

where  $\mathbb{B}(\xi)$  denotes the discrete operator calculated as in the standard displacement/rotation based formulation. The remaining steps proceed in the way outlined above.

Since the strain parameters  $\epsilon_{(e)}$  are eliminated at the element level, the resulting shell finite elements have the same nodal degrees-of-freedom as the displacement/rotation based elements.

**6.2 Assumed strain technique adopted in this work.** Within the considered shell theory the generalized strains consist of the stretching strains  $\epsilon(\xi)$  and the bending strains  $\kappa(\xi)$ . Since the locking effect is due to  $\epsilon(\xi)$  only, there is no need to apply the assumed strain technique to the bending strains. Thus the most general case we shall consider here is based on the following interpolation of the stretching strains

$$\begin{aligned}\epsilon_1(\xi) &= \sum_{i=1}^m \sum_{j=1}^{m_2} L_i^{(1)}(\xi_1) L_j^{(2)}(\xi_2) \bar{\epsilon}_{1(i,j)}, \\ \epsilon_2(\xi) &= \sum_{i=1}^{m_2} \sum_{j=1}^m L_i^{(2)}(\xi_2) L_j^{(1)}(\xi_1) \bar{\epsilon}_{2(i,j)},\end{aligned}\tag{6.6}$$

where  $\bar{\epsilon}_{1(i,j)}$  and  $\bar{\epsilon}_{2(i,j)}$  are the values of the strains calculated at the sampling points and  $L_i^{(1)}(\xi_1)$  and  $L_j^{(2)}(\xi_2)$  are interpolating functions. Consistently with (6.6) the discrete operator for the assumed strain technique is given by

$$\begin{aligned}\bar{B}_1(\xi) &= \sum_{i=1}^m \sum_{j=1}^{m_2} L_i^{(1)}(\xi_1) L_j^{(2)}(\xi_2) \bar{B}_{1(i,j)}, \\ \bar{B}_2(\xi) &= \sum_{i=1}^{m_2} \sum_{j=1}^m L_i^{(2)}(\xi_2) L_j^{(1)}(\xi_1) \bar{B}_{2(i,j)},\end{aligned}\tag{6.7}$$

where  $\bar{B}_{1(i,j)}$  and  $\bar{B}_{2(i,j)}$  are the values of the standard operator  $B(\xi)$  calculated at the sampling points. Here, following the relevant literature, we have assumed that the interpolation scheme distinguishes preferable directions.

For a different choice of sampling points and interpolating functions various particular elements can be constructed, where all elements, like the standard displacement/rotation elements, have six degrees of freedom at each nodal point.

**6.3 ASC elements.** In order to gain some insight into the problem we shall include in our analysis two elements formulated within the concept of the assumed strain

technique: a four node element, designated ASCe4, and a nine node element, designated ASCe9.<sup>3</sup>

The element ASCe4 has been constructed following an approach first presented in Bathe and Dvorkin.<sup>4</sup> The sampling points of this element are shown in Fig. 11 and the interpolating functions are assumed in the form

$$\begin{aligned} L_1^{(1)}(\xi) &= 1, \\ L_1^{(2)}(\xi) &= \frac{1}{2}(1+\xi), \quad L_2^{(2)}(\xi) = (1-\xi), \end{aligned} \quad (6.8)$$

where  $\xi = \xi_1$  or  $\xi = \xi_2$ .

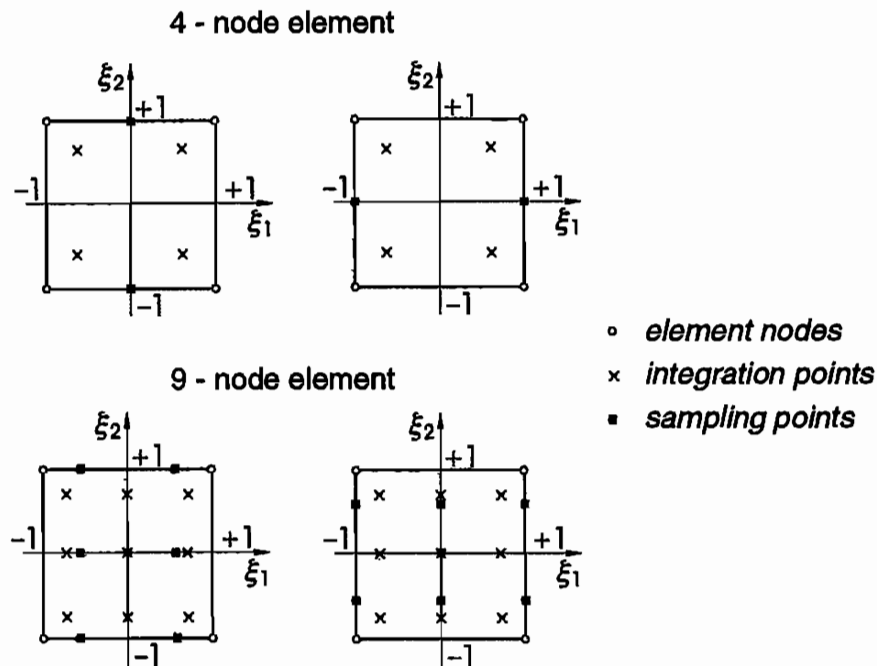


Fig. 11

The element ASCe9 has been constructed following Huang and Hinton<sup>5</sup>. The sampling points of this element are shown in Fig. 11 and the interpolating functions are assumed in the form

<sup>3</sup> Both elements were developed by CHRÓŚCIELEWSKI [1994], and we refer the reader to this work for all details.

<sup>4</sup> BATHE AND DVORKIN [1985, 1986].



$$\begin{aligned} L_4^{(1)}(\xi) &= \frac{1}{2}(1 + \sqrt{3}\xi), & L_4^{(1)}(\xi) &= \frac{1}{2}(1 - \sqrt{3}\xi), \\ L_4^{(2)}(\xi) &= \frac{1}{2}\xi(\xi + 1), & L_2^{(2)}(\xi) &= (1 + \xi^2), & L_3^{(2)}(\xi) &= \frac{1}{2}\xi(\xi - 1). \end{aligned} \quad (6.9)$$

---

<sup>5</sup> HUANG AND HINTON [1986].

## Chapter IV

# Numerical analysis of linearly elastic shells

### 1. Tested shell finite elements

**Linearly elastic constitutive equations.** The shell governing equations derived in Chapt. II as well as the shell finite elements formulated in Chapt. III, when used together with appropriate constitutive relations, are equally applicable to thin or thick shell structures undergoing small or finite strain elastic deformation.<sup>1</sup> However, in order to have the possibility to compare our solutions with the results reported in the literature, we shall consider in this paper only small strain problems. For this class of problems we shall use the following form of the two-dimensional stress-strain relations (written here in terms of physical components)

$$\begin{aligned} N^{(11)} &= C(\varepsilon_{(11)} + \nu\varepsilon_{(22)}), & N^{(22)} &= C(\varepsilon_{(22)} + \nu\varepsilon_{(11)}), \\ N^{(12)} &= C(1-\nu)\varepsilon_{(12)}, & N^{(21)} &= C(1-\nu)\varepsilon_{(21)}, \\ Q^{(1)} &= \frac{1}{2}\alpha_s C(1-\nu)\varepsilon_{(1)}, & Q^{(2)} &= \frac{1}{2}\alpha_s C(1-\nu)\varepsilon_{(2)}, \\ M^{(11)} &= D(\kappa_{(11)} + \nu\kappa_{(22)}), & M^{(22)} &= D(\kappa_{(22)} + \nu\kappa_{(11)}), \\ M^{(12)} &= D(1-\nu)\kappa_{(12)}, & M^{(21)} &= D(1-\nu)\kappa_{(12)}, \\ M^{(1)} &= \alpha_t D(1-\nu)\kappa_{(1)}, & M^{(2)} &= \alpha_t D(1-\nu)\kappa_{(2)}. \end{aligned} \quad (1.1)$$

Here the classical stiffnesses are defined by

$$C = \frac{Eh_0}{1-\nu^2}, \quad D = \frac{Eh_0^3}{12(1-\nu^2)}, \quad (1.2)$$

---

<sup>1</sup> Some of these features have been demonstrated in CHRÓSCIELEWSKI, MAKOWSKI AND STUMPF [1992] in the context of rubber-like shells using the constitutive equations derived in MAKOWSKI AND STUMPF [1987].

where  $E$  denotes Young's modulus,  $\nu$  is the Poisson ration,  $\alpha_s$  and  $\alpha_t$  stand for the shear and torsional coefficient, respectively.

The constitutive equations (1.1) may be viewed as simplest generalization of the classical ones. In particular, upon symmetrization and omitting the constitutive relations for the drilling couples they reduce to the form generally accepted in the Mindlin-Reissner shell theory. Moreover, it can be shown that for smooth, relatively thin shells undergoing small strain deformation the contribution of strains  $\kappa_{(1)}, \kappa_{(2)}$  to the two-dimensional strain energy function is of higher order small and can be neglected (taking  $\alpha_t = 0$ ). However, from the computational point of view it is convenient to retain this small contribution and thus to preserve the complete structure of the general shell theory.

***Catalogue of elements and designations.*** In this chapter we present the numerical analysis of a number of problems, which illustrate the basic aspects of the finite element formulation given in the preceding chapter. The considered problems consist of standard test examples as well as a detailed analysis of special aspects not sufficiently examined in the literature. For a unified presentation of the results the following designations will be used:

- $K \times L$  – finite element mesh, where  $K$  and  $L$  denote the number of elements along corresponding edges of the shell,
- $FI, URI$  – full and uniform reduced integration rule, respectively,
- $fil.$  – stabilization procedure with corresponding filtering coefficient,
- $u, v, w$  – displacements along global coordinate axis  $x, y$  and  $z$ , respectively, which are specified in each example.

In order to evaluate the performance of the developed finite elements we shall present a comparison of our solutions with those reported in the literature as well as our solutions obtained within different formulations of plate and shell finite elements. The complete list of tested elements are presented in Plate 1 and Plate 2. The elements displayed in Plate 1 were described in detail in the previous chapter. A short description and the references to the original literature of the elements displayed in Plate 2 is presented below.

Plate 1

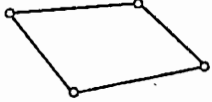

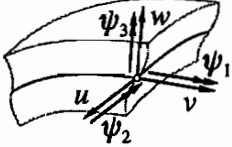
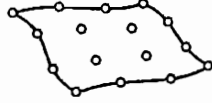

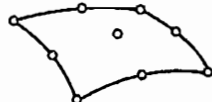
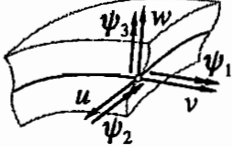
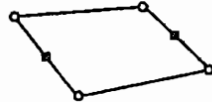

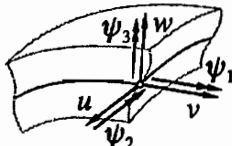
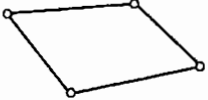

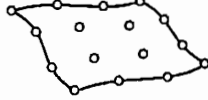
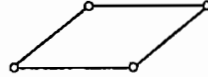
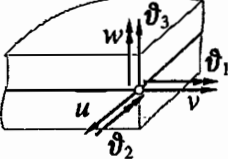
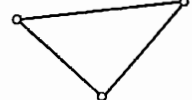
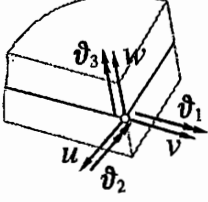
<p>designation number of nodes</p>	<p>nodal degrees of freedom</p>	<p>formulation integration scheme</p>
<p>CAMe4</p> 	<p>6dof/node</p>	<p>Displacement / rotation based formulation.</p>
<p>CAMe9</p> 		<p>Full (FI) or uniform reduced (URI) integration.</p>
<p>CAMe16</p> 		<p>Stabilization procedure in case of URI integration.</p>
<p>MIXe4 SEMe4</p> 		<p>6dof/node</p>
<p>MIXe9 SEMe9</p> 		
<p>ASCe4</p>  <p>■ sampling points</p>	<p>6dof/node</p>	<p>Assumed strain formulation</p>
<p>ASCe9</p>  <p>■ sampling points</p>		

Plate 2

designation number of nodes	nodal degrees of freedom	formulation integration scheme
SELe4 	5dof/node	Standard degenerated shell elements with five degrees-of-freedom per node.
SELe9 		Full (FI) or uniform reduced (URI) integration.
SELe16 		Stabilization procedure in case URI.
BOX 	6dof/node 	4-node rectangular plate element with six degrees-of-freedom per node.  The element is formulated on the basis of van Karman plate theory.
CAT 	6dof/node 	3-node triangular flat shell element with six degrees-of-freedom per node..  The stiffness matrix is obtain by direct superposition of: - plane membrane stiffness, - bending stiffness, - in-plane rotational stiffness.

**SEL elements.** In order to obtain a deeper insight into the performance of various shell finite elements, we include in our numerical analysis a family of three Lagrange elements with 4-, 9-, and 16-nodes, designated as SELe4, SELe9 and SELe16, respectively. These are standard degenerated shell elements<sup>2</sup> having five degrees-of-freedom per node, three displacements and two rotations. Like in the case of CAM elements, in the evaluation of element matrices and vectors either full or uniform reduced integration rule is used. In the later case the stabilization procedure is also included in the same way as in the CAM elements.

Let us recall that the basic concept underlying the formulation of the so-called degenerated shell elements relies on modifying a three-dimensional brick element by assuming a linear shape function in thickness direction while retaining any shape functions in the two remaining (surface) directions. The basic assumptions invoked here are nothing else than the classical Mindlin-Reissner hypothesis according to which: 1) Initially normal fibres to the reference surface remain straight and inextensible, 2) The normal stresses can be neglected (plane stress hypothesis). As a result of the finite element isoparametric discretization together with the assumption 1) the resulting finite element has at each node 5 dof: three displacements  $\mathbf{u}_k = (u, v, w)_k$  and two rotations  $\boldsymbol{\theta}_k = (\theta_1, \theta_2)_k$  as shown in Fig. 1.

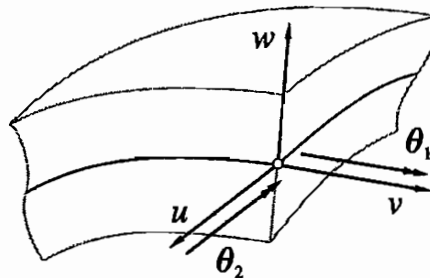


Fig. 1

**BOX element.** In the subsequent analysis we include also results of an earlier developed plate element (designated BOX). This is a  $C^1$  non-conforming flat rectangular element based on the von Kármán theory of thin plates.<sup>3</sup> It has six

<sup>2</sup>These elements were developed in CHRÓSCIELEWSKI [1994] following the formulation due to BATHE [1982].

<sup>3</sup>The element was worked out by CHRÓSCIELEWSKI [1983] along, in principle, the concept of LEE AND HARRIS [1978].

degrees-of-freedom at each node with rotational degrees defined as suitable derivatives of the displacements (Fig. 2). The main characteristics of the element are the following. Relative to a fixed Cartesian coordinate system  $\{x, y, z\}$  the in-plane (tangential) and normal components of the displacement field are denoted by  $u$ ,  $v$  and  $w$ , respectively. The  $z$ -coordinate is taken in thickness direction so that  $w$  denotes the normal deflection of the plate. The nodal degrees of freedom are defined by  $(u, v, w, \vartheta_x, \vartheta_y, \vartheta_z)_k$ ,  $k=1,2,3,4$ , and the polynomial shape functions are chosen in such a way that the compatibility between the displacements  $v$  and  $w$  are satisfied for adjacent elements, which are joined at the non-zero angle along their common  $x$ -axis. This enforces the preferential orientation by setting the  $x$ -axis for both the global and local coordinate system parallel to the longitudinal direction of the members. In the analysis of structures, for which the  $y$ -axis is naturally distinguished, the role of  $x$ - and  $y$ -axis is reversed and thus the element is applicable in both cases. The 6th dof  $\vartheta_z$ , which is created by introducing higher order terms in the interpolation of  $v$  (or  $u$  when the  $y$ -axis has the preferential orientation), also serves to provide in-plane rotational stiffness to avoid a singular matrix, when adjacent elements connected to a node are all coplanar. It should be noted here that while  $\vartheta_x = w_{,x}$  and  $\vartheta_y = w_{,y}$  have the geometric meaning of small rotations about corresponding axes already at the continuum formulation stage, the rotational dof  $\vartheta_z$  is introduced at the discretization level, and its geometric interpretation is not so direct. This is in contrast to the formulation of CAM, MIX, SEM and ASC elements, where all three rotational dof have a clear geometric meaning.

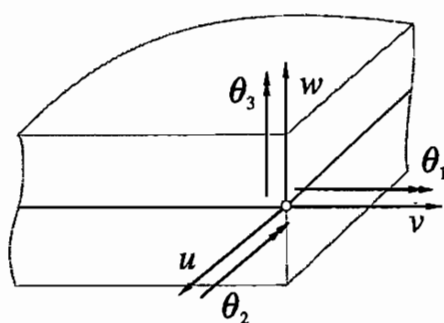


Fig. 2

**CAT element.** This is a simple 3-node triangular flat element with six degrees-of-freedom per node.<sup>1</sup> The element stiffness matrix is obtained by superposition of CST (Constant Strain Triangular), DKT (Discrete Kirchhoff Theory) and an in-plane rotational stiffness.

## 2. Smooth shell problems

A shell, which is geometrically represented by a smooth reference surface and which has neither column supports nor stiffeners, is called here a smooth one. If, in addition, the thickness is relatively small in comparison with the two other dimensions, and if the strains remain infinitesimally small everywhere in the shell space, then the classical Mindlin-Reissner or equivalent kinematical hypotheses seem to be reasonable assumptions. When such assumptions are used together with conventional finite element formulations, the resulting standard elements have five DOF per node, which is entirely enough to analyse shell problems in the aforementioned cases (with the exception of flat elements). Then the main aspects of various formulations of this kind are the accuracy and the reliability of the shell elements, which can be verified through numerical test examples. The primary aim lying behind the effort to develop shell elements with all six DOF per node is to remove the limitation of the standard elements with five DOF per node and extend their range of applicability. Contrary to the 5 DOF/node elements, the 6 DOF/node elements are applicable not only to all regular, but also to all irregular shell structures. In this sense, regular shell problems should be regarded as a first step in an assessment of the correctness of the shell element formulation with six DOF per node. With this in mind, we present as first example a problem, which became a standard test example in the literature.

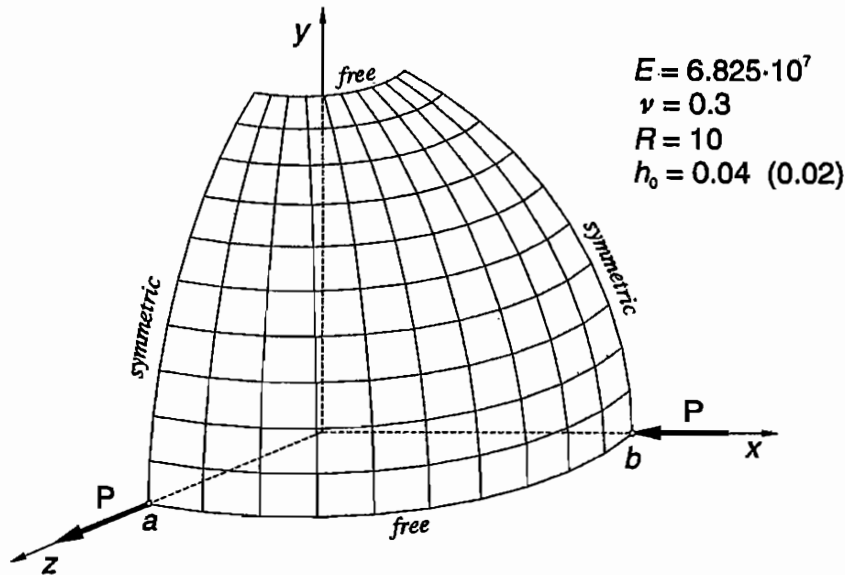
**Example 1. Pinched hemisphere.** The doubly-curved shell shown in Fig. 1.1, which has been proposed by MacNeal and Harder<sup>2</sup>, is commonly regarded as a reliable test to assess the ability of the finite elements to describe the inextensional bending behavior. It appears also to be a good example for checking the ability of the element to handle rigid body modes, since most sections of the shell rotate almost rigidly under the given load. For the linear solutions the displacements  $w_a = -u_b = 0.094$  the force directions with reference force value  $P_{ref} = 1$  suggested by MacNeal and Harder are taken for the normalization (no analytical solution is available).

---

<sup>1</sup> CHRÓSCIELEWSKI, GÓRSKI AND IWICKI [1993,1994].

<sup>2</sup> MACNEAL AND HARDER [1985].





**Fig. 1.1** Pinched hemisphere with a  $18^\circ$  hole at the top subjected to four radial point forces normal to its surface at equal distances around its equator. Due to the bi-symmetry only one quarter is discretized using a regular mesh  $n \times n$  element.

In our formulation of various shell finite elements the sixth DOF (drilling rotation) enters the picture through the underlying shell theory. Hence, it plays the same role independently of the particular finite element formulation. However, different formulations have their own characteristics, which may influence the solutions in a hardly predictable manner. Accordingly, we first examine this aspect. From the results presented in Fig. 1.2 it can be seen that for a wide range of acceptable values of the torsional coefficient  $\alpha_t$ , typically  $\alpha_t < 1$ , no differences in the solutions are observed within the same type of element. This characteristic behavior is found to be independent of the type of finite element formulation (displacement/rotation, semi-mixed, assumed strains). Some differences observed within this range of values of  $\alpha_t$  between the solutions obtained by using different elements are typical for their formulation. The same characteristics have been observed in all other regular shell problems, which we have extensively studied. It will be shown in the following chapters that this property is also preserved in the examples of folded and kinked shell problems. The coincidence of the observed properties supports the applied methodology, which is quite different from the techniques used in the literature. For higher values of the torsional parameter  $\alpha_t$ , typically  $\alpha_t > 1$ , the calculated displacements and rotations appear to be sensitive to the type of formulation. The smallest sensitivity is observed for the higher order

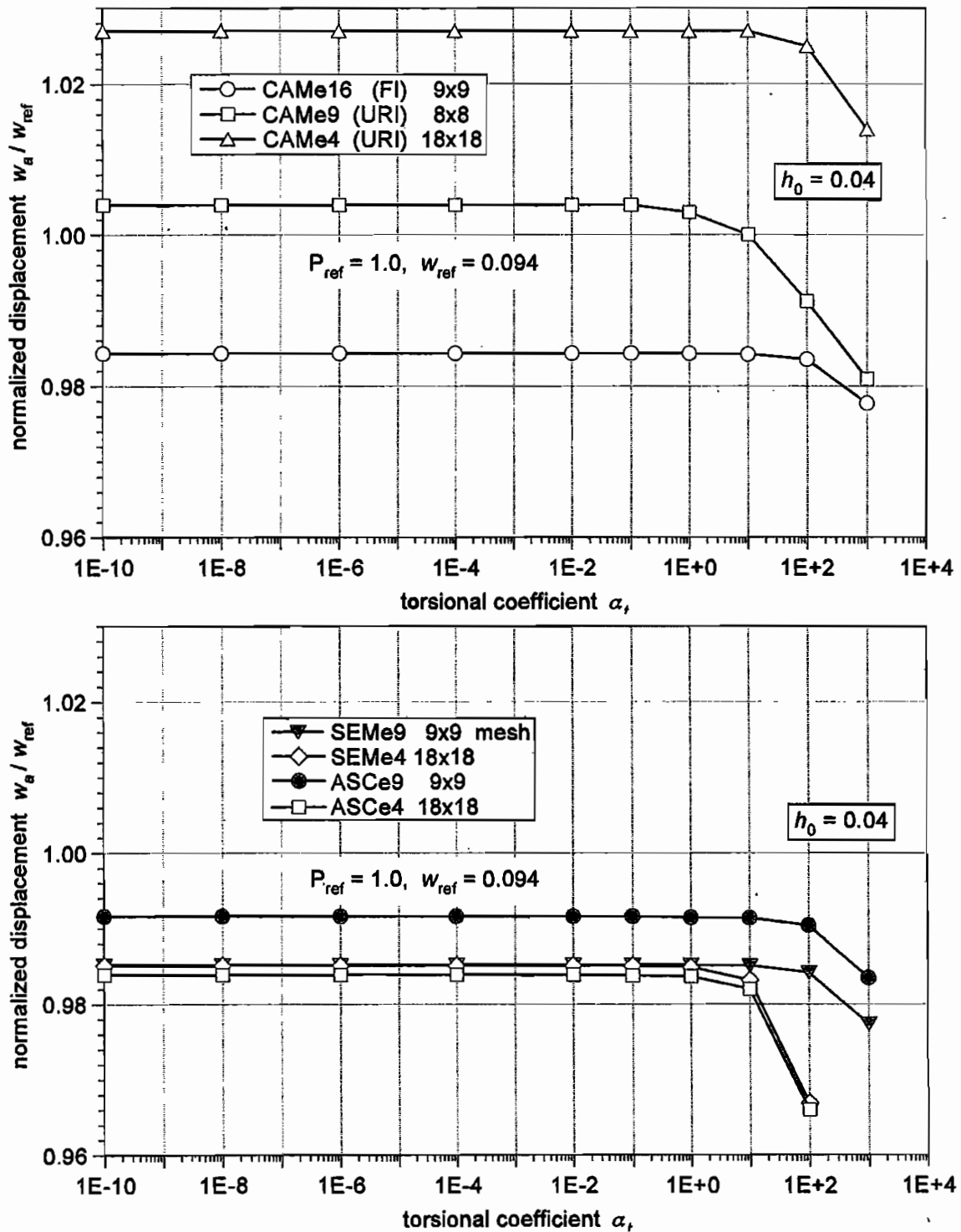


Fig. 1.2 Pinched hemisphere (linear solutions). Investigation of the influence of the torsional coefficient within different finite element formulations.

displacement/rotation based elements (sixteen node CAM element) with full integration, while the biggest influence of the values of  $\alpha_i$  is observed for the under-integrated elements. This clearly demonstrates the well-known fact that the use of the reduced integration is generally accompanied by zero energy modes and high sensitivity of the solutions to small imperfections of any kind. The general conclusion, which may be drawn from our analysis, is the statement that within the acceptable range of values of the torsional parameter we are free to use any value, and this will not influence the results.

In the case of smooth shell problems the elements with five and six DOF per node should lead to correct solutions with comparable accuracy. However, the experience shows that when the sixth DOF is built into the standard 5 DOF/node elements their performance can be remarkably spoiled or may even lead to erratic solutions. Indeed, the results reported in the literature<sup>1</sup> clearly show that the performance of the elements with drilling DOF can strongly depend on the manner, in which the drilling DOF is built into the element. A detailed study of Chen<sup>2</sup> has shown that as far as the convergence and accuracy are concerned the standard flat CST (Constant Strain Triangular) element is superior to the Allman's triangular element with drilling DOF. It is then necessary that elements with six DOF per node are first carefully tested on standard test examples of regular shell problems.

In Fig. 1.3 we present some selected results of convergence tests for linear solutions obtained by our elements, and a comparison with the corresponding results presented in the literature for alternative finite element formulations. Except our SELe16 element and the comparable S16 element due to Stander et al., all other elements include drilling DOF. A good coincidence between the CAM and SEL solutions shows that for regular shells no difference should be expected, whether one uses the elements with 5 DOF or 6 DOF per node. The same property is also observed in the case of nonlinear solutions in the advanced range of nonlinearity (on the scale usually presented in the literature no essential differences would be seen) shown in Fig. 1.4 and Fig. 1.5.

It is a well-known fact, that when the full integration is applied to evaluate the stiffness matrices, the locking effect is much more severe for lower order elements

---

<sup>1</sup> See e.g. JETTEUR AND FREY [1986], JAAMEL, FREY AND JETTEUR [1989] or a review article by FREY [1989].

<sup>2</sup> CHEN [1992]

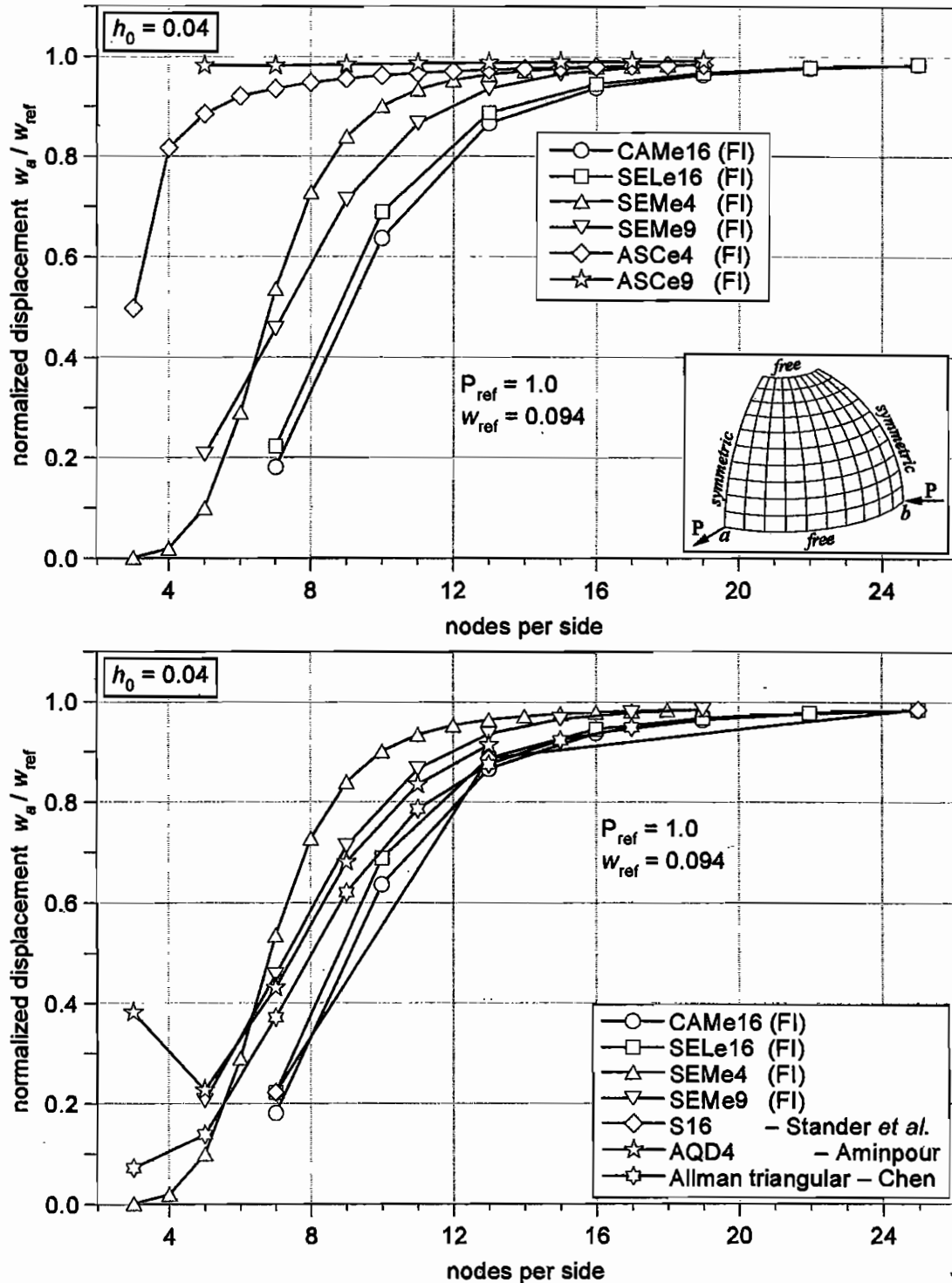


Fig. 1.3 Pinched hemisphere (linear solutions). Analysis of the convergence of our elements and representative results of the literature (below).

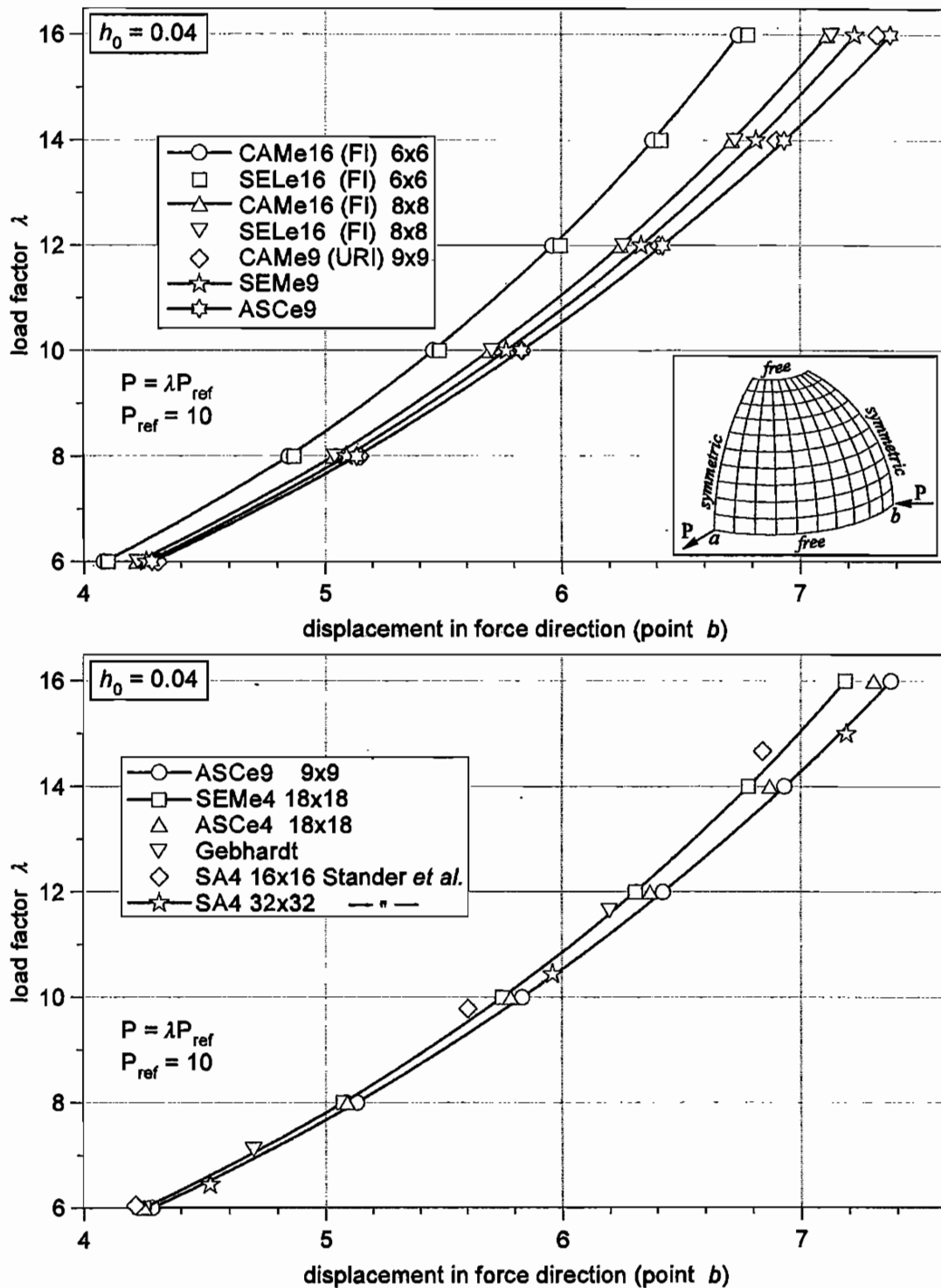


Fig. 1.4 Pinched hemisphere. Nonlinear solutions in the advanced range of the deformation.

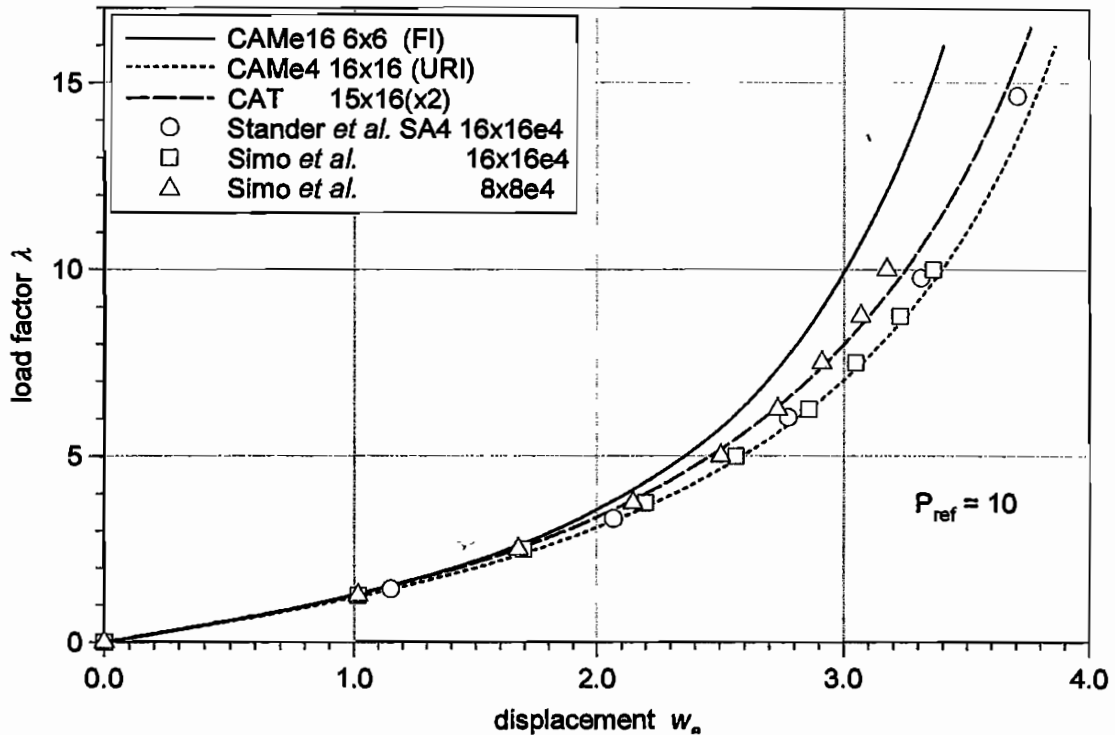


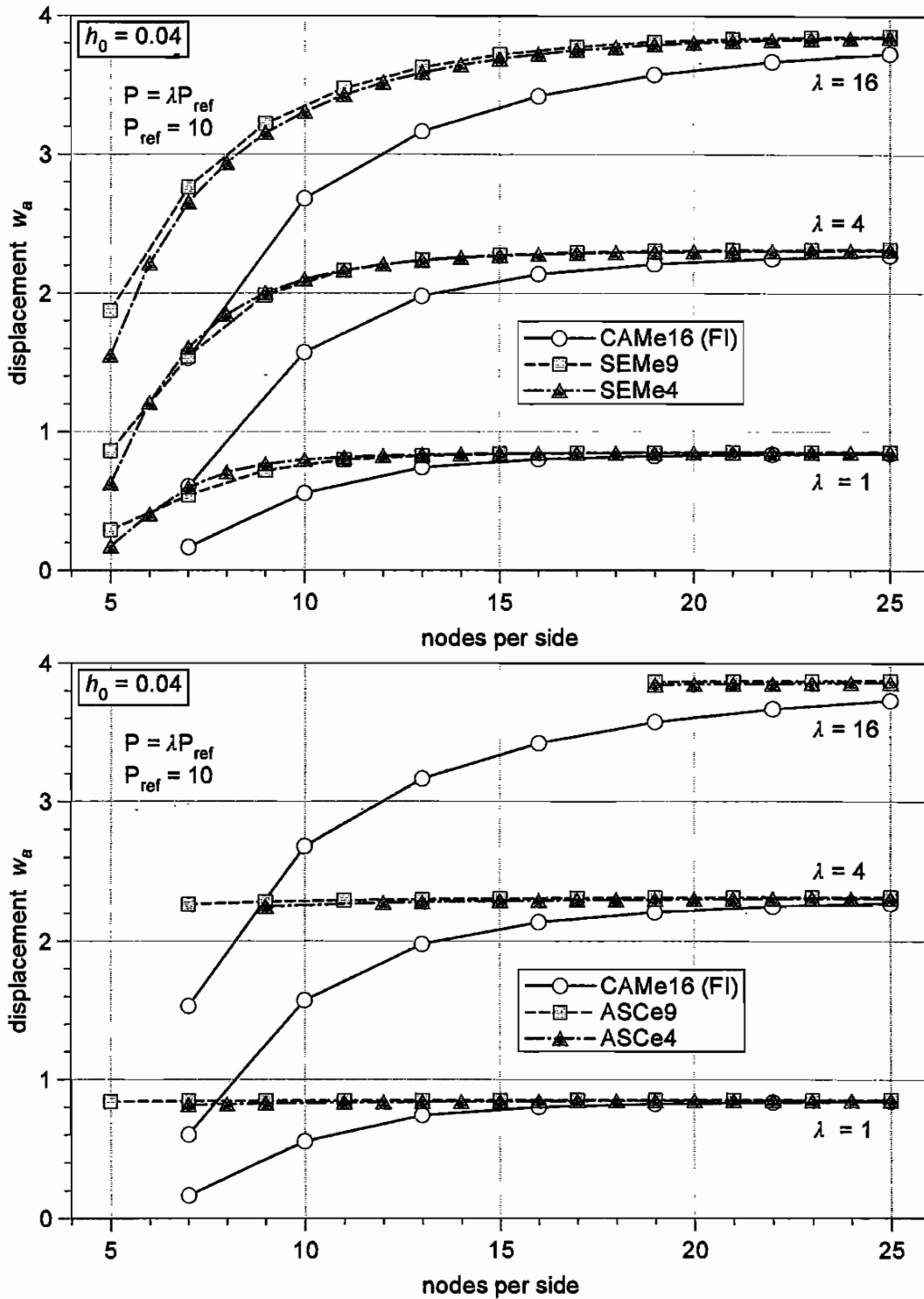
Fig. 1.5 Pinched hemisphere (nonlinear solutions).

than for higher order ones. It was also observed that for the latter elements this effect decreases with increasing nonlinear deformation. However, this is not the rule. The results presented in Fig. 1.6 clearly demonstrate just the opposite.

In Fig. 1.7 we present the results of the convergence tests for the same shell geometry but for a twice smaller thickness, where also a comparison with the solutions presented by Simo<sup>1</sup> is shown. Like for the thick shell (Fig. 1.3), the best convergence is obtained by using the ASCe9 element. However, this element suffers from the uniform rate of convergence at lower discretizations. This characteristic property is typical for all elements, which are polluted by spurious modes.

In overall, when the element formulations are comparable, a good coincidence of the obtained solutions is observed independently whether or not these elements include drilling DOF. This is the case for our CAME16 and SELe16 elements, and

<sup>1</sup> SIMO [1993].



**Fig. 1.6** Pinched hemisphere (nonlinear solutions). Analysis of the locking effect with full integration rule for increasing load level.

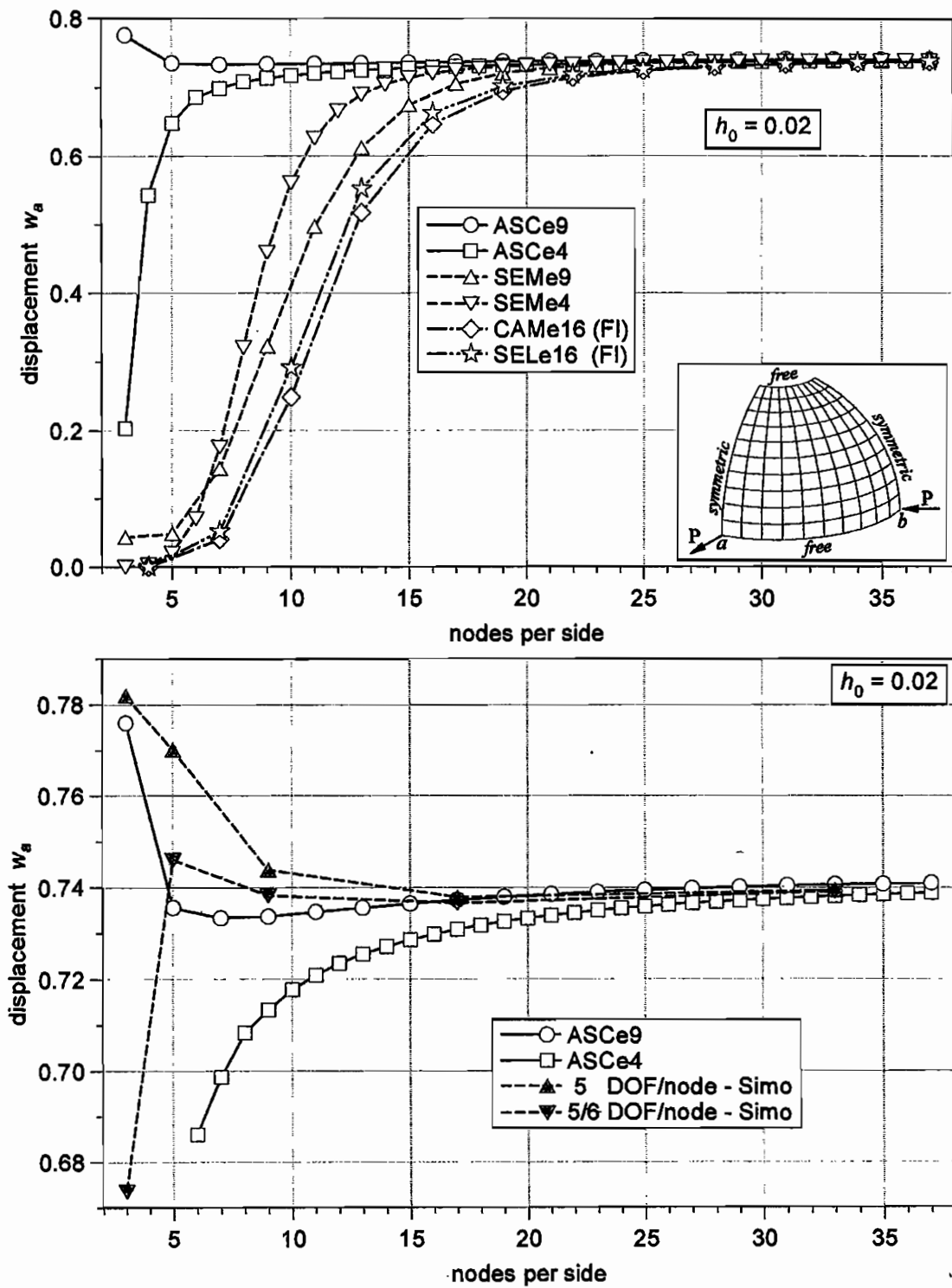
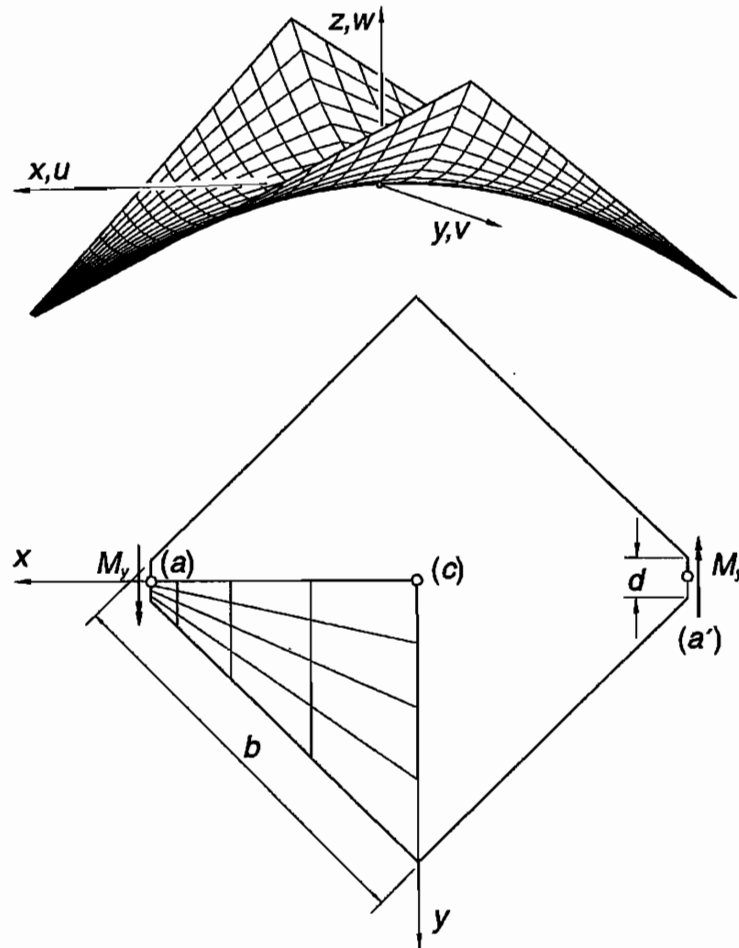


Fig. 1.7 Thin pinched hemisphere (linear solutions). Convergence study.



for the S16 element of Stander et al.<sup>1</sup>, all being 16 node elements based on the standard Lagrange interpolation. We have also found, that most reliable are the solutions obtained by using the CAME16 element with full integration, whenever they are not dominated by the locking effect. The solutions presented in the remaining part of the work will support this conclusion.

**Example 2. Hyperbolic paraboloidal shell.** The problem shown in Fig. 2.1 was proposed by Basar and Ding<sup>2</sup> for testing a large rotation shell theory and assessment of finite elements in flexure for warped meshes.



**Fig. 2.1** Hyperbolic paraboloidal shell is loaded by two opposite moments applied at the supported edges, which can move in the normal direction to the shell surface. The graded mesh for one quarter is used in the analysis.

<sup>1</sup> STANDER, MATZENMILLER AND RAMM [1989].

<sup>2</sup> BASAR AND DING [1990], see also DING [1989].

This problem has been subsequently considered by Stander et al.<sup>1</sup> and Wriggers and Gruttmann.<sup>2</sup> Unfortunately, the results presented in these papers were presented in graphic form only. Nevertheless, within an accuracy of graphic presentation there can be observed good coincidence of our solutions (Fig. 2.2) with those obtained in the aforementioned papers. The numerical values of our solutions are given in Tab.2.1 and Tab.2.2. The computed deformed configurations are shown in Fig. 2.3 and Fig. 2.4.

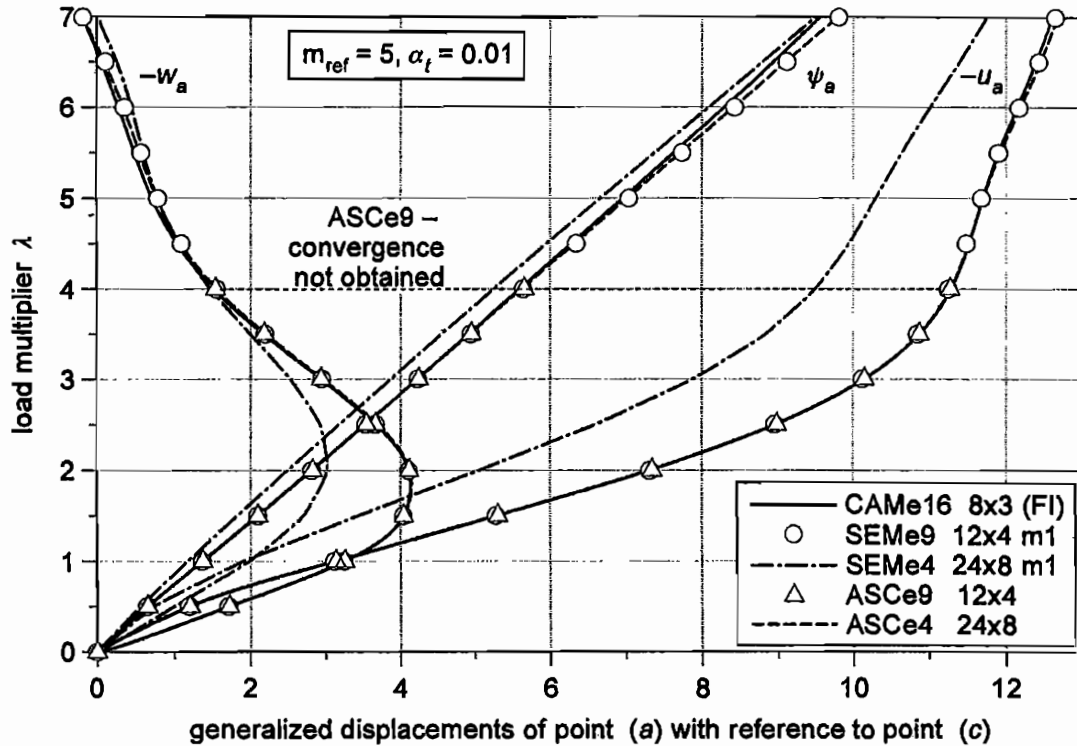


Fig. 2.2 Hyperbolic paraboloidal shell. Nonlinear solutions.

<sup>1</sup> STANDER, MATZENMILLER AND RAMM [1989].

<sup>2</sup> WRIGGERS AND GRUTTMANN [1993].

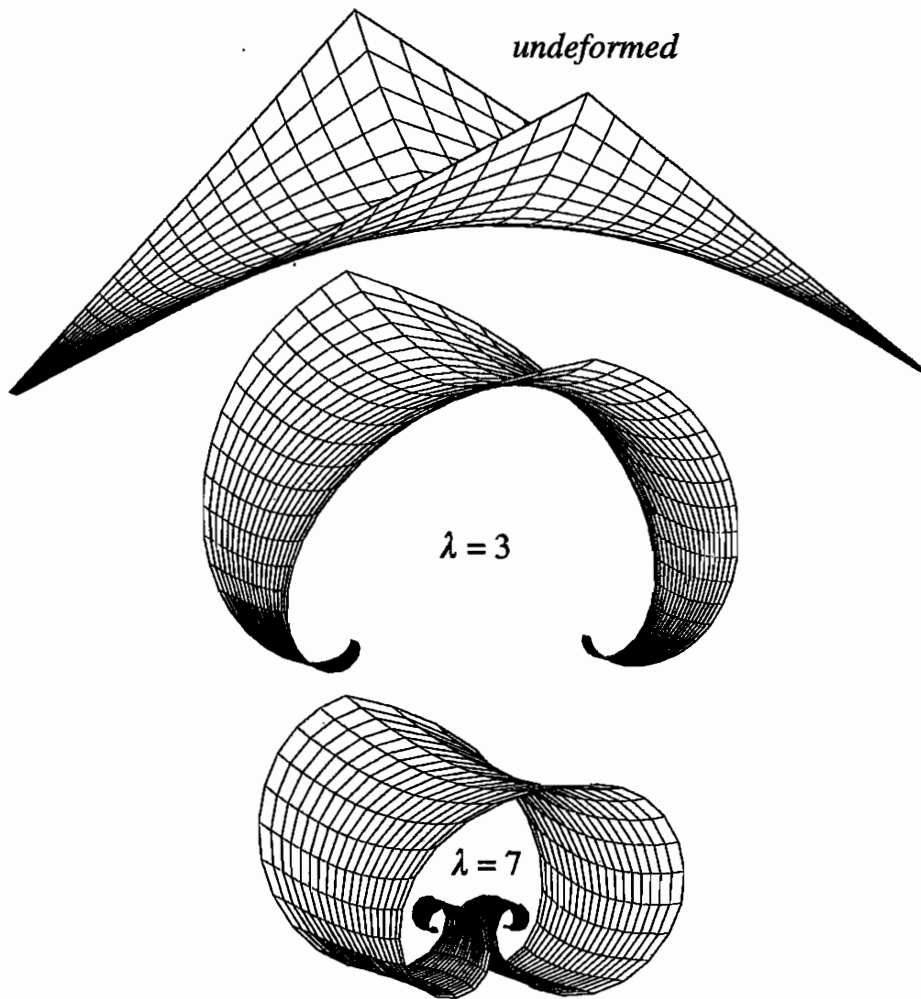


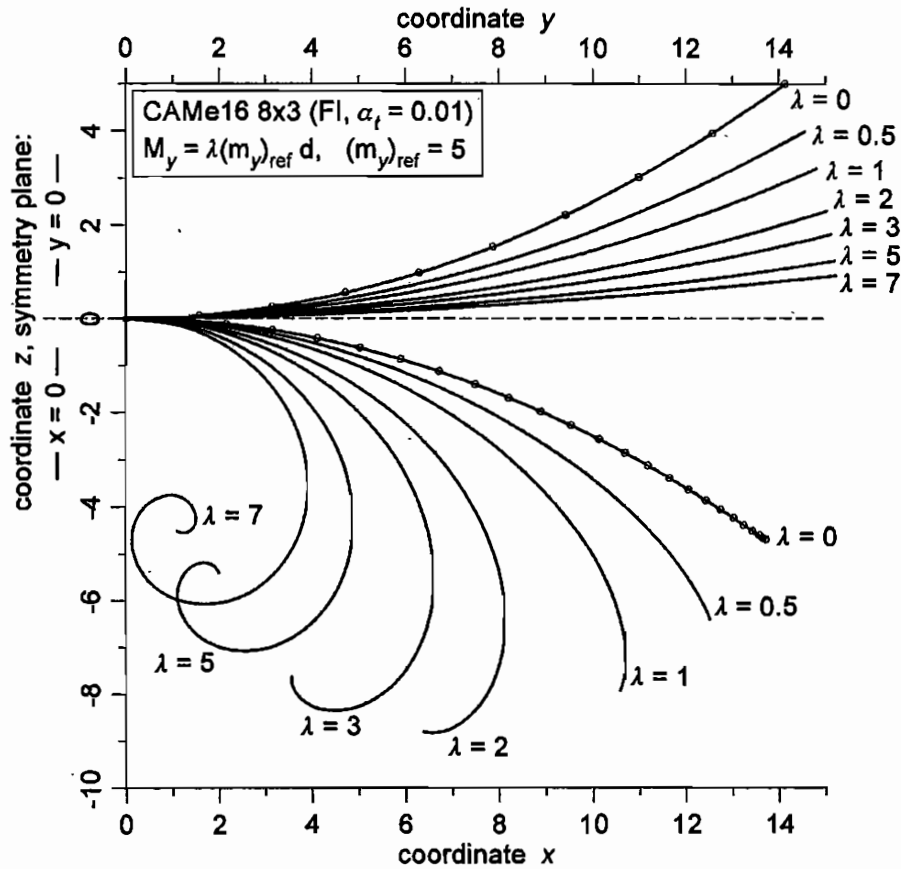
Fig. 2.3 Hyperbolic paraboloidal shell. Computed deformed configurations.

Tab. 2.1 Hyperbolic paraboloidal shell - linear solutions.

element	mesh	$-u_a$	$-w_a$	$q_a$	$q_c$	$\psi_a$
present study						
CAMe16 (FI)	4x2	1.5466	2.9978	2.2578	2.9308	1.1447
	8x3	1.5805	3.0804	2.3073	2.9950	1.1581
	12x4	1.5827	3.0854	2.3105	2.9992	1.1588
SELe16 (FI)	4x2	1.5478	2.9991	2.2595	2.9330	1.1521
	8x3	1.5833	3.0849	2.3114	3.0003	1.1670
SEMe4	24x8	1.0508	1.8685	1.5340	1.9912	1.0193
SEMe9	12x4	1.5778	3.0757	2.3033	2.9899	1.1571
ASCe4	24x8	1.5735	3.0742	2.2970	2.9817	1.1498
ASCe9	12x4	1.5934	3.1036	2.3261	3.0195	1.1655

Tab. 2.1 Hyperbolic paraboloidal shell - nonlinear solution

load $M=\lambda M_0$	CAMe16 8x3	SEMe4 24x8	SEMe9 12x4	ASCe4 24x8	ASCe9 12x4
$\lambda$	horizontal displacement ( $-u$ )				
0.5	1.1967	0.72533	1.1938	1.1900	1.2036
1.0	3.1205	1.9090	3.1145	3.1068	3.1343
1.5	5.2935	3.4203	5.2850	5.2775	5.3115
2.0	7.3228	5.0543	7.3111	7.3093	7.3414
2.5	8.9708	6.5973	8.9534	8.9616	8.9850
3.0	10.146	7.8827	10.121	10.140	10.150
3.5	10.883	8.8394	10.849	10.876	10.875
4.0	11.298	9.4945	11.258	11.289	11.283
5.0	11.713	10.293	11.691	11.715	
6.0	12.144	11.013	12.169	12.185	
7.0	12.609	11.765	12.653	12.673	
	vertical displacement ( $-w$ )				
0.5	1.7158	0.99151	1.7128	1.7135	1.7231
1.0	3.2409	1.9796	3.2384	3.2431	3.2495
1.5	4.0395	2.6974	4.0392	4.0506	4.0456
2.0	4.1129	3.0127	4.1145	4.1322	4.1147
2.5	3.6615	2.9227	3.6654	3.6858	3.6595
3.0	2.9389	2.5305	2.9477	2.9654	2.9377
3.5	2.1730	1.9958	2.1922	2.2022	2.1818
4.0	1.5175	1.4721	1.5530	1.5533	1.5400
5.0	0.70999	0.77856	0.78316	0.76938	
6.0	0.28066	0.44253	0.35229	0.34064	
7.0	-0.19178	0.00929	-0.18490	-0.19091	
	rotation				
0.5	37.037	31.559	36.996	36.802	37.163
1.0	78.421	67.168	78.381	78.020	78.645
1.5	120.00	104.49	120.03	119.53	120.37
2.0	161.10	142.82	161.30	160.67	161.72
2.5	201.73	181.84	202.22	201.46	202.71
3.0	241.92	221.33	242.84	241.98	243.38
3.5	281.71	261.15	283.22	282.28	283.68
4.0	321.12	301.21	323.43	322.39	324.14
5.0	398.77	381.93	403.31	402.20	
6.0	474.61	462.92	482.75	481.59	
7.0	547.25	543.94	561.91	560.66	



**Fig. 2.4** Hyperbolic paraboloidal shell. Computed deformed configurations of normal sections  $x = 0$  and  $y = 0$ .

**Example 3. Clamped skew plates.** This example (Fig. 3.1) is chosen to demonstrate the performance of the developed shell elements in the analysis of problems with irregular meshes. This problem was first examined by Pica et al.<sup>1</sup>

The comparison of the solutions reported by these authors with our own results is shown in Fig. 3.2, where a full coincidence of the vertical deflection can be seen.

<sup>1</sup> PICA, WOOD AND HINTON [1980].

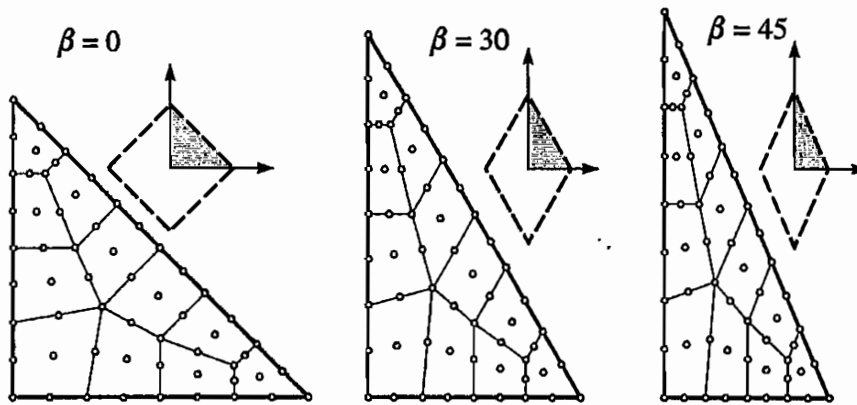


Fig. 3.1 Clamped skew plates under uniform distributed load.

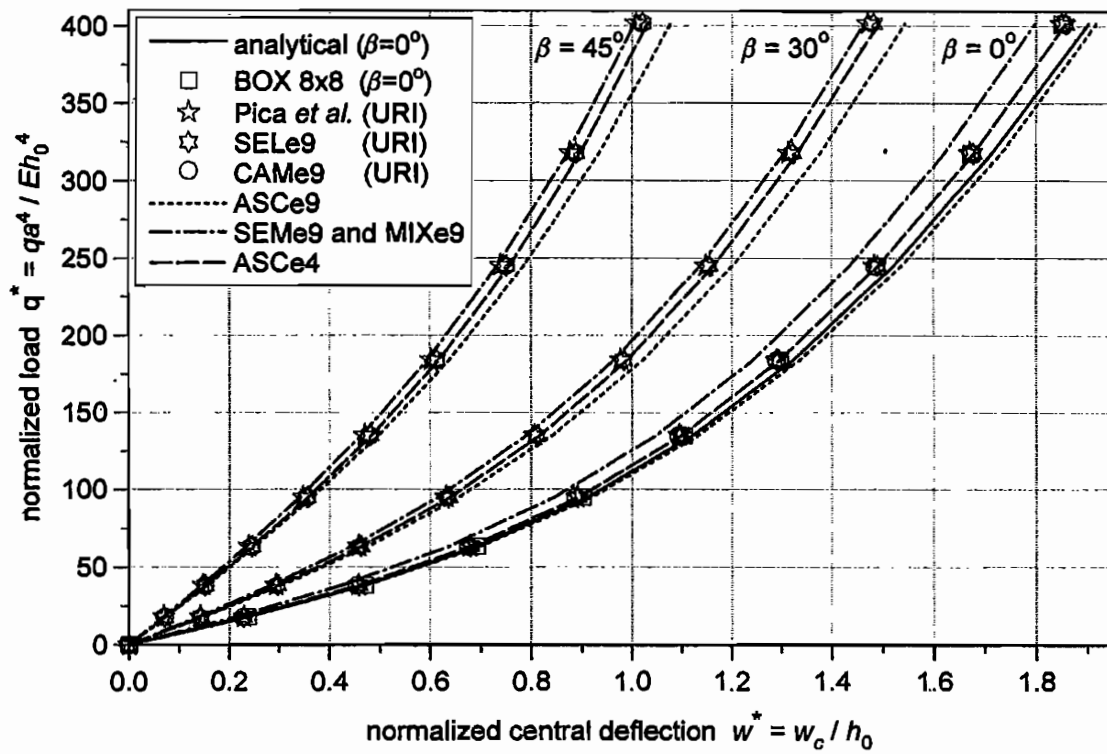
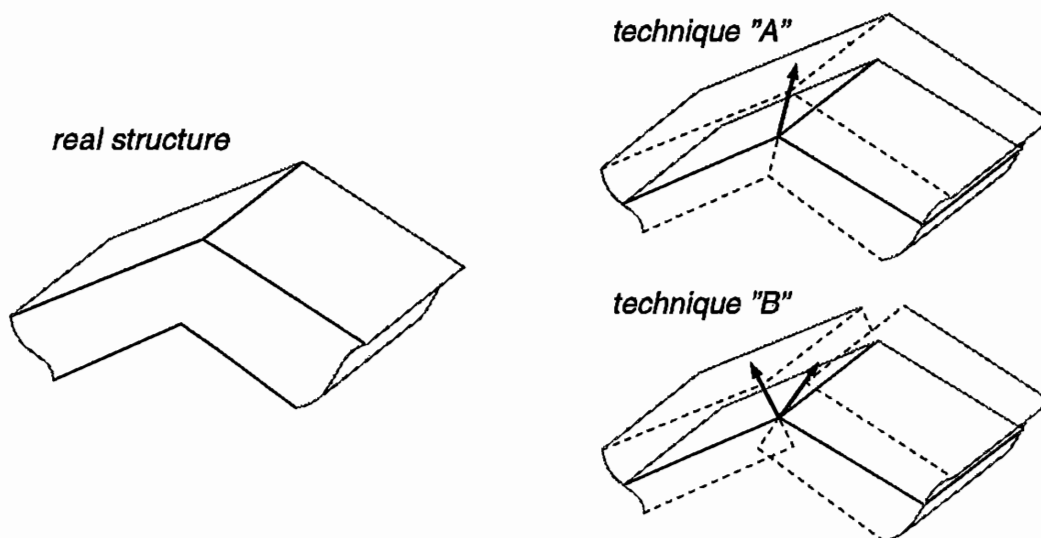


Fig. 3.2 Clamped skew plates. Nonlinear solutions.

### 3. Folds and kinks in shell structures

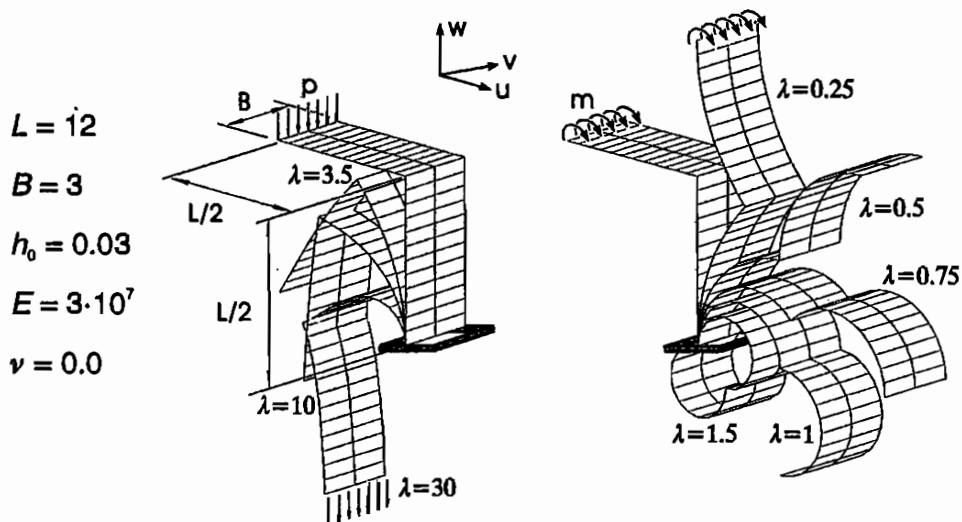
A large and important class of engineering structures are multi-shells. They are characterized by highly irregular multi-featured geometries consisting of folds, kinks, branches, etc., along which several structural components are rigidly interconnected. While the complexity of the underlying geometry and loading makes such structures hardly tractable by analytical methods, the finite element method appears to be a particularly suitable tool for their analysis. However, in the case of shell elements with 5 DOF per node difficulties arise at the shell intersections in assembling element matrices and vectors into the global ones. Obviously, this does not concern the elements with all 6 DOF per node. In all our CAM, MIX, SEM and ASC elements the six nodal degrees of freedom (three translational and three rotational) are defined either relative to local triads attached to the nodes of the element, or with respect to an arbitrarily specified unique global basis. Using standard rules they can be transformed uniquely from one basis to another. Their representations with respect to local triads are usually used for the analysis of regular shells. Transformations to the global basis are required in the case of irregular shell and plate structures in order to assemble global stiffness matrices and load (external and residual) vectors. When applying the shell elements with 5 DOF per node to irregular structures obvious difficulties appear due to the lack of the sixth (drilling) DOF.



**Fig. 1** Two possible techniques to use shell elements with 5 DOF per node for the analysis of shell and plate structures involving kinks.

In the analysis of irregular structures the simplest case is the one, where two structural elements are rigidly interconnected along a junction as sketched in Fig. 1. Then it is always possible to define a field of local triads with a director field continuous across the junctions (technique "A"). Such triads then serve as basis for the assemblage of global matrices and vectors. Hence, the standard 5 DOF per node elements can be assembled into the global stiffness matrix with no additional efforts. We have included this technique in the SEL elements. The second possible technique "B" involves the transformation of 5 DOF in local triads into 6 DOF with respect to a global basis. While both techniques are pointed out in the literature, there is an apparent lack of illustrative numerical test examples, which would provide a deeper insight into possible influence of both techniques on the predicted solutions. A few examples presented below aim at providing insight into this aspect.

**Example 1. Right angle cantilever plate.** The first example, the right angle cantilever plate (actually beam) clamped at one end and loaded either by distributed forces or distributed moments applied at the other free end (Fig. 1.1), is essentially one-dimensional. Hence, no difficulties in obtaining the solution should be expected. Indeed, we have found that the deflections predicted by the 6DOF/node CAM elements and 5DOF/node SEL elements coincide entirely with the analytical solution for the pure bending problem in the fully nonlinear range. The same complete coincidence was observed with other loading.

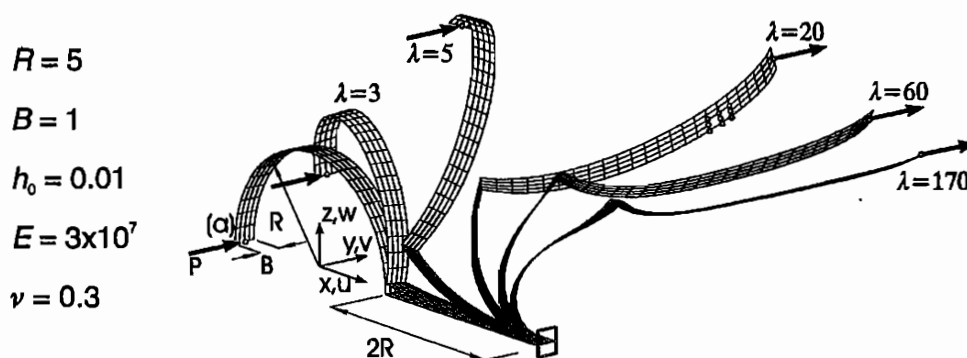


**Fig. 1.1** Right angle shell. Data of the structures and computed deformed configurations.



**Example 2. Sickle-shell.** The second example in this class (Fig. 2.1), which we have examined, was called by Simo<sup>1</sup> a sickle-shell problem. Besides the results at the very low load level (actually, within the linear range) no details were presented in the aforementioned work. The complete non-linear solution together with the deformed shapes of the structure are shown in Fig. 2.2 and the numerical values are given in Tab. 2.1. Again, a full agreement is observed between the solutions obtained with CAM and SEL elements.

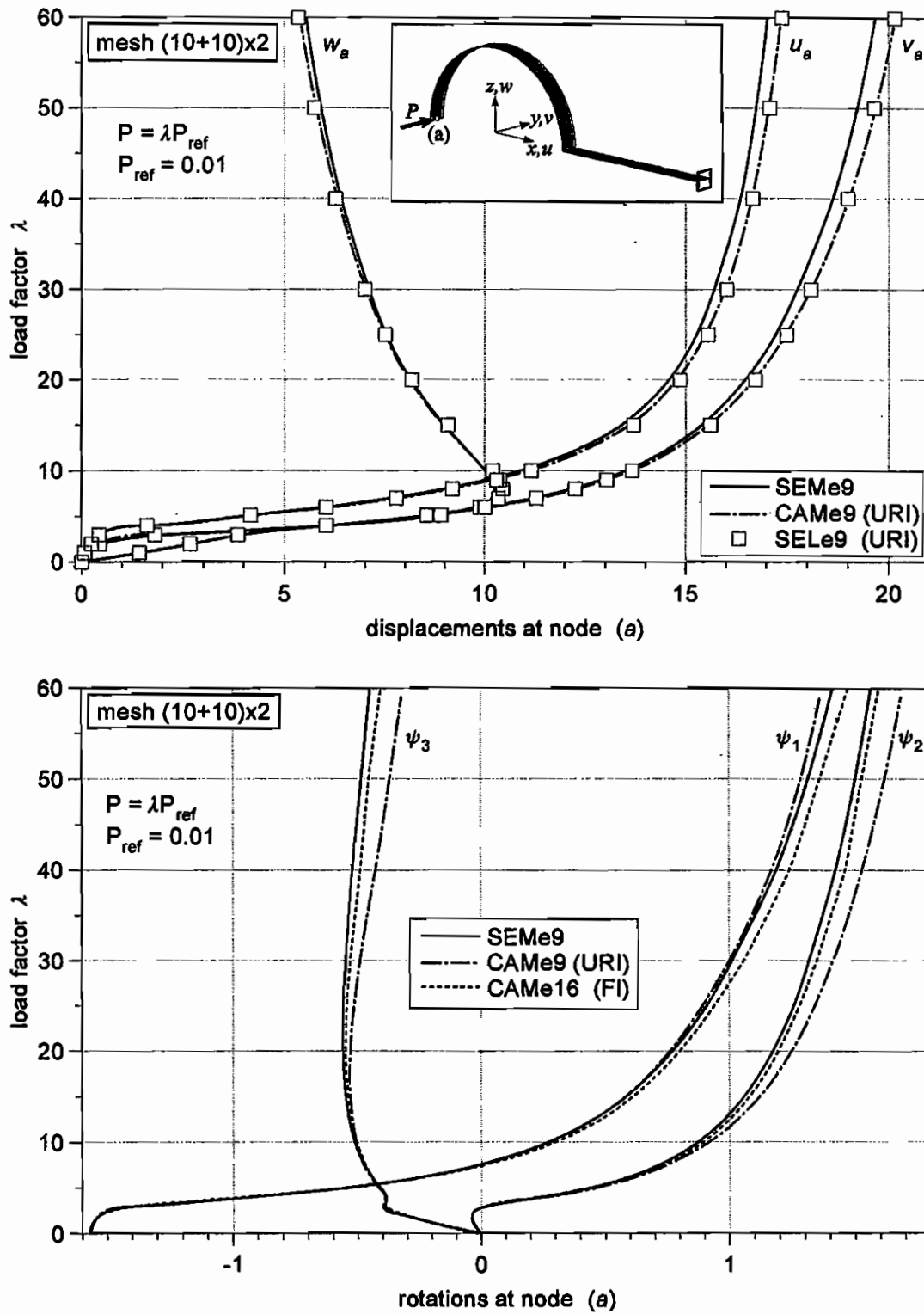
From these results it becomes evident that this type of problems cannot be regarded as a reliable test for the applicability of shell finite elements to analyse irregular shell structures. Actually, from the analysis of a C-shaped beam considered in our previous work<sup>2</sup>, one can conclude that the standard 5 DOF/node elements can be applied with moderate reliability to kinked structures only in the case, when the deformation along interconnections is not dominant.



**Fig. 2.1** Sickle-shell problem. The computed configurations within the highly nonlinear range of deformation coincide to the extent not distinguishable on this scale, whether CAM, SEM or SEL elements are used.

<sup>1</sup> SIMO [1993].

<sup>2</sup> CHRÓŚCIELEWSKI, MAKOWSKI AND STUMPF [1994], see CHRÓŚCIELEWSKI [1994] for more detailed analysis.



**Fig. 2.2** Sickle-shell problem. Load-displacement/rotation paths obtained by using different shell elements.

**Tab. 2.1** Sickle shell. Nonlinear solutions, mesh (8+12)x2

load <sup>*)</sup>	horizontal displacement $v_a$			vertical displacement $w_a$		
$\lambda$	CAMe9 <sup>**)</sup>	SEMe9	SELe9 <sup>**)</sup>	CAMe9 <sup>**)</sup>	SEMe9	SELe9 <sup>**)</sup>
1.	1.460	1.457	1.424	0.09619	0.1068	0.09119
2.	2.740	2.734	2.669	0.46141	0.5164	0.4410
3.	3.970	3.987	3.839	1.989	2.227	1.803
4.	6.214	6.166	6.013	6.194	6.187	6.026
6.	10.11	10.01	10.01	9.772	9.752	9.878
8.	12.30	12.18	12.26	10.28	10.26	10.45
10.	13.65	13.51	13.66	10.04	10.02	10.20
15.	15.58	15.40	15.61	8.962	8.984	9.065
20.	16.68	16.47	16.72	8.096	8.136	8.151
25.	17.47	17.22	17.50	7.470	7.515	7.485
30.	18.09	17.78	18.09	7.002	7.048	6.979
40.	19.02	18.63	19.00	6.303	6.380	6.254
50.	19.68	19.23	19.65	5.782	5.901	5.737
60.	20.18	19.67	20.15	5.380	5.534	5.336

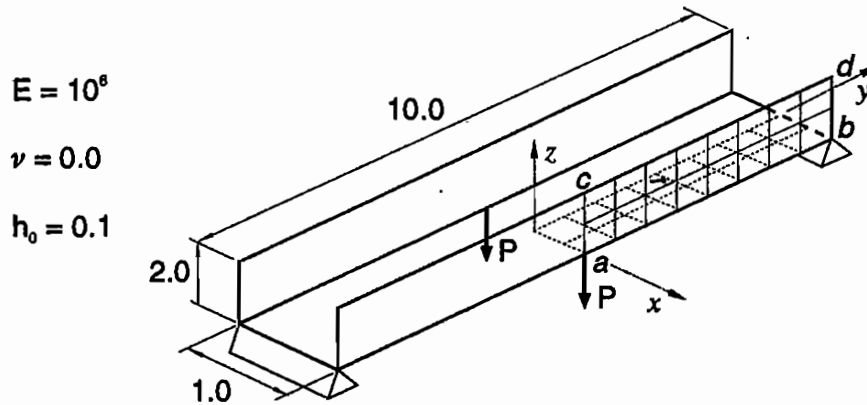
<sup>\*)</sup> $P = \lambda P_{ref}$ ,  $P_{ref} = 0.01$ , <sup>\*\*)</sup>URI integration

**Tab. 2.2** Sickle shell. Nonlinear solutions, mesh (8+12)x2

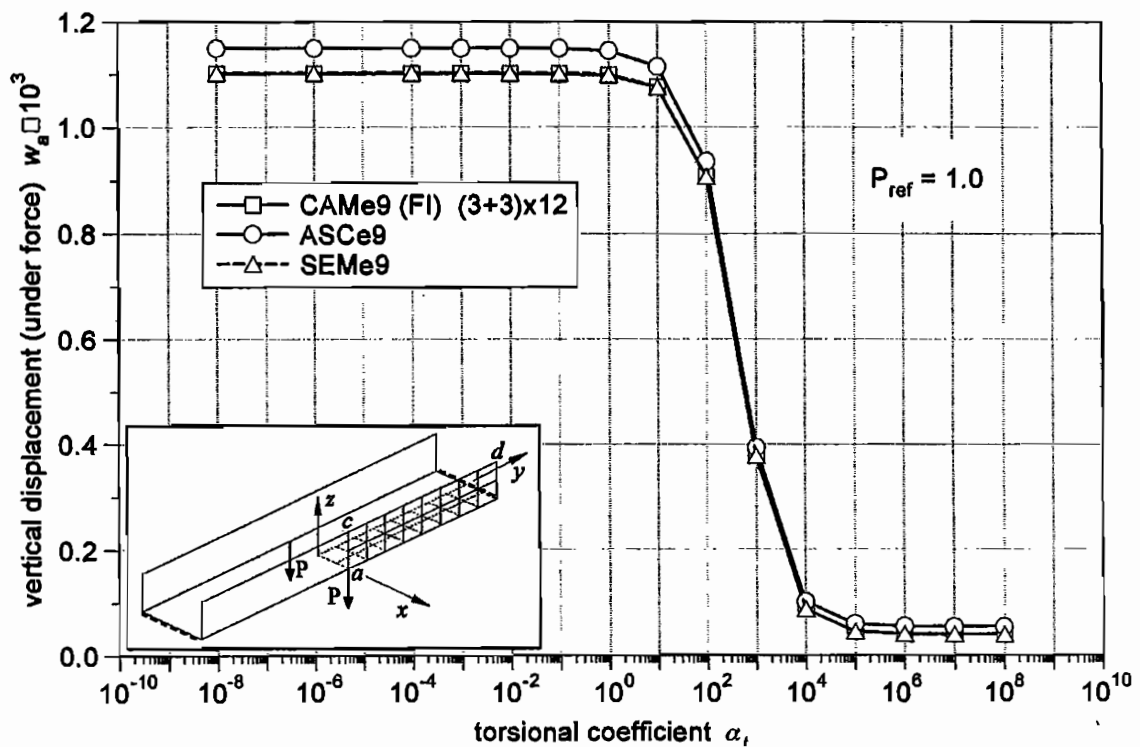
load <sup>*)</sup>	CAMe9 (URI)			SEMe9		
$\lambda$	$\psi_1$	$\psi_2$	(-) $\psi_3$	$\psi_1$	$\psi_2$	(-) $\psi_3$
1.	-1.565	-0.02503	0.1766	-1.563	-0.02546	0.1761
2.	-1.536	-0.03679	0.3212	-1.531	-0.03620	0.3192
3.	-1.392	0.02263	0.3982	-1.368	0.03244	0.3885
4.	-0.9186	0.2691	0.3904	-0.9197	0.2594	0.3857
6.	-0.2720	0.5995	0.4435	-0.2794	0.5758	0.4380
8.	0.06669	0.7879	0.4839	0.05997	0.7545	0.4826
10.	0.2795	0.9180	0.5056	0.2722	0.8738	0.5117
15.	0.5834	1.122	0.5299	0.5847	1.060	0.5486
20.	0.7623	1.249	0.5317	0.7735	1.175	0.5602
25.	0.8945	1.343	0.5164	0.9107	1.258	0.5591
30.	1.002	1.416	0.4917	1.020	1.323	0.5506
40.	1.172	1.530	0.4272	1.189	1.425	0.5210
50.	1.287	1.621	0.3701	1.316	1.504	0.4846
60.	1.372	1.694	0.3170	1.415	1.567	0.4488

<sup>\*)</sup> $P = \lambda P_{ref}$ ,  $P_{ref} = 0.01$

**Example 3. Folded plate.** In order to obtain a deeper insight into the modelling of junctions and their possible influence on the predicted solutions, we consider the problem shown in Fig. 3.1.



**Fig. 3.1** Plated structure. Due to the bi-symmetry only a quarter need to be discretized.



**Fig. 3.2** Plated structure (linear solutions). Analysis of the torsional coefficient.

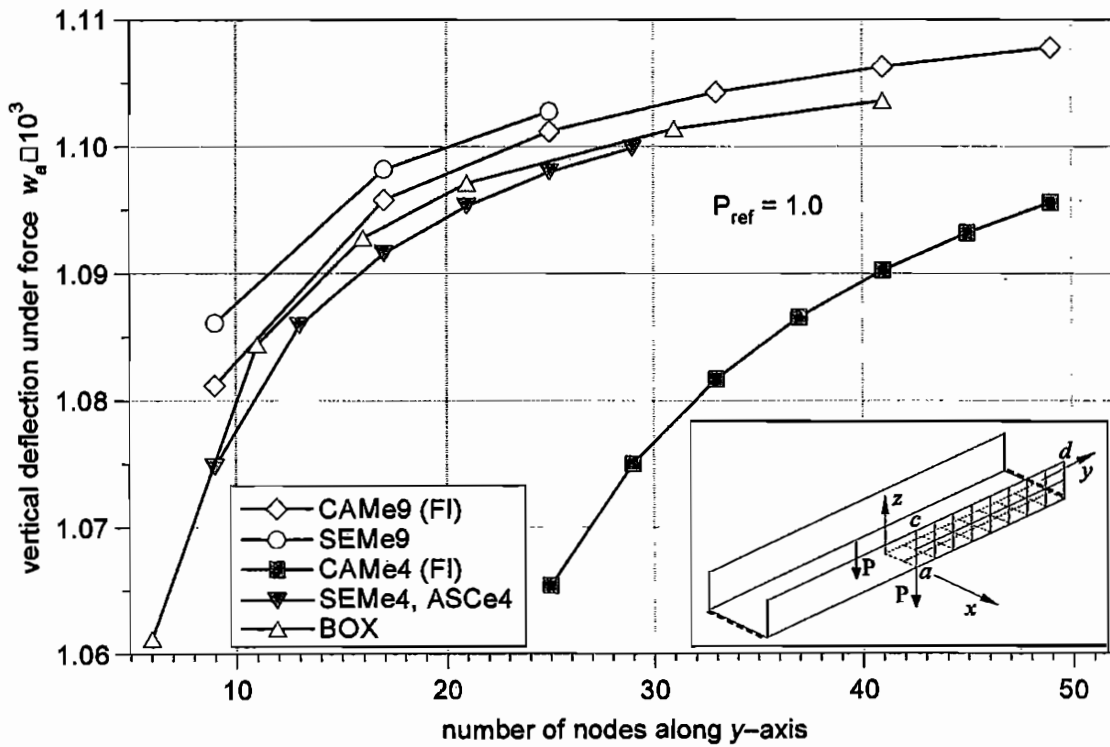
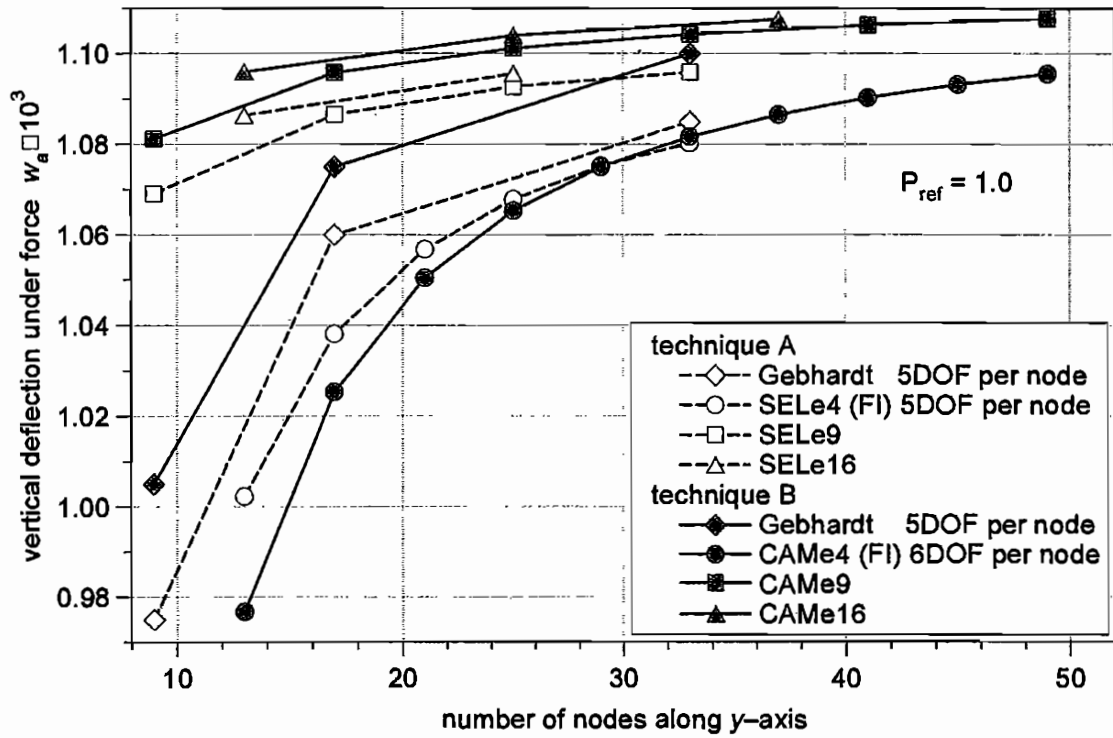
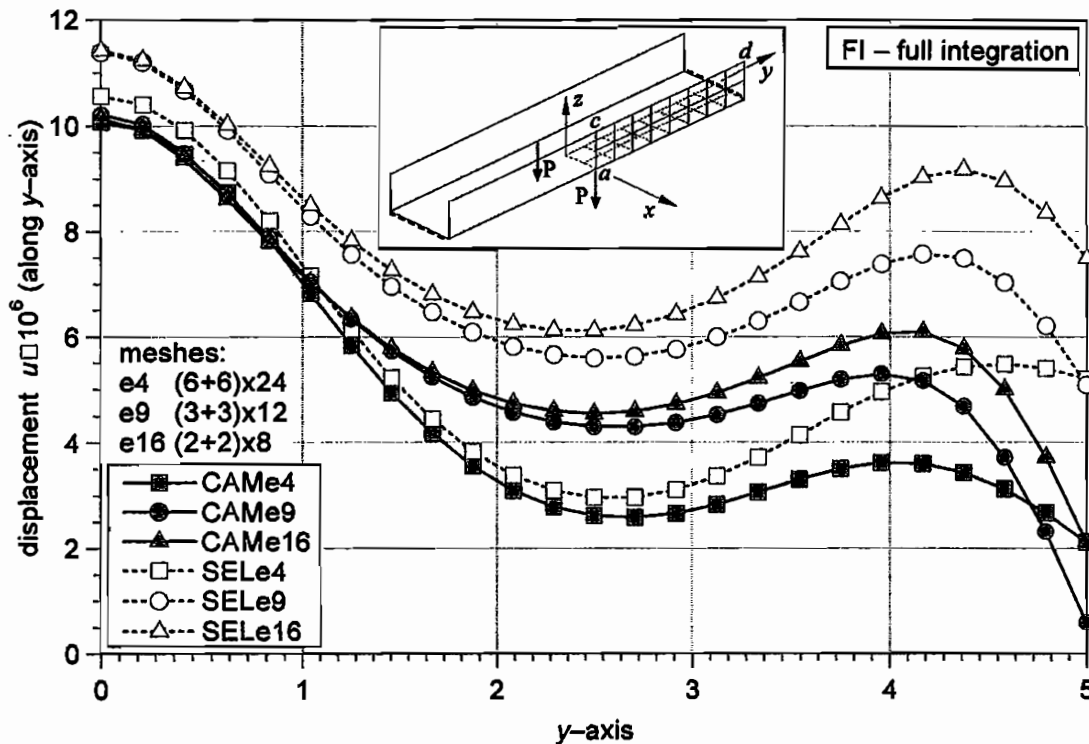


Fig. 3.3 Plated structure. Convergence study of linear solutions.

The results presented in Fig. 3.2 demonstrate that, like for smooth shells, the torsional coefficient  $\alpha$ , has no influence on the solutions as long as its values remain within the appropriate range. It is also remarkable that the range itself is actually problem-independent (see next chapters).



**Fig. 3.4** Plated structure. Horizontal displacements  $u$  along (c)-(d) line of the vertical plate predicted by CAM and SEL elements with full integration rule.

Within the linear range of deformation this example was analysed by Gebhardt<sup>1</sup> using a standard degenerated element with 5 DOF per node, together with the use of either techniques "A" or "B" to model the connection of horizontal and vertical plates. The results presented in that work and reproduced in Fig. 3.3 show that the technique "B" leads to a vertical displacement under the force, which is slightly smaller than the one obtained by using the technique "A". We carried out a detailed convergence study showing that SEL elements give also lower values of the displacements than CAM elements with the same number of nodes. Keeping in mind that our SEM and ASC elements exhibit convergence to the same values as the CAM elements, this example clearly indicates that the technique used to model

<sup>1</sup> GEBHARDT [1990].

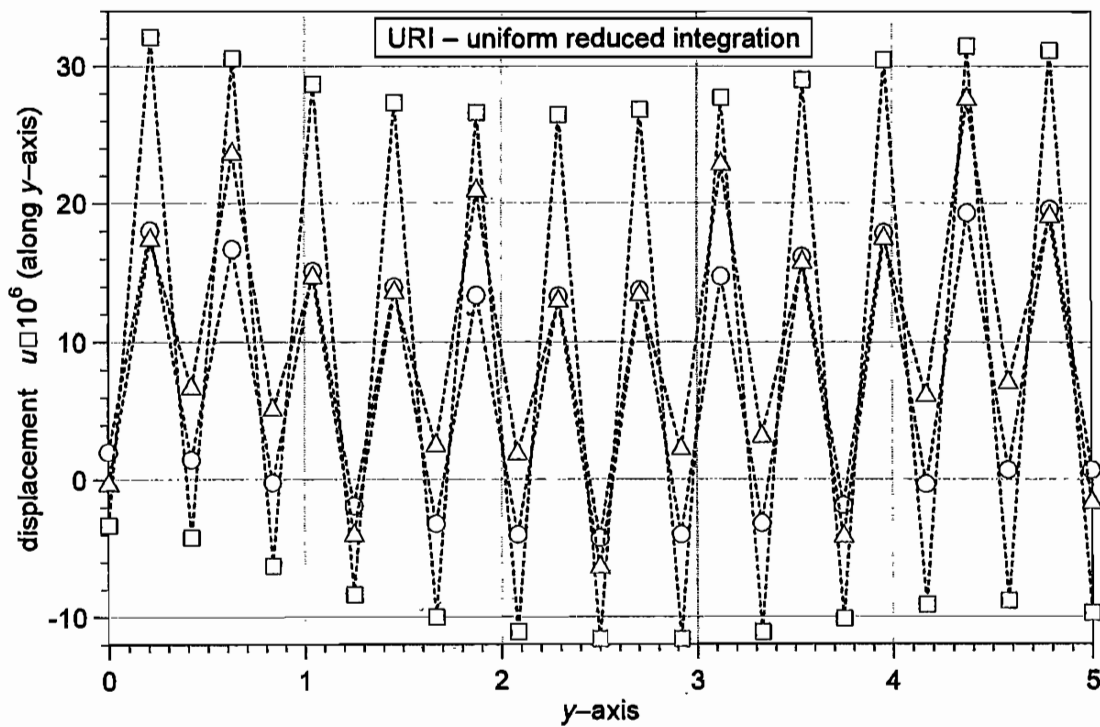
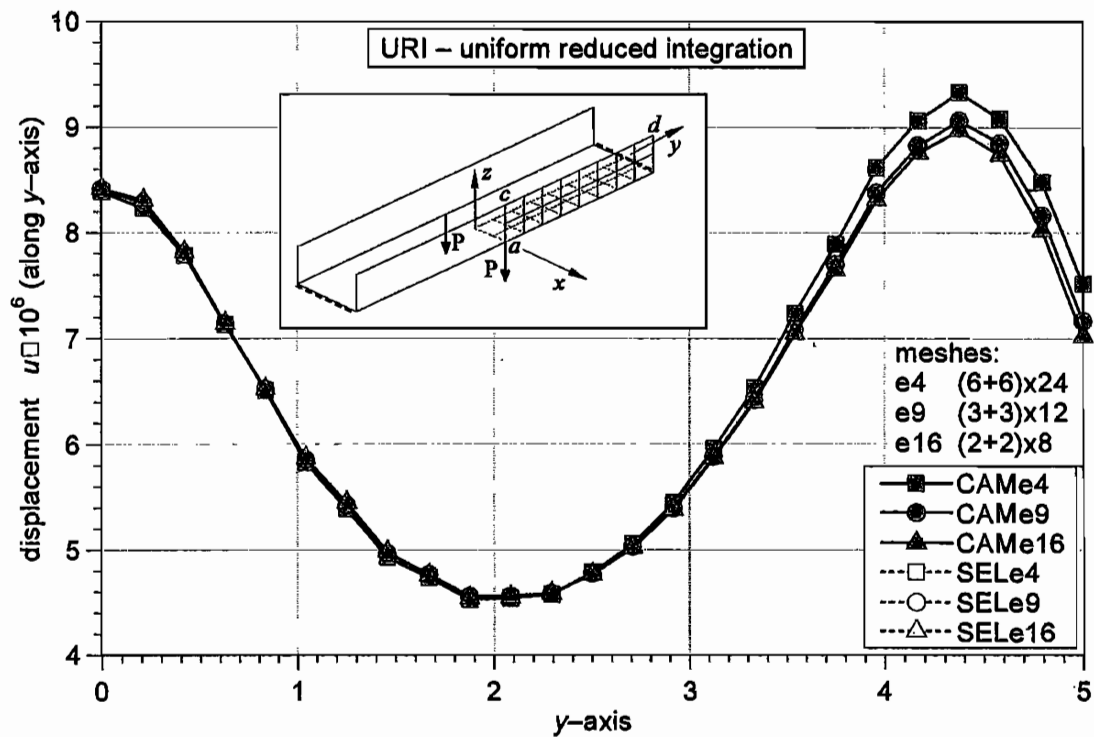
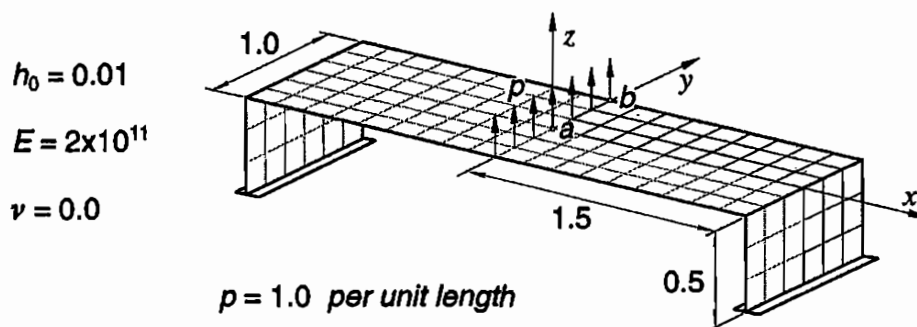


Fig. 3.5 Plated structure. Horizontal displacements  $u$  along (c)-(d) line of the vertical plate predicted by CAM and SEL elements with reduced integration rule.

junctions of irregular structures may influence the predicted solutions. As about the vertical displacement under the force, the differences between the CAM and SEL element solutions are not of great importance. However, the horizontal displacements along the vertical plate predicted by these elements differ quite essentially (Fig. 3.4). Moreover, it is very interesting to point out that the drilling degree of freedom formulated on the shell theory basis (CAM, SEM, ASC elements) stabilize the solutions, when the uniform reduced integration rule is applied (Fig. 3.5).

**Example 4. Plated structure.** When dealing with the problem of shell intersections, it should be mentioned that a rigorous description of strain and stress distributions in the vicinity of folds, kinks, branches, etc., falls outside of the realm of any shell theory in the same way as none of the shell theories can correctly describe the stress and deformation states within the boundary layer even of regular shells. Besides this well-known fact, the shell-theory-based solutions yield an appropriate description of those states outside of the vicinity of intersections and boundaries. In order to illustrate this point, we examine finally an example presented by Bathe et al.<sup>2</sup> and shown in Fig. 4.1.



**Fig. 4.1** Folded plate structure. Owing to the bi-symmetry of the geometry and the loading only the indicated quarter of the structure is discretized by finite elements using the regular mesh  $n \times (3n+n)$ , where  $n$  denotes the number of elements across the width of the vertical and horizontal plates.

As in the previous example, only linear solutions are given here. It was pointed out in Bathe et al. that problems of this kind may be analysed using Timoshenko beam finite elements (beam model), shell finite elements (shell model), or three-dimensional finite elements (3D-model). From the results presented in Bathe et al. and reproduced in Fig. 4.2 it can be seen that the vertical deflections under the

<sup>2</sup>BATHE, LEE, AND BUCALEM [1990].



load line predicted by shell and 3D models coincide quite well. Obviously, the beam model cannot account for the varying deflection along the width of the structure, but this effect predicted by the shell model coincides very well with the results obtained by using the 3D-model. From the results presented in Fig. 4.3 it is also seen that a complete agreement with the results of Bathe et al. is obtained, when CAM elements are used, even with coarse meshes. However, the SEL element, which is comparable with the shell element applied in Bathe et al., gives slightly smaller deflections (both are 16 node degenerated elements with 5 DOF per node). The noted difference is presumably due to a different modelling of the junction of horizontal and vertical plates. In Bathe et al. the technique "B" was applied, while in the case of SEL element here the technique "A" as explained above is used. Thus, this example illustrates again the effect of the modelling of junctions on the predicted displacements. It is also interesting to note that in the solution of this problem neither locking effects nor zero-energy modes are observed (Fig. 4.3).

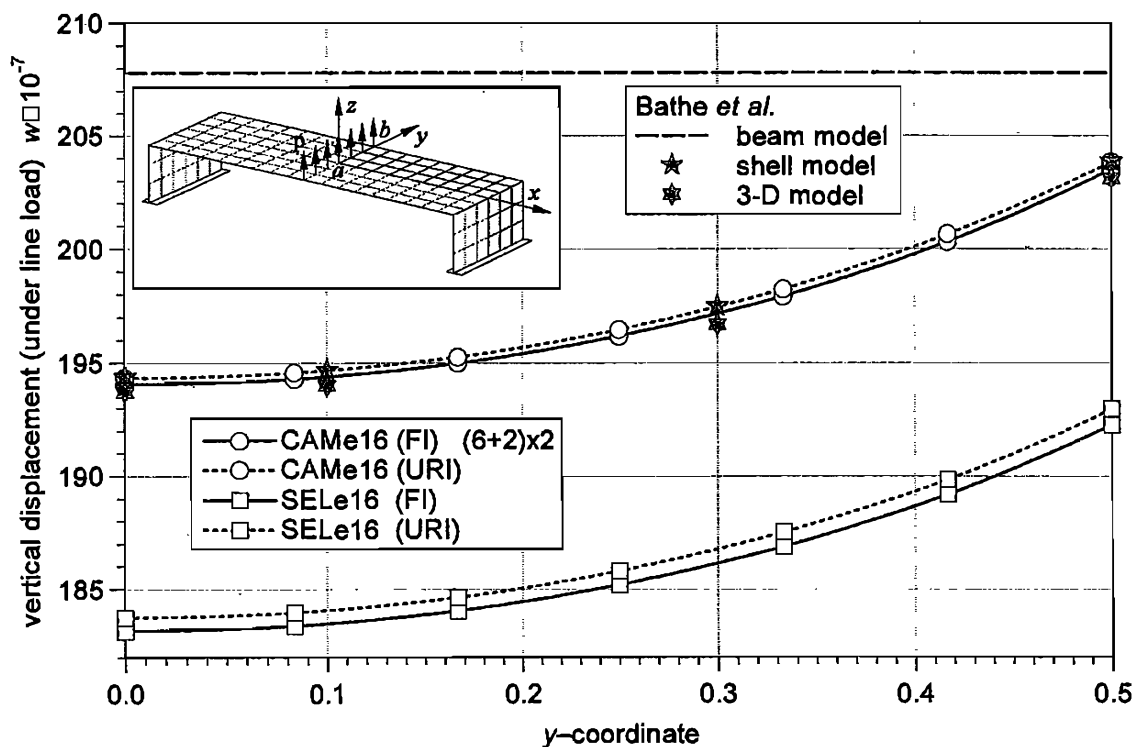


Fig. 4.2 Folded plate structure. Vertical deflection under the load line.

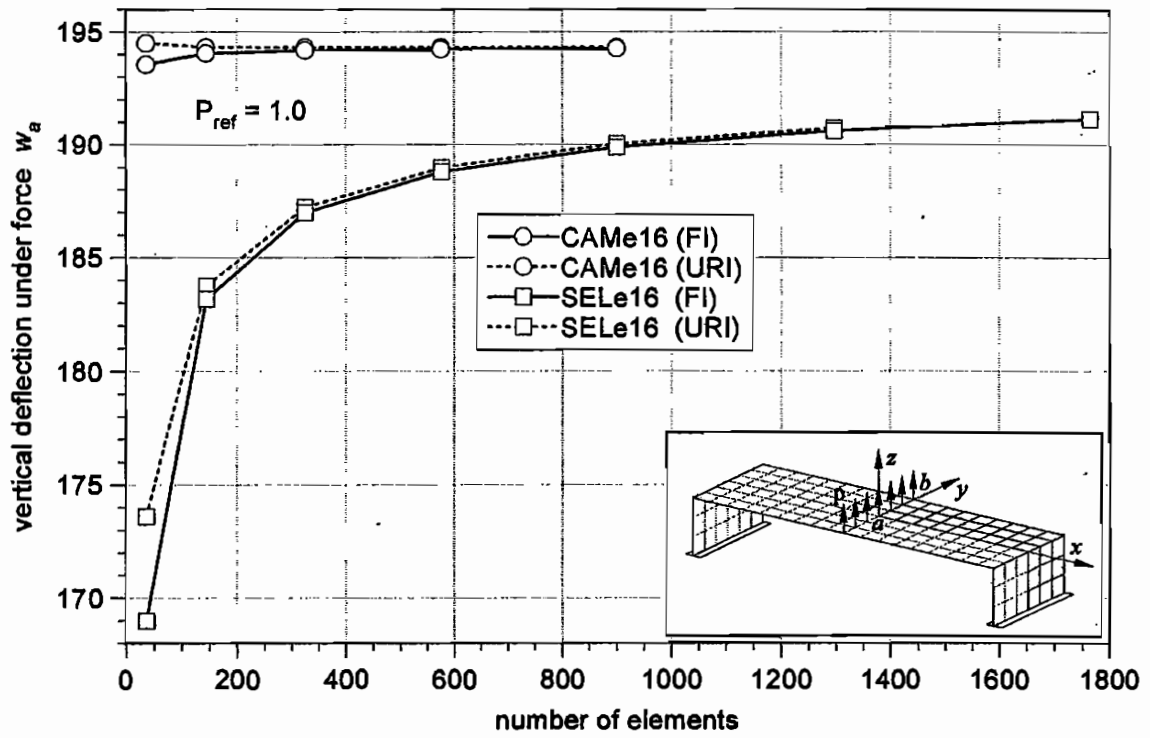
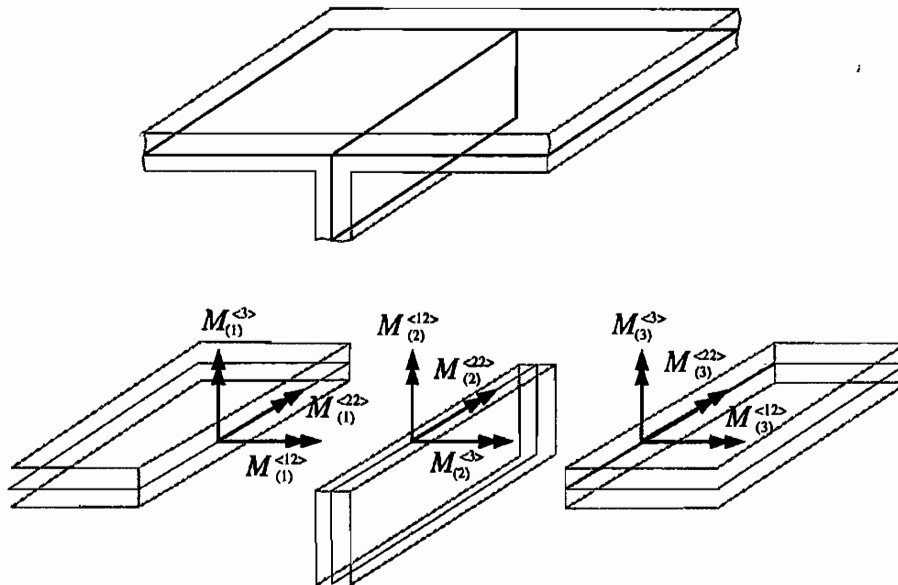


Fig. 4.3 Folded plate structure. Convergence study.

#### 4. Folded plate structures

Thin- or thick-walled folded plate structures, such as single or multicell box girders, corrugated flooring decks and unstiffened or stiffened prismatic or non-prismatic plate structures, constitute a special class of multi-shell structures. Being of particular engineering importance with own specific characteristics, they attract much attention in engineering computations. Some special methods, such as the finite strip method, for example, were worked out, which are valid for a limited class of problems. Folded plate structures also provide an attractive set of problems to verify the performance of general shell finite elements.



**Fig. 1** Branching of stress resultant couples at the T-profile plate (shell) intersection.

From the computational point of view structures of this kind are simpler to analyse than general multi-shells, because they can be modelled by using plate and facet shell finite elements. On the other hand, folded plate structures typically contain multi-intersections, and as such they are more difficult to model than the shell structures containing solely single folds and kinks. A common type of intersection has the T-profile sketched in Fig. 1. Along the common edge the plates are rigidly connected causing coupling between the in-plane and bending response. It is apparent that there is no way to define in a continuous manner the director field across such an intersection. Therefore, technique "A" (used in our SEL elements)

is ruled out and finite elements with only 5 dof per nodes cannot be applied. On the other hand, it is occasionally claimed in the literature that the technique "B" can still be applied to such structures, but we are not aware of representative numerical solutions to support this statement. It seems that if this would be possible the solutions may differ from the results obtained with the shell finite elements including drilling couples (as in our CAM, SEM, ASC elements). This can be seen, if one writes the moment equilibrium equations at the junction. For example, the moment equilibrium about the vertical direction for elements with drilling couples reads (using notation explained in Fig. 1)

$$M_{(1)}^{(3)} + M_{(2)}^{(12)} + M_{(3)}^{(3)} = 0.$$

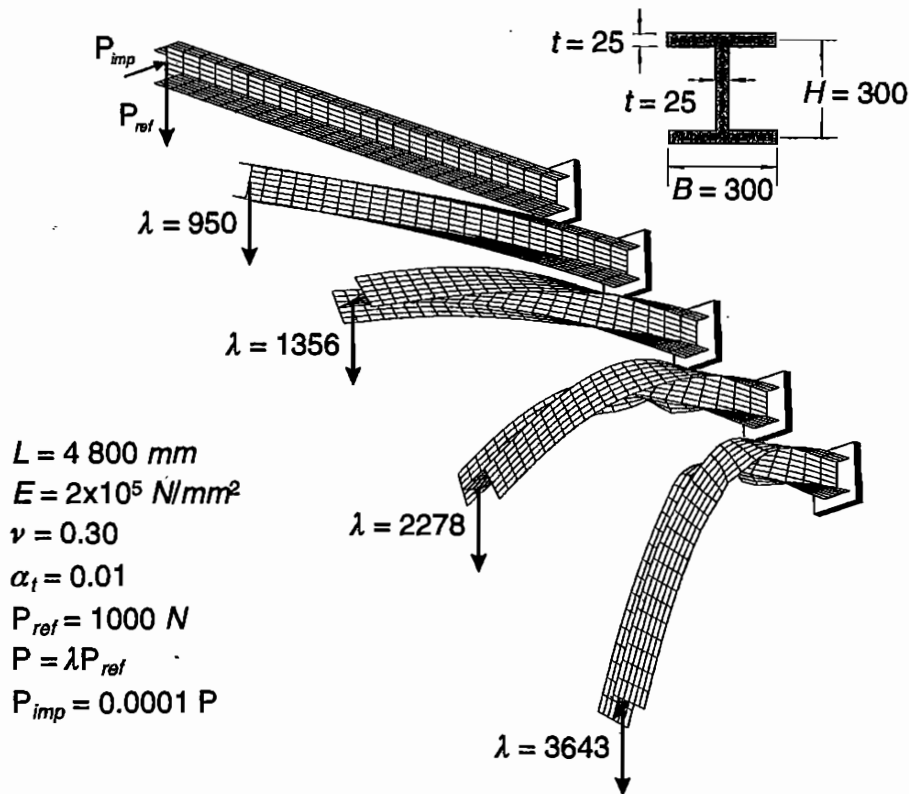
In the case of elements with 5 dof per node this condition would reduce to the form  $M_{(2)}^{(12)} = 0$ , thus enforcing the twisting couple in the vertical plate to vanish along the junction. This simply shows that shell (or plate) finite elements, which do not account for the drilling couples, do not allow a proper description of the shell behavior at the junction of adjacent structural components. It should be noted that this is true also for kinked structures, independently whether one applies the technique "A" or "B". This fact might explain some differences in the results obtained by using SEL elements and those based on elements with drilling DOF, as it has been outlined in the previous chapter.

**Example 1. I-shaped beam.** To verify the suitability of different shell elements for general applications including folded structures, we found a particularly attractive and fairly simple but challenging problem first considered by Talbot and Dhatt.<sup>1</sup> It consists of a long I-shaped beam clamped at one end and loaded by a vertical force applied at the center of the other free end (Fig. 1.1). The attractiveness of the problem lies in the results reported in the aforementioned paper, which put shades on the effectiveness and accuracy of the flat shell finite elements, which are often considered in the literature. In their study Talbot and Dhatt examined three flat triangular shell elements being the superposition of bending and membrane elements. The bending formulation of all three elements was based on a discrete Kirchhoff model, the classical 3-node DKT element, and a newly developed 6-node DKTP element. The membrane (in-plane) behavior is based on the constant (CST), linear (LST) and quadratic (QST) strain approximation. Their suitable compositions yield the following shell elements: a 3-node DCT element (DKT + CST), a 3-node DQT element (DKT + QST), a 6-node DLT element (DKTP +

---

<sup>1</sup> TALBOT AND DHATT [1987].

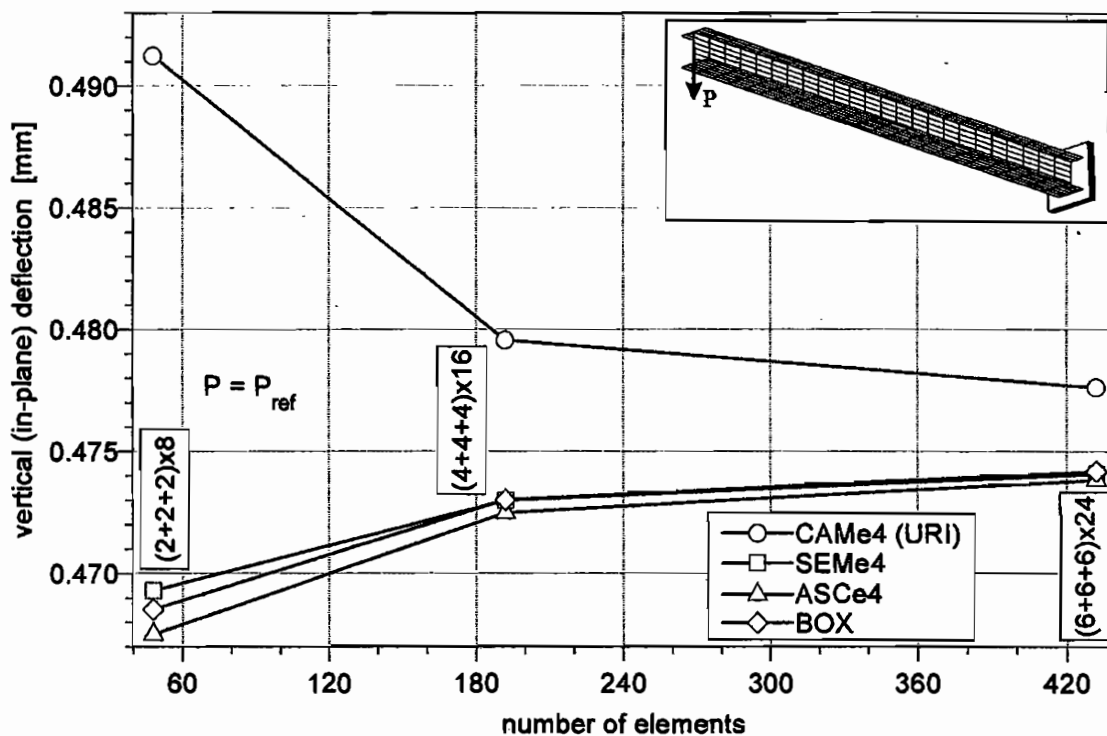
LST). All elements have six degrees of freedom per node. The rotational nodal parameters are defined in terms of derivatives of the displacements, and thus they do not coincide with real rotations as in our formulation of the shell elements. Of these elements, when applied to the problem shown in Fig. 1.1, DQT and DCT fail entirely to provide a correct solution even in the initial range of the deformation. The critical value of the load predicted by the DLT element is close to the analytical solution of the classical beam theory (see Tab. 1.2). The DQT element exhibits divergence at the critical load, while DCT element diverges even for a refined mesh without buckling. From these results due to Talbot and Dhatt one can see that this seemingly simple problem may provide a better test to assess the performance of shell finite elements than those usually examined in the literature.



**Fig. 1.1** Lateral buckling of I-shaped cantilever beam. Problem definition and computed deformed configurations in the full range of the deformation.

Within the linear range we have found a quite good coincidence of the displacements computed by using all our tested elements (CAM, SEM, ASC) and the plate element (BOX). Partial results are shown in Fig. 1.3. The complete analysis of the problem includes the nonlinear solutions and the determination of

the critical load corresponding to bifurcation of the solution. As it is seen in Fig. 1.4, for monotonously increasing values of the applied load the beam behaves nearly linearly, remaining all the time within the plane of symmetry. At the critical value  $P_{cr}$  the secondary equilibrium path, corresponding to the lateral buckling of the beam, bifurcates from the primary path. In order to determine the critical load the perturbation force of intensity 1/1000th of the vertical force  $P$  has been applied in the out-of-plane direction. This force has subsequently been removed, and the critical value of the vertical load has then been determined by reducing its value until the out-of-plane displacement reached the zero value. The critical loads computed in this way for different elements and meshes are collected in Tab. 1.2 and Fig. 1.4.



**Fig. 1.2** I-shaped cantilever beam. Convergence study of the four node elements (linear solutions).

Unlike the linear solutions, the observed differences in the values of the critical load are quite big and all results, except those predicted by BOX element, lie above the values obtained by Talbot and Dhatt. This shows that perhaps a very fine mesh would be needed in order to obtain the correct result of the critical load (which obviously need not coincide with the one predicted by the classical beam theory). It should also be noted that the critical load is attained at the in-plane

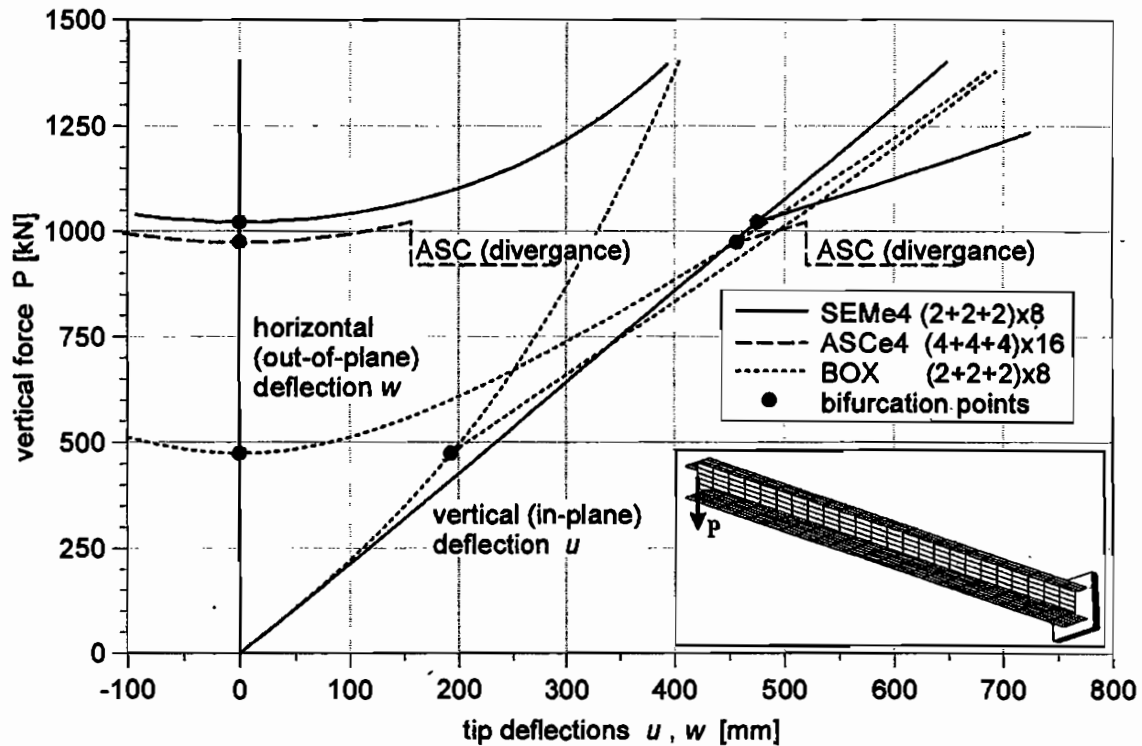
vertical deflection, which exceeds the height of the beam. The magnitude of these deflections is far beyond the validity of the von Karman plate theory, what explains, why the critical value predicted by the BOX element is much below the one obtained by using the shell elements.

**Tab. 1** Linear solutions

4-node elements				
element	mesh			
	(2+2+2)x8	(4+4+4)x16	(6+6+6)x24	
CAMe4 (FI)	0.2499	0.3871	0.4313	
CAMe4 (URI)	0.4913	0.4796	0.4776	
MIXe4	0.4675	0.4725		
SEMe4	0.4693	0.4730	0.4741	
ASCe4	0.4675	0.4725	0.4738	
BOX	0.4685	0.4730	0.4742	
9-node elements				
	mesh			
		(2+2+2)x8		(4+4+4)x16
CAMe9 (FI)		0.4735		0.4747
CAMe9 (URI)		0.4758		
MIXe9		0.4739		
SEMe9		0.4740		0.4750
ASCe9		0.4887		
16-node elements				
	mesh			
			(2+2+2)x8	
CAMe16 (FI)			0.4746	
CAMe16 (URI)			0.4759	

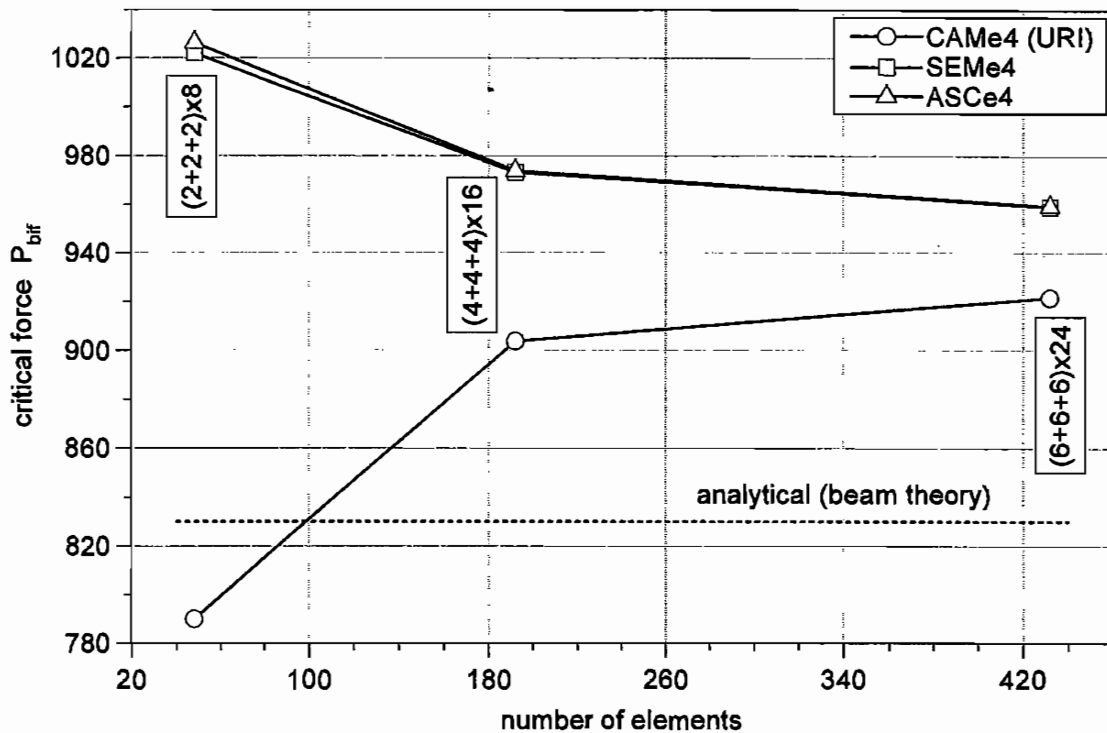
The complete solutions in the full nonlinear range obtained for different discretizations by using different elements are shown in Fig. 1.5 and Fig. 1.6. In the nonlinear analysis of this problem two observed phenomena are worth mentioning. First, as indicated in Fig. 1.3, the ASC element fails to converge at the initial post-buckling range. Second, there are quantitative differences between the solutions. The most dramatic differences appear in the range of highly nonlinear deformation. We have no clear explanation of this fact. The basic problem with the displacement/rotation based  $C^0$  elements lies in the fact that the application of

the full integration scheme to evaluate the element matrices results in an over stiff solution (locking effect). A common way to avoid this effect is the application of underintegration. However, this generally leads to spurious modes, which may essentially change the predicted behavior of the structure. However, in this example no essential locking effect has been observed. It is also remarkable that within the linear solutions the under integration results in a convergence from above. This property is opposite to the one observed for elements with full integration (Fig. 1.2). For the the critical load this property is just opposite (Fig. 1.4).



**Fig. 1.3** I-shaped cantilever beam. Primary (pre-buckling) and secondary (post-buckling) nonlinear solutions in the initial range of the deformation.





**Fig. 1.4** I-shaped cantilever beam. Convergence study of the critical load predicted by different four node elements.

**Tab. 2** Critical load

element	mesh	$P_{bif}$
CAME4 (URI)	(2+2+2)x8	790.1
	(4+4+4)x16	903.8
	(6+6+6)x24	921.7
SEMe4	(2+2+2)x8	1022.1
	(4+4+4)x16	973.2
	(6+6+6)x24	959.3
ASCe4	(2+2+2)x8	1026.3
	(4+4+4)x16	973.8
	(6+6+6)x24	959.3
BOX	(2+2+2)x8	474.1
	(4+4+4)x16	464.6
CAME9 (FI)	(2+2+2)x8	973.3
CAME9 (URI)	(2+2+2)x8	941.2
SEMe9	(2+2+2)x8	955.8
CAME16 (FI)	(2+2+2)x8	938.0
Talbot and Datt (DLT element)		834.2
analytical (beam theory)		830.0

Tab. 3 Post-buckling nonlinear solutions, mesh 2x2x2x8

CAMe9 (FI)				SEMe9			
P	u	v	w	P	u	v	w
973.25	457.07	25.941	0.000	955.85	449.72	250.84	0.000
973.41	457.28	25.983	9.000	955.98	449.93	251.25	9.000
975.43	459.98	26.532	33.632	962.25	458.38	26.835	57.654
998.88	490.96	32.946	113.88	981.66	484.36	32.190	114.55
1064.0	578.94	52.537	212.73	1049.7	573.46	51.735	211.93
1263.5	814.05	113.40	342.60	1241.6	808.96	112.59	342.24
1497.9	1066.9	194.96	423.94	1468.8	1062.2	193.93	423.32
1762.7	1319.2	294.26	479.27	1719.0	1314.2	292.60	477.80
2052.3	1564.0	409.27	517.04	1985.5	1558.7	406.77	515.71
2372.4	1799.1	538.68	543.53	2381.7	1969.4	650.15	551.04
2917.6	2130.7	756.63	567.49	2981.7	2445.6	1026.8	537.06
3556.3	2434.5	998.52	576.99	3480.1	2721.4	1304.5	507.53

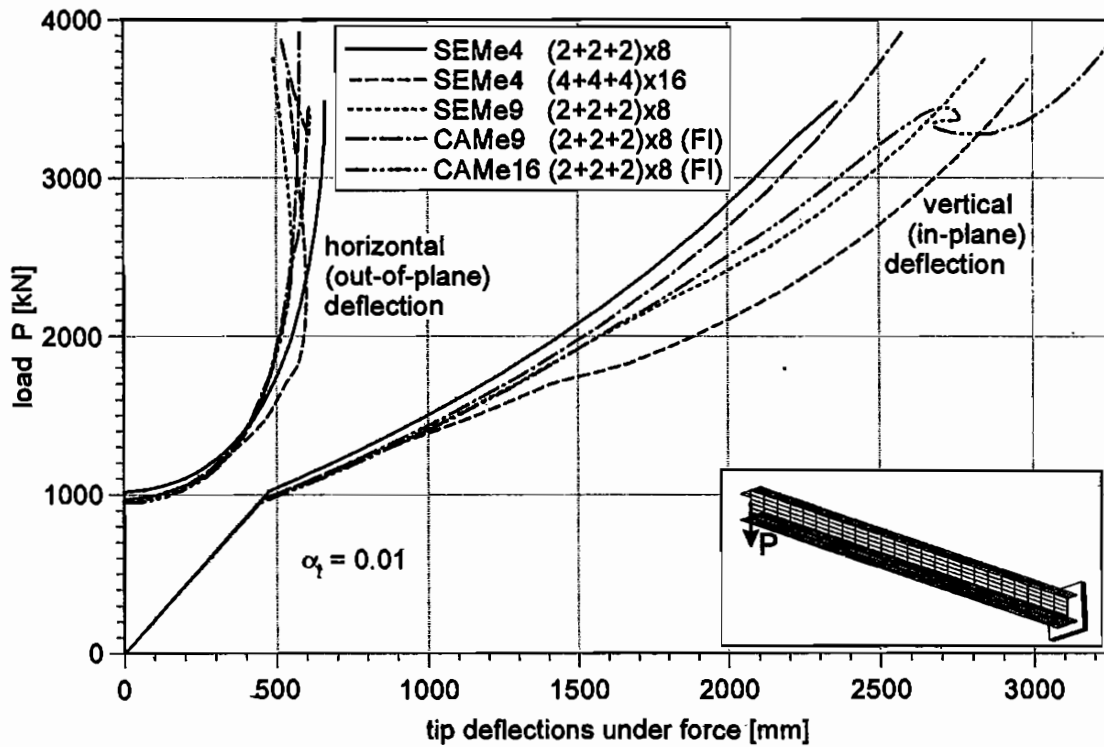
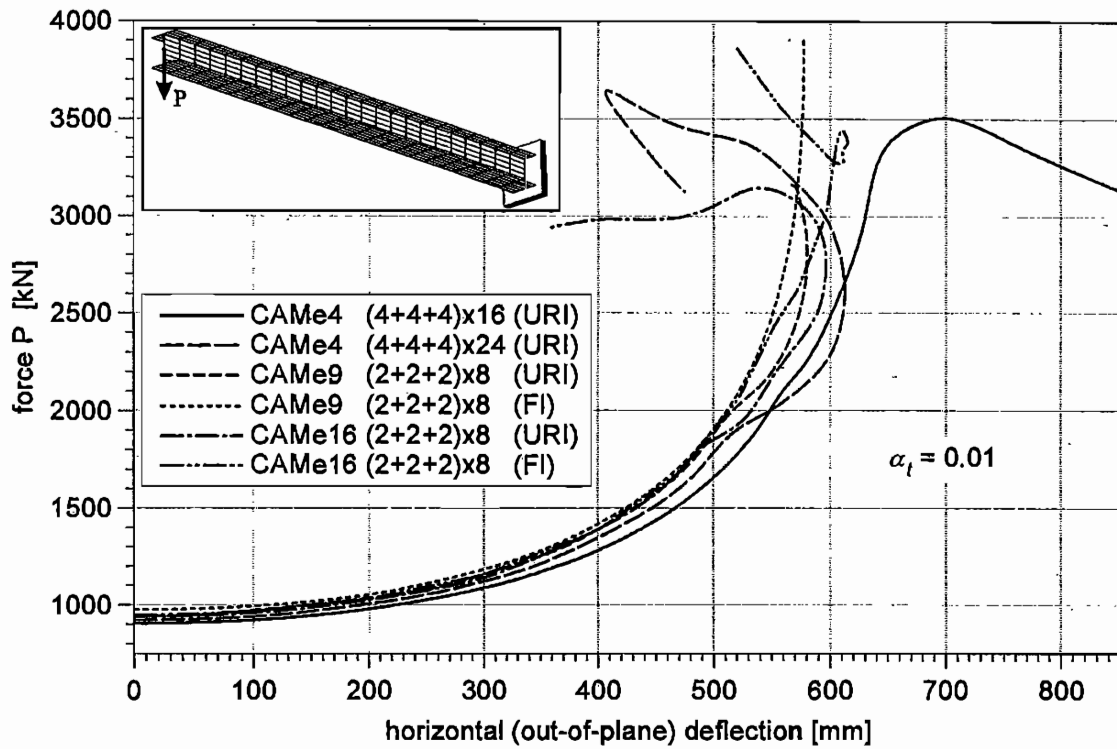


Fig. 1.5 I-shaped cantilever beam. A comparison of the displacements predicted by SEM and CAM elements in the complete range of the deformation.

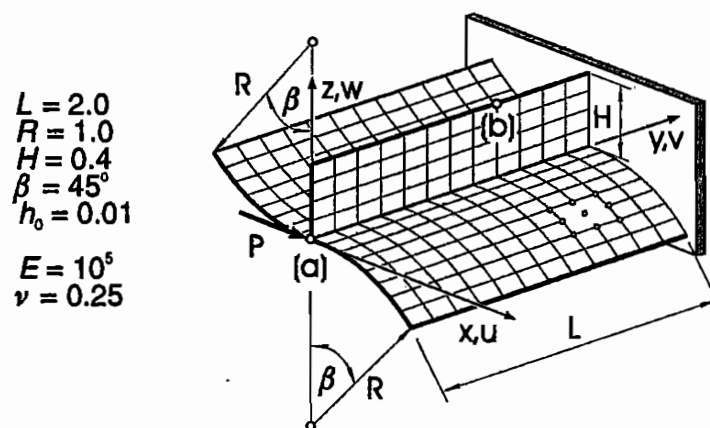


**Fig. 1.6** I-shaped cantilever beam. A comparison of the displacements predicted by CAM elements in the post-buckling range by using full and uniform reduced integration.

## 5. Irregular shell structures

All examples considered in the previous chapters have been selected from the literature, where partial numerical results were available. The examples have illustrated various aspects of the finite element analysis of plate and shell structures. We close our analysis with a new example, which essentially combines all specific features of the previous shell problems.

**Example .1 Stiffened doubly curved cylindrical panel.** A shell structure of the kind shown in Fig. 1.1 accommodates the characteristics, which are typical for light stiffened cylindrical panels often used in the aircraft and aerospace industry.



**Fig. 1.1** Stiffened doubly curved cylindrical panel. Data of the problem and computed deformed configurations (element - CAMe16 FI) in the advanced nonlinear range (secondary path II).

Such structures exhibit a more complex behavior. The main difficulty in the non-linear analysis of such structures is associated with the existence of both stable and unstable equilibrium paths in the postbuckling range. In order to obtain a complete picture of the behavior of such structures one needs to have a really reliable shell finite element capable of efficiently capturing their geometry and their deformation, as well as an effective solution procedure enabling to locate all singular points along the complete equilibrium paths.

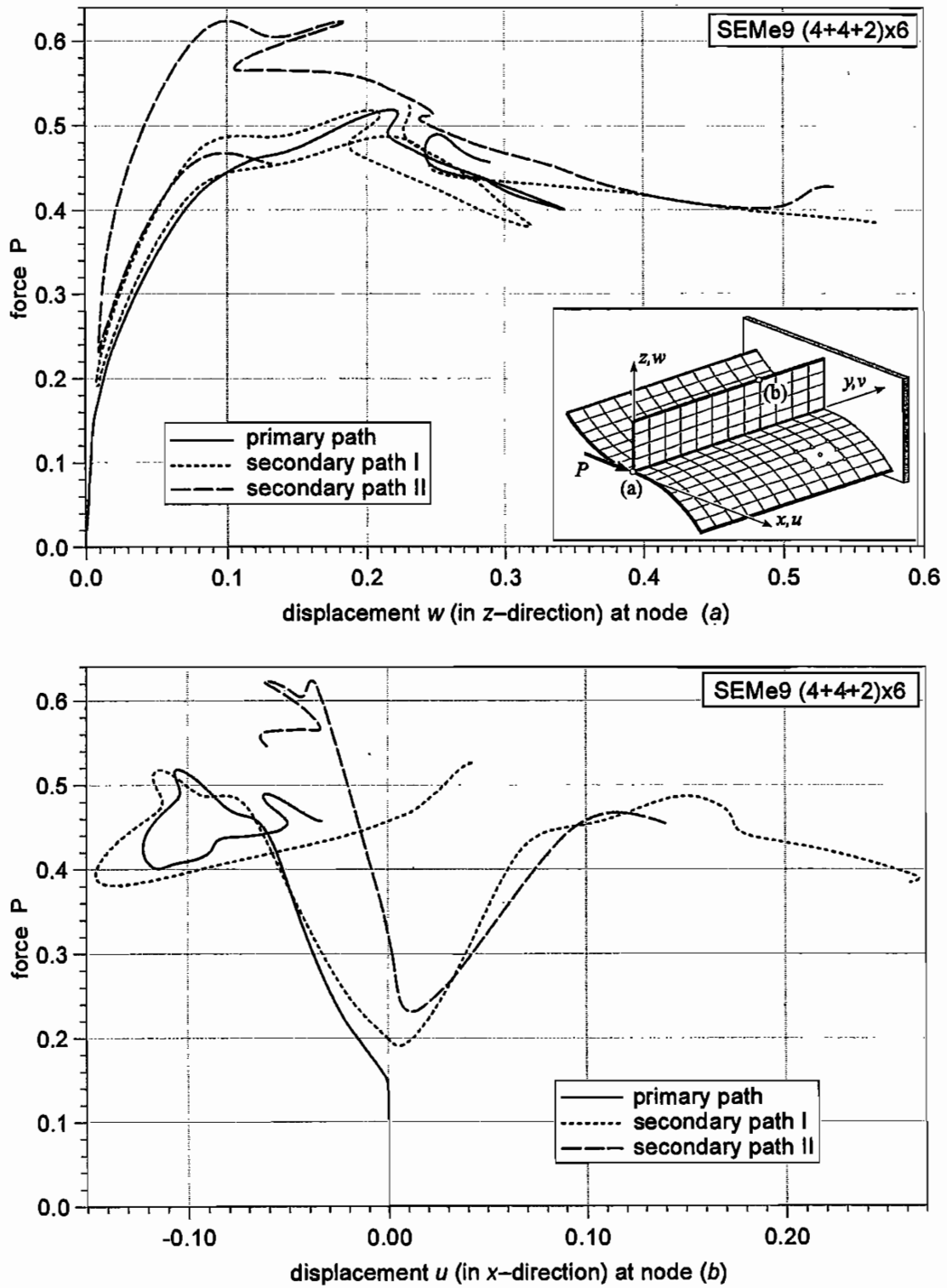
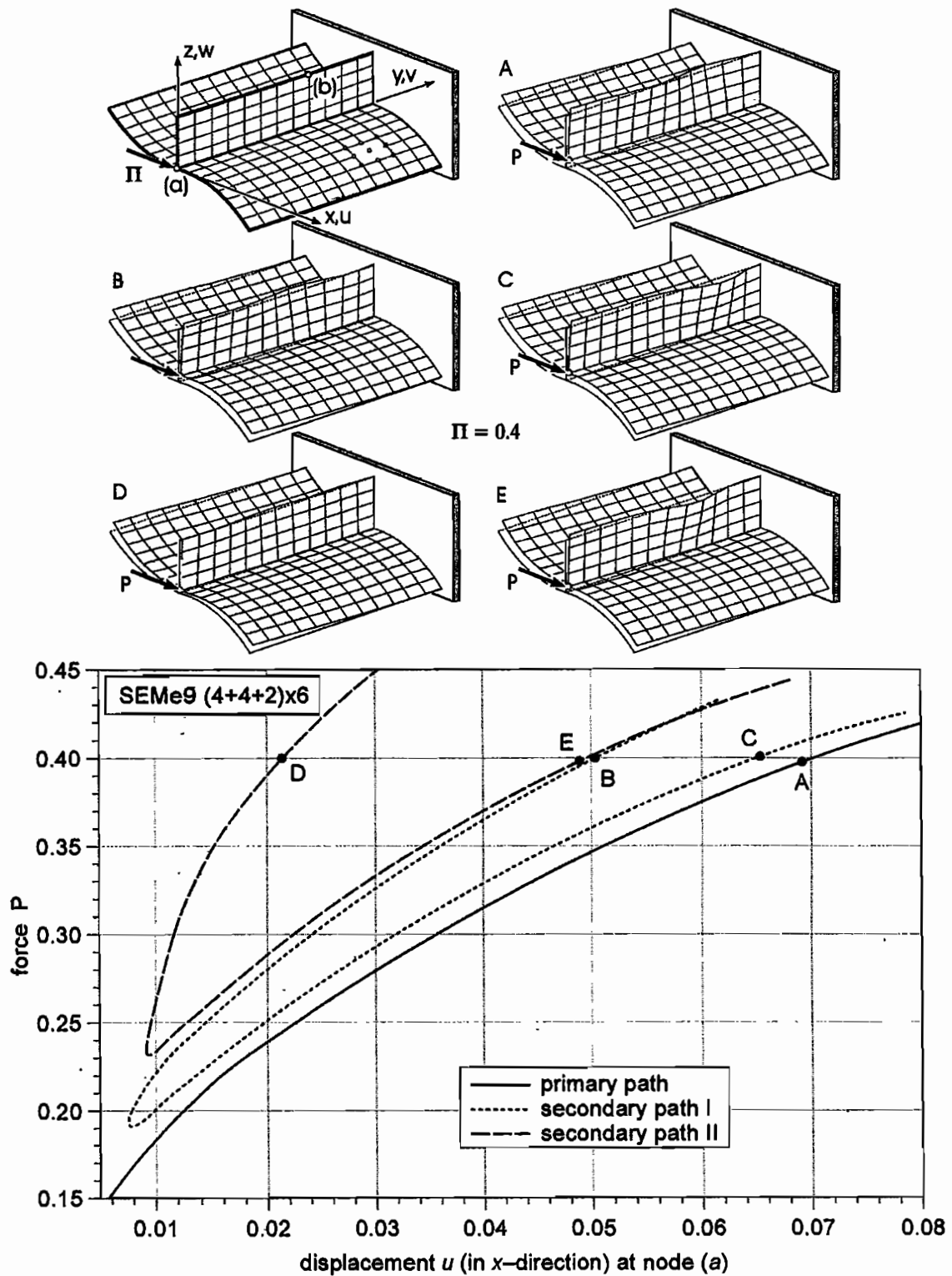
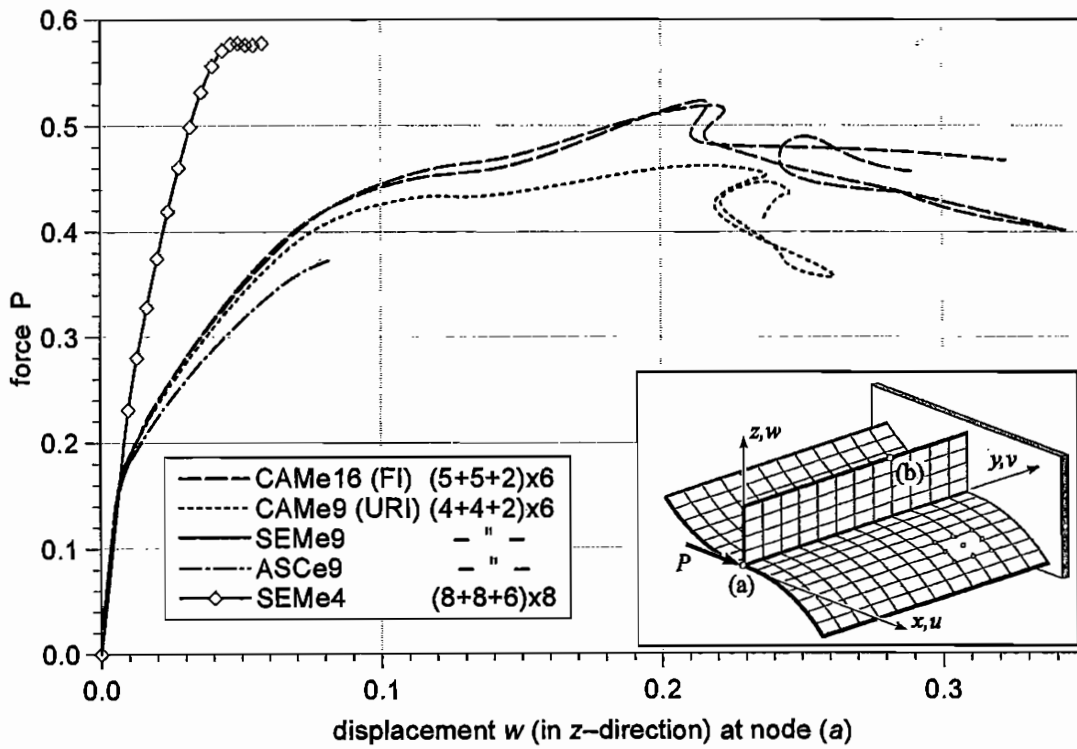
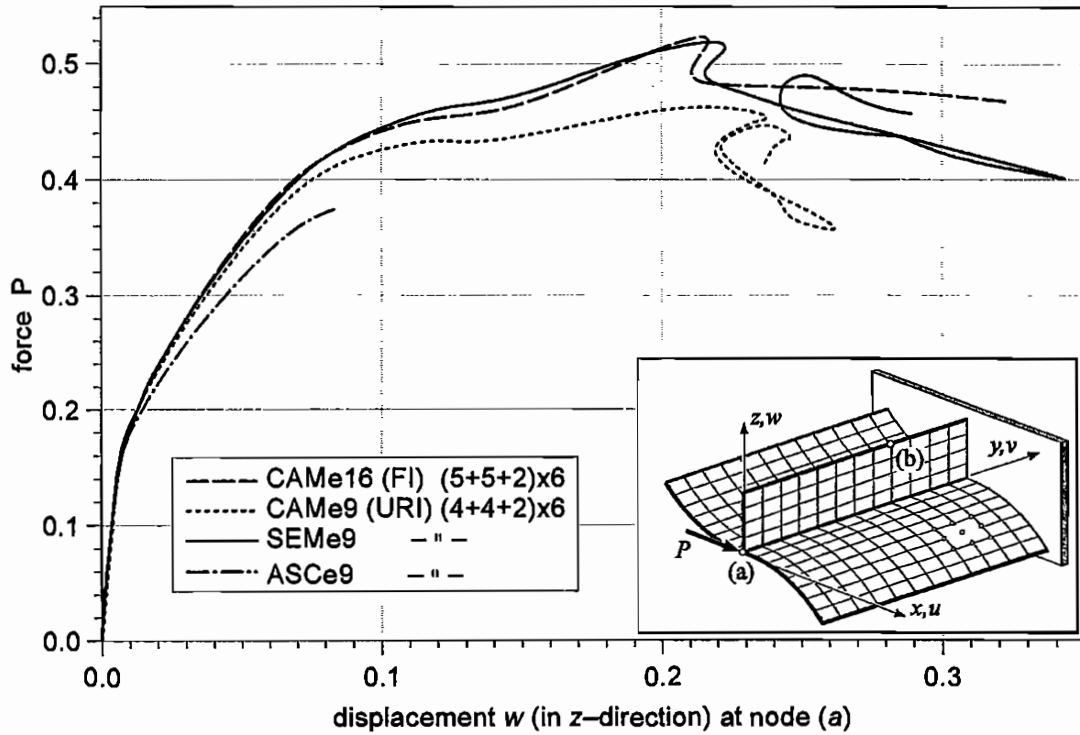


Fig. 1.2 Stiffened doubly curved cylindrical panel. Load-displacement curves for two points.



**Fig. 1.3** Stiffened doubly curved cylindrical panel. Load-displacement curves and the corresponding deformed configurations for the indicated load level.



**Fig. 1.4** Stiffened doubly curved cylindrical panel. A comparison of the load-displacement curves obtained by using different elements.

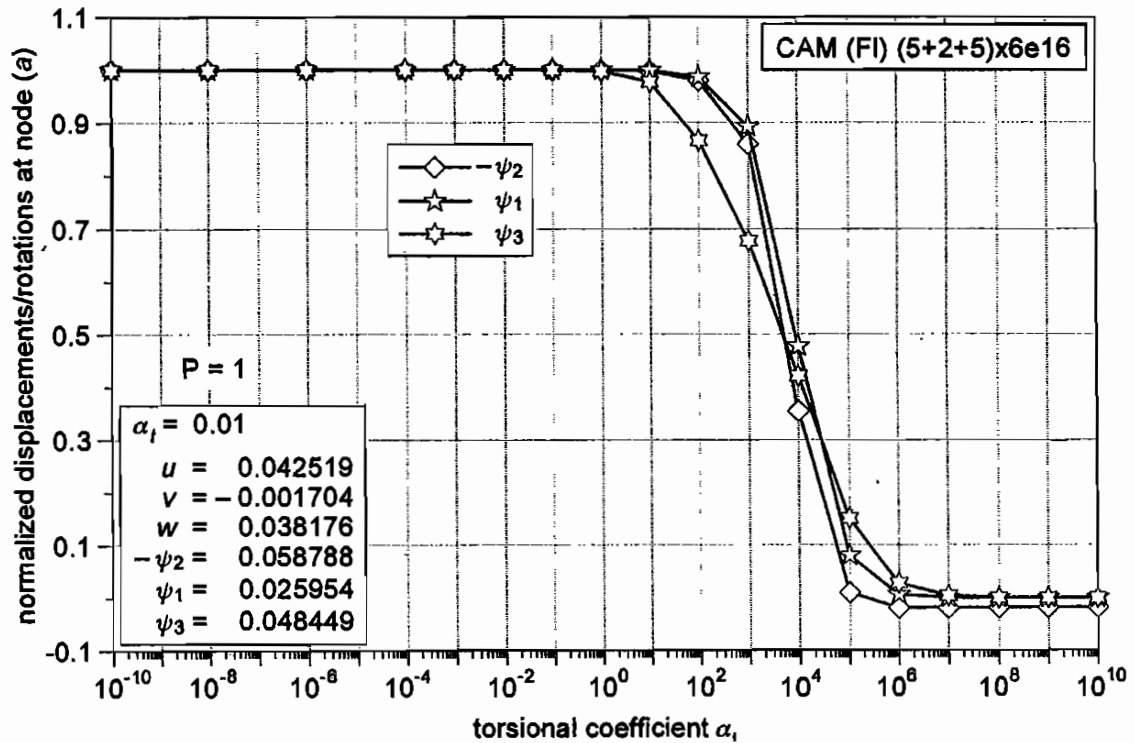
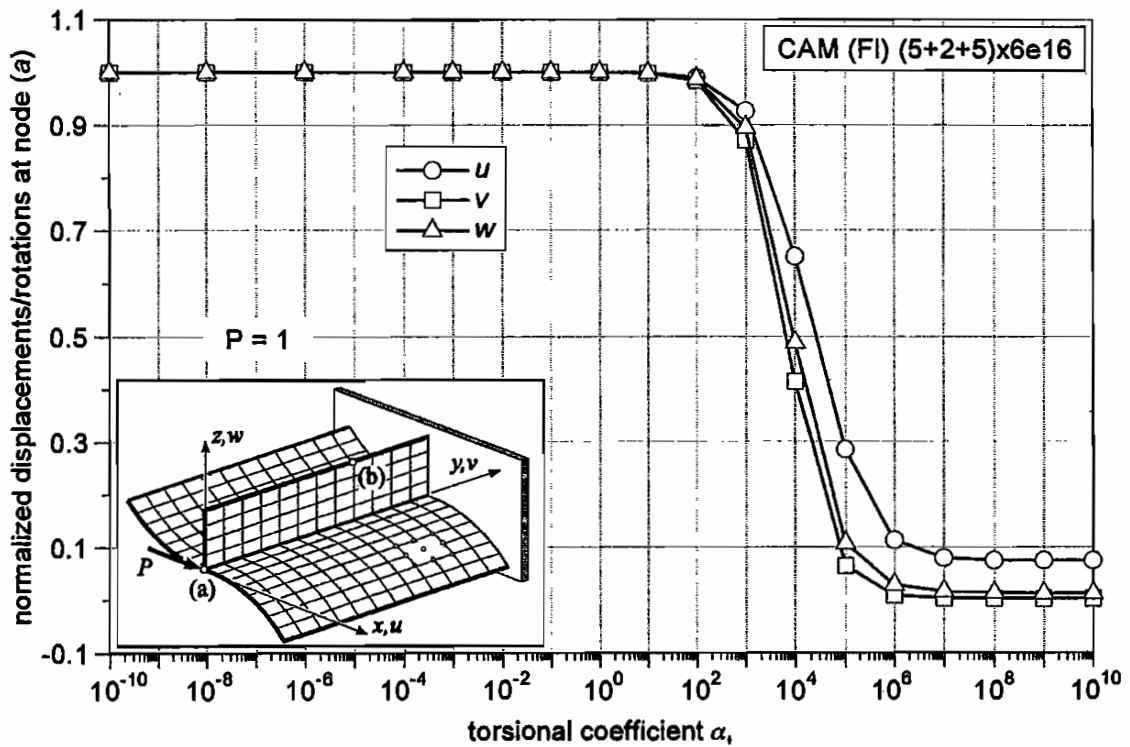
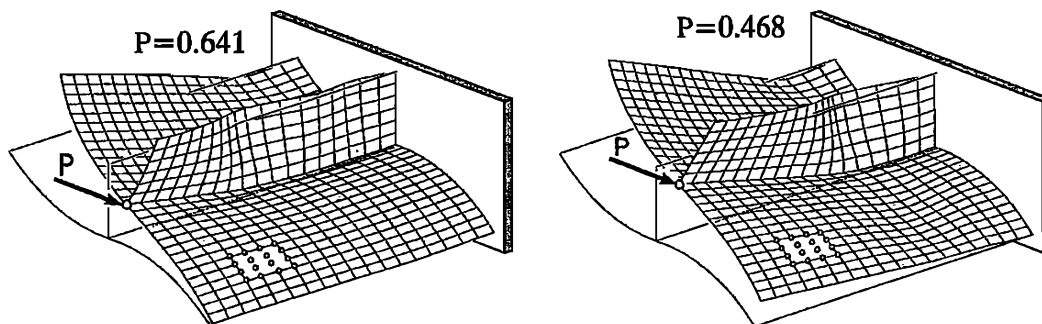


Fig. 1.6 Stiffened doubly curved cylindrical panel. A study of the influence of the torsional parameter (linear solutions).



For the particular problem shown in Fig. 1.2 partial solutions consisting of the primary and two secondary equilibrium paths (the primary path is one, which starts at the undeformed configuration of the structure) are presented in Fig. 1.2. As it can be seen in Fig. 1.2, different equilibrium paths are associated with a varying number of wave deformation patterns of the stiffener. This kind of deformation is due to a strong coupling of the membrane and bending deformations. It is very likely that this coupling may be strongly affected by the technique used to model shell intersections, and thus by the technique the drilling degree of freedom is built into the shell elements. In particular, it would be very interesting to compare our results with solutions obtained by finite elements with an alternative modeling of shell intersections proposed in the literature. Solving this problem with different shell elements we have found, in general, a fairly good coincidence of the results in the initial deformation range. However, in the advanced range of non-linear deformation the solutions predicted by different elements exhibit a more or less varying behavior of the structure, as it is seen in Fig. 1.4, where partial results are presented. Presumably, these differences would be smaller for refined finite element meshes.<sup>1</sup> Our analysis of this example ends with a clear demonstration, that as for smooth and kinked shell structures the torsional coefficient has no influence on the solution as long as it lies within the admissible range (Fig. 1.5). The observed property for the full range is of the same type as for smooth shell structures thus showing that the choice of this parameter is problem-independent.



**Fig. 1.5** Stiffened doubly curved cylindrical panel. Computed deformed configurations (secondary equilibrium path).

<sup>1</sup> All numerical results presented in this work were obtained on PC computers and therefore we were not able to use finer meshes.

## References

- AHMAD, S., IRONS, B.M. AND ZIENKIEWICZ, O.C. [1971], *Analysis of thick and thin shell structures by curved finite elements*. Int. J. Num. Meth. Eng., Vol. 2, pp. 419-451.
- ALLMAN, D.J. [1984], *A compatible triangular element including vertex rotations for plane elasticity analysis*. Comp. Struct., Vol. 19, pp. 1-8.
- ALLMAN, D.J. [1988], *Evaluation of the constant strain triangular with drilling rotations*. Int. J. Num. Meth. Eng., Vol. 26, pp. 2645-2655.
- ALLMAN, D.J. [1994], *A basic flat facet finite element for the analysis of general shells*. Int. J. Num. Meth. Eng., Vol. 37, pp. 19-35.
- ARGYRIS, J.H. AND SCHARPF, D.W. [1971], *Finite element theory of plates and shells including transverse shear strain effects*. In: B. Fraeijs de Veubeke, ed., High Speed Computing of Elastic Structures, pp. 253-292, Université de Liege.
- ARGYRIS, J.H. AND TENEK, L. [1994], *An efficient and locking-free flat anisotropic plate and shell triangular element*. Comp. Meth. Appl. Mech. Eng., Vol. 118, pp. 63-119.
- BAŞAR, Y. AND DING, Y. [1990], *Finite-rotation elements for the non-linear analysis of thin shell structures*. Int. J. Solids Struct., Vol. 26, pp. 83-97.
- BAŞAR, Y., DING, Y. AND KRÄTZIG, W.B. [1992], *Finite-rotation shell elements via mixed formulation*. Comput. Mech., Vol. 10, pp. 289-306.
- BATHE, K.-J. [1982], *Finite Element Procedures in Engineering Analysis*. Prentice-Hall, Inc., Englewood Cliffs, New Jersey.
- BATHE, K.-J. [1986], *Some advances in finite element procedures for nonlinear structural and thermal problems*. In: Computational Mechanics – Advances and Trends (ed. A.K. Noor), The American Society of Mechanical Engineering, New York.
- BATHE, K.-J. AND DVORKIN, E.N. [1985], *A four-node plate bending element based on Mindlin/Reissner plate theory and mixed interpolation*. Int. J. Num. Meth. Eng., Vol. 21, pp. 367-383.
- BATHE, K.-J. AND DVORKIN, E.N. [1986], *A formulation of general shell elements - the use of mixed interpolation of tensorial components*. Int. J. Num. Meth. Eng., Vol. 22, pp. 697-722.
- BATHE, K.-J., LEE, N.-S. AND BUCALEM, M.L. [1990], *On the use of hierarchical models in engineering analysis*. Comp. Meth. Appl. Mech. Eng., Vol. 82, pp. 5-26.
- BELYTSCHKO, T. [1986], *A review of recent developments in plate and shell elements*. In: A.K. Noor, ed., Computational Mechanics - Advances and Trends. The American Society of Mechanical Engineering, New York.
- CHEN, H.C. [1992], *Evaluation of Allman triangular membrane element used in general shell analysis*. Comput. Struct., Vol. 43, pp. 881-887.
- CHRÓŚCIELEWSKI, J. [1983], *Numerical analysis of ribbed plates in the range of geometric and material nonlinearities with the use of the finite element method* (in Polish). PhD Thesis, Gdańsk University of Technology, Gdańsk 1983.
- CHRÓŚCIELEWSKI, J. [1995], *Family of  $C^0$  finite elements in six parameter nonlinear theory of shells* (in Polish). Zeszyty Naukowe Politechniki Gdańskiej, Gdańsk (to be published).

- CHRÓSCIELEWSKI, J., GÓRSKI, J. AND IWICKI, P. [1993], *A three-node flat finite element in nonlinear shell and folded structure analysis*. Proc. XI Polish Conf. on Computer Methods in Mechanics, pp. 179-186, Kielce-Cedzyna, 11-14 May 1993.
- CHRÓSCIELEWSKI, J., GÓRSKI, J. AND IWICKI, P. [1994], *An analysis of the DCT 3-node triangular flat shell finite element*. Zeszyty Naukowe Politechniki Gdańskiej, Gdańsk 1994.
- CHRÓSCIELEWSKI, J., MAKOWSKI, J. AND STUMPF, H. [1992], *Genuinely resultant shell finite elements accounting for geometric and material non-linearity*. Int. J. Num. Meth. Eng., Vol. 35, pp. 63-94.
- CHRÓSCIELEWSKI, J., MAKOWSKI, J. AND STUMPF, H. [1994], *Finite element analysis of smooth, folded and multi-shell structures*. Comp. Meth. Appl. Mech. Eng. (submitted).
- DHATT, G., MARCOTTE, L. AND MATTE, Y. [1986], *A new triangular discrete Kirchhoff plate/shell element*. Int. J. Num. Meth. Engng, Vol. 23, pp. 453-477.
- DING, Y. [1987], *Finite-Rotations-Elemente zur geometrisch nichtlinearen Analyse allgemeiner Flachentragwerke*, Institut für Konstruktiven Ingenieurbau, Mitteilung Nr. 89-6, Ruhr-Universität Bochum.
- DONEA, J. AND BELYTSCHKO, T. [1992], *Advances in computational mechanics*. Nuclear Eng. and Design, Vol. 134, pp. 1-22.
- DVORKIN, E.N. AND BATHE, K.-J. [1984], *A continuum mechanics based four-node shell element for general nonlinear analysis*. Eng. Comput., Vol. 1, pp. 77-88.
- FOX, D.D. AND SIMO, J.C. [1992], *A drill rotation formulation for geometrically exact shells*. Comp. Meth. Appl. Mech. Eng., Vol. 98, pp. 329-343.
- FREY, F. [1989], *Shell finite elements with six degrees of freedom per node*. In: A.K. Noor, T. Belytschko and J.C. Simo, eds., *Analytical and Computational Models of Shells* (ASME, CED-Vol. 3, New York, 1989).
- GALLAGHER, R.H. [1976], *Problems and progress in thin shell finite element analysis*. In: D.G. Ashwell and R.H. Gallagher, eds., *Finite Elements for Thin Shells and Curved Members* (John Wiley and Sons, London, 1976).
- GEBHARDT, H. [1990], *Finite Element Konzepte für schubelastische Schalen mit endlichen Drehungen*. PhD Thesis, Schriftenreihe Heft 10, Institut für Baustatik, Universität Fridericiana Karlsruhe.
- HUANG, H.-C. AND HINTON, E. [1986], *A new nine node degenerated shell element with enhanced membrane and shear interpolation*. Int. J. Num. Meth. Eng., Vol. 22, pp. 73-92.
- HUGHES, T.J.R. AND BREZZI, F. [1989], *On drilling degrees of freedom*. Comp. Meth. Appl. Mech. Eng., Vol. 72, pp. 105-121.
- Struct., Vol. 9, pp. 445-457.
- HUGHES, T.J.R. AND CARNOY, E. [1983], *Nonlinear finite element formulation accounting for large membrane strains*. Comp. Meth. Appl. Mech. Eng., Vol. 39, pp. 69-82.
- HUGHES, T.J.R. AND LIU, W.K. [1981], *Nonlinear finite element analysis of shells: Part I. Three-dimensional shells*. Comp. Meth. Appl. Mech. Eng., Vol. 26, pp. 331-362.
- FELIPPA, C.A. AND MILITELLO, C. [1992], *Membrane triangles with corner drilling freedoms - II. The ANDES element*. Finite Elements in Analysis and Design, Vol. 12, pp. 189-221.
- FOX, D.D. AND SIMO, J.C. [1992], *A drill rotation formulation for geometrically exact shells*. Comput. Meth. Appl. Mech. Eng., Vol. 98, pp. 329-343.
- FREY, F. [1989], *Shell finite elements with six degrees of freedom per node*. In: *Analytical and Computational Models of Shells* (eds A.K. Noor, T. Belytschko and J.C. Simo), pp. 291-316. ASME, CED-Vol. 3, New York.

- IRONS, B.M. AND AHMAD, S. [1975], *Techniques of Finite Elements*. Ellis Horwood Limited, New York.
- JAAMEI, S., FREY, F. AND JETTEUR, PH. [1989], *Nonlinear thin shell finite element with six degrees of freedom per node*. *Comp. Meth. Appl. Mech. Eng.*, Vol. 75, pp. 251-266.
- JETTEUR, PH. AND FREY, F. [1986], *A four node Marguerre element for non-linear shell analysis*. *Eng. Comput.*, Vol. 3, pp. 276-282.
- VAN KEULEN, F., BOUT, A., AND ERNST, L.J. [1993], *Nonlinear thin shell analysis using a curved triangular element*. *Comp. Meth. Appl. Mech. Eng.*, Vol. 103, pp. 315-343.
- VAN KEULEN, F. [1993], *A geometrically nonlinear curved shell element with constant stress resultants*. *Comp. Meth. Appl. Mech. Eng.*, Vol. 106, pp. 315-352.
- LEE, H.P. AND HARRIS, P.J. [1978], *Post-buckling strength of thin-walled members*. *Comput. Struct.*, Vol. 1, pp. 689-702.
- MACNEAL, R.H. AND HARDER, R.L. [1985], *A proposed standard set of problems to test finite element accuracy*. *Finite Elements in Analysis and Design*, Vol. 1, pp. 3-20.
- MACNEAL, R.H. AND HARDER, R.L. [1988], *A refined four-noded membrane element with rotational degrees of freedom*. *Comput. Structures*, Vol. 28, 1988, pp. 75-84.
- MAKOWSKI, J. AND STUMPF, H. [1986], *Finite strains and rotations in shells*. In: W. Pietraszkiewicz, ed., *Finite Rotations in Structural Mechanics*. Springer-Verlag, Berlin.
- MAKOWSKI, J. AND STUMPF, H. [1988], *Geometric structure of fully nonlinear and linearized Cosserat type shell theory*. *Mitt. Institut für Mechanik*, Nr. 62, Ruhr-Universität Bochum.
- MAKOWSKI, J. AND STUMPF, H. [1990], *Buckling equations for elastic shells with rotational degrees of freedom undergoing finite strain deformation*. *Int. J. Solids Struct.*, Vol. 3, pp. 353-368.
- MAKOWSKI, J. AND STUMPF, H. [1994], *Mechanics of irregular shell structures*. *Mitt. Institut für Mechanik*, Nr. 95, Ruhr-Universität Bochum.
- ORAL, S. AND BARUT, A. [1991], *A shear-flexible facet shell element for large deflection and instability analysis*. *Comp. Meth. Appl. Mech. Eng.*, Vol. 93, pp. 415-431.
- PARISCH, H. [1991], *An investigation of a finite rotation four node assumed strain shell element*. *Int. J. Num. Meth. Eng.*, Vol. 31, pp. 127-150.
- PIAN, T.H.H. AND SUMIHARA, K. [1984], *Rational approach for assumed stress finite elements*. *Int. J. Num. Meth. Eng.*, Vol. 2, pp. 1685-1695.
- PIAN, T.H.H. AND WU, C.-C. [1988], *A rational approach for choosing stress terms for hybrid finite element formulations*. *Int. J. Num. Meth. Eng.*, Vol. 26, pp. 2331-2343.
- PICA, A., WOOD, R.D. AND HINTON, E. [1979], *Finite element analysis of geometrically nonlinear plate behaviour using a Mindlin formulation*. *Comp. Struct.*, Vol. 11, pp. 203-215.
- SALEEB, A.F., CHANG, T.Y., GRAF, W. AND YINGYEUNYONG, S. [1989], *A hybrid/mixed model for non-linear shell analysis and its applications to large-rotation problems*. *Int. J. Num. Meth. Eng.*, Vol. 29, pp. 407-446.
- SIMO, J.C. [1993], *On a stress resultant geometrically exact shell model. Part VII: Shell intersections with 5/6 DOF finite element formulations*. *Comp. Meth. Appl. Mech. Eng.*, Vol. 108, pp. 319-339.
- SIMO, J.C. AND ARMERO, F. [1992], *Geometrically non-linear enhanced strain mixed methods and the method of incompatible modes*. *Int. J. Num. Meth. Eng.*, Vol. 33, pp. 1413-1449.
- SIMO, J.C., FOX, D.D. AND RIFAI, M.S. [1990], *On a stress resultant geometrically exact shell model. Part III: Computational aspects of the nonlinear theory*. *Comp. Meth. Appl. Mech. Eng.*, Vol. 79, pp. 2-70.

- SIMO, J.C. AND HUGHES, T.J.R. [1986], *On the variational foundations of assumed strain methods*. ASME J. Appl. Mech., Vol. 53, pp. 51-54.
- SIMO, J.C. AND RIFAI, M.S. [1990], *A class of mixed assumed strain methods and the method of incompatible modes*. Int. J. Num. Meth. Eng., Vol. 29, pp. 1595-1638.
- STANDER, N., MATZENMILLER, A. AND RAMM, E. [1989], *An assessment of assumed strain methods in finite rotation shell analysis*. Eng. Comput., Vol. 6, pp. 58-66.
- TALBOT, M. AND DHATT, G. [1987], *Three discrete Kirchhoff elements for shell analysis with large geometrical non-linearities and bifurcations*. Eng. Comput., Vol. 4, pp. 15-22.
- TAYLOR, R.L. [1988], *Finite element analysis of linear shell problems*. In: The Mathematics of Finite Elements and Applications VI (ed. J.R. Whiteman), pp. 191-203, Academic Press, Ltd., London.
- VU-QUOC, L. AND MORA, J.A. [1989], *A class of simple and efficient degenerated shell elements - analysis of global spurious-mode filtering*. Comp. Meth. Appl. Mech. Eng., Vol. 74, pp. 117-175.
- WEMPNER, G. [1989], *Mechanics and finite elements of shells*. Appl. Mech. Rev., Vol. 42, pp. 129-142.
- WRIGGERS, P. AND GRUTTMANN, F. [1993], *Thin shells with finite rotations-formulated in Biot stresses: Theory and finite element formulation*. Int. J. Num. Meth. Eng., Vol. 36, pp. 2049-2071.
- YANG, H.T.Y., SAIGAL, S. AND LIAW, D.G. [1990], *Advances of thin shell finite elements and some applications - Version I*. Comput. Structures, Vol. 35, pp. 481-504.
- ZIENKIEWICZ, O.C. AND TAYLOR, R. L. [1989], *The Finite Element Method. Vol. I Basic Formulation of Linear Problems*. McGraw-Hill Book Comp., London.
- ZIENKIEWICZ, O.C., TAYLOR, R.L. AND TOO, J.M. [1971], *Reduced integration technique in general-analysis of plates and shells*. Int. J. Num. Meth. Eng., Vol. 3, pp. 275-29.

### **Mitteilungen aus dem Institut für Mechanik**

- Nr. 1      Theodor Lehmann:  
Große elasto-plastische Formänderungen
- Nr. 2      Bogdan Raniecki/Klaus Thermann:  
Infinitesimal Thermoelasticity and Kinematics of Finite Elastic-Plastic Deformations. Basic Concepts
- Nr. 3      Wolfgang Krings:  
Beitrag zur Finiten Element Methode bei linearem, viskoelastischem Stoffverhalten
- Nr. 4      Burkhard Lücke:  
Theoretische und experimentelle Untersuchung der zyklischen elastoplastischen Blechbiegung bei endlichen Verzerrungen
- Nr. 5      Knut Schwarze:  
Einfluß von Querschnittsverformungen bei dünnwandigen Stäben mit stetig gekrümmter Profilmittellinie
- Nr. 6      Hubert Sommer:  
Ein Beitrag zur Theorie des ebenen elastischen Verzerrungszustandes bei endlichen Formänderungen
- Nr. 7      H. Stumpf/F. J. Biehl:  
Die Methode der orthogonalen Projektionen und ihre Anwendung zur Berechnung orthotroper Platten
- Nr. 8      Albert Meyers:  
Ein Beitrag zum optimalen Entwurf von schnelllaufenden Zentrifugenschalen
- Nr. 9      Berend Fischer:  
Zur zyklischen, elastoplastischen Beanspruchung eines dickwandigen Zylinders bei endlichen Verzerrungen
- Nr. 10      Wojciech Pietraszkiewicz:  
Introduction to the Non-Linear Theory of Shells
- Nr. 11      Wilfried Ullenboom:  
Optimierung von Stäben unter nichtperiodischer dynamischer Belastung
- Nr. 12      Jürgen Güldenpfennig:  
Anwendung eines Modells der Vielkristallplastizität auf ein Problem gekoppelter elasto-plastischer Wellen
- Nr. 13      Pawel Rafalski:  
Minimum Principles in Plasticity
- Nr. 14      Peter Hilgers:  
Der Einsatz eines Mikrorechners zur hybriden Optimierung und Schwingungsanalyse
- Nr. 15      Hans-Albert Lauer:  
Optimierung von Stäben unter dynamischer periodischer Beanspruchung bei Beachtung von Spannungsrestriktionen
- Nr. 16      Martin Fritz:  
Berechnung der Auflagerkräfte und der Muskelkräfte des Menschen bei ebenen Bewegungen aufgrund von kinematographischen Aufnahmen

- Nr. 17 H. Stumpf/F. J. Biehl:  
Approximations and Error Estimates in Eigenvalue Problems of Elastic Systems with Application to Eigenvibrations of Orthotropic Plates
- Nr. 18 Uwe Kolberg:  
Variational Principles and their Numerical Application to Geometrically Nonlinear v. Karman Plates
- Nr. 19 Heinz Antes:  
Über Fehler und Möglichkeiten ihrer Abschätzung bei numerischen Berechnungen von Schalenträgwerken
- Nr. 20 Czeslaw Wozniak:  
Large Deformations of Elastic and Non-Elastic Plates, Shells and Rods
- Nr. 21 Maria K. Duszek:  
Problems of Geometrically Non-Linear Theory of Plasticity
- Nr. 22 Burkhard von Bredow:  
Optimierung von Stäben unter stochastischer Erregung
- Nr. 23 Jürgen Preuss:  
Optimaler Entwurf von Tragwerken mit Hilfe der Mehrzielmethode
- Nr. 24 Ekkehard Großmann:  
Kovarianzanalyse mechanischer Zufallsschwingungen bei Darstellung der mehrfachkorrelierten Erregungen durch stochastische Differentialgleichungen
- Nr. 25 Dieter Weichert:  
Variational Formulation and Solution of Boundary-Value Problems in the Theory of Plasticity and Application to Plate Problems
- Nr. 26 Wojciech Pietraszkiewicz:  
On Consistent Approximations in the Geometrically Non-Linear Theory of Shells
- Nr. 27 Georg Zander:  
Zur Bestimmung von Verzweigungslasten dünnwandiger Kreiszyylinder unter kombinierter Längs- und Torsionslast
- Nr. 28 Pawel Rafalski:  
An Alternative Approach to the Elastic-Viscoplastic Initial-Boundary Value Problem
- Nr. 29 Heinrich Oeynhausen:  
Verzweigungslasten elastoplastisch deformierter, dickwandiger Kreiszyylinder unter Innendruck und Axialkraft
- Nr. 30 F.-J. Biehl:  
Zweiseitige Eingrenzung von Feldgrößen beim einseitigen Kontaktproblem
- Nr. 31 Maria K. Duszek:  
Foundations of the Non-Linear Plastic Shell Theory
- Nr. 32 Reinhard Piltner:  
Spezielle finite Elemente mit Löchern, Ecken und Rissen unter Verwendung von analytischen Teillösungen
- Nr. 33 Petrisor Mazilu:  
Variationsprinzip der Thermoplastizität  
I. Wärmeausbreitung und Plastizität

- Nr. 34      **Helmut Stumpf:**  
Unified Operator Description, Nonlinear Buckling and Post-Buckling Analysis of Thin Elastic Shells
- Nr. 35      **Bernd Kaempf:**  
Ein Extremal-Variationsprinzip für die instationäre Wärmeleitung mit einer Anwendung auf thermoelastische Probleme unter Verwendung der finiten Elemente
- Nr. 36      **Alfred Kraft:**  
Zum methodischen Entwurf mechanischer Systeme im Hinblick auf optimales Schwingungsverhalten
- Nr. 37      **Petrisor Mazilu:**  
Variationsprinzipie der Thermoplastizität  
II. Gekoppelte thermomechanische Prozesse
- Nr. 38      **Klaus-Detlef Mickley:**  
Punktweise Eingrenzung von Feldgrößen in der Elastomechanik und ihre numerische Realisierung mit Fundamental-Splinefunktionen
- Nr. 39      **Lutz-Peter Nolte:**  
Beitrag zur Herleitung und vergleichende Untersuchung geometrisch nichtlinearer Schalentheorien unter Berücksichtigung großer Rotationen
- Nr. 40      **Ulrich Blix:**  
Zur Berechnung der Einschnürung von Zugstäben unter Berücksichtigung thermischer Einflüsse mit Hilfe der Finite-Element-Methode
- Nr. 41      **Peter Becker:**  
Zur Berechnung von Schallfeldern mit Elementmethoden
- Nr. 42      **Dietmar Bouchard:**  
Entwicklung und Anwendung eines an die Diskrete-Fourier-Transformation angepaßten direkten Algorithmus zur Bestimmung der modalen Parameter linearer Schwingungssysteme
- Nr. 43      **Uwe Zdebel:**  
Theoretische und experimentelle Untersuchungen zu einem thermo-plastischen Stoffgesetz
- Nr. 44      **Jan Kubik:**  
Thermosdiffusion Flows in a Solid with a Dominant Constituent
- Nr. 45      **Horst J. Klepp:**  
Über die Gleichgewichtslagen und Gleichgewichtsbereiche nichtlinearer autonomer Systeme
- Nr. 46      **J. Makowsky/L.-P. Nolte/H. Stumpf:**  
Finite In-Plane Deformations of Flexible Rods - Insight into Nonlinear Shell Problems
- Nr. 47      **Franz Karl Labisch:**  
Grundlagen einer Analyse mehrdeutiger Lösungen nichtlinearer Randwertprobleme der Elastostatik mit Hilfe von Variationsverfahren
- Nr. 48      **J. Chrosielewski/L.-P. Nolte:**  
Strategien zur Lösung nichtlinearer Probleme der Strukturmechanik und ihre modulare Aufbereitung im Konzept MESY
- Nr. 49      **Karl-Heinz Bürger:**  
Gewichtsoptimierung rotationssymmetrischer Platten unter instationärer Erregung



- Nr. 50      Ulrich Schmid:  
Zur Berechnung des plastischen Setzens von Schraubenfedern
- Nr. 51      Jörg Frischbier:  
Theorie der Stoßbelastung orthotroper Platten und ihre experimentelle Überprüfung am Beispiel einer unidirektional verstärkten CFK-Verbundplatte
- Nr. 52      W. Tarnpczynski:  
Strain history effect in cyclic plasticity
- Nr. 53      Dieter Weichert:  
Zum Problem geometrischer Nichtlinearitäten in der Plastizitätstheorie
- Nr. 54      Heinz Antes/Thomas Meise/Thomas Wiebe:  
Wellenausbreitung in akustischen Medien  
Randelement-Prozeduren im 2-D Frequenzraum und im 3-D Zeitbereich
- Nr. 55      Wojciech Pietraszkiewicz:  
Geometrically non-linear theories of thin elastic shells
- Nr. 56      Jerzy Makowski/Helmut Stumpf:  
Finite strain theory of rods
- Nr. 57      Andreas Pape:  
Zur Beschreibung des transienten und stationären Verfestigungsverhaltens von Stahl mit Hilfe eines nichtlinearen Grenzflächenmodells
- Nr. 58      Johannes Groß-Weege:  
Zum Einspielverhalten von Flächentragwerken
- Nr. 59      Peihua LIU:  
Optimierung von Kreisplatten unter dynamischer nicht rotationssymmetrischer Last
- Nr. 60      Reinhard Schmidt:  
Die Anwendung von Zustandsbeobachtern zur Schwingungsüberwachung und Schadensfrüherkennung auf mechanische Konstruktionen
- Nr. 61      Martin Pitzer:  
Vergleich einiger FE-Formulierungen auf der Basis eines inelastischen Stoffgesetzes
- Nr. 62      Jerzy Makowsky/Helmut Stumpf:  
Geometric structure of fully nonlinear and linearized Cosserat type shell theory
- Nr. 63      O. T. Bruhns:  
Große plastische Formänderungen - Bad Honnef 1988
- Nr. 64      Khanh Chau Le/Helmut Stumpf/Dieter Weichert:  
Variational principles of fracture mechanics
- Nr. 65      Guido Obermüller:  
Ein Beitrag zur Strukturoptimierung unter stochastischen Lasten
- Nr. 66      Herbert Diehl:  
Ein Materialmodell zur Berechnung von Hochgeschwindigkeitsdeformationen metallischer Werkstoffe unter besonderer Berücksichtigung der Schädigung durch Scherbänder
- Nr. 67      Michael Geis:  
Zur Berechnung ebener, elastodynamischer Rißprobleme mit der Randelementmethode

- Nr. 68 **Günter Renker:**  
Zur Identifikation nichtlinearer strukturmechanischer Systeme
- Nr. 69 **Berthold Schieck:**  
Große elastische Dehnungen in Schalen aus hyperelastischen inkompressiblen Materialien
- Nr. 70 **Frank Szepan:**  
Ein elastisch-viskoplastisches Stoffgesetz zur Beschreibung großer Formänderungen unter Berücksichtigung der thermomechanischen Kopplung
- Nr. 71 **Christian Scholz:**  
Ein Beitrag zur Gestaltoptimierung druckbelasteter Rotationsschalen
- Nr. 72 **J. Badur/H. Stumpf:**  
On the influence of E. and F. Cosserat on modern continuum mechanics and field theory
- Nr. 73 **Werner Fornefeld:**  
Zur Parameteridentifikation und Berechnung von Hochgeschwindigkeitsdeformationen metallischer Werkstoffe anhand eines Kontinuums-Damage-Modells
- Nr. 74 **J. Sączuk/H. Stumpf:**  
On statical shakedown theorems for non-linear problems
- Nr. 75 **Andreas Feldmüller:**  
Ein thermoplastisches Stoffgesetz isotrop geschädigter Kontinua
- Nr. 76 **Ulfert Rott:**  
Ein neues Konzept zur Berechnung viskoplastischer Strukturen
- Nr. 77 **Thomas Heinrich Pingel:**  
Beitrag zur Herleitung und numerischen Realisierung eines mathematischen Modells der menschlichen Wirbelsäule
- Nr. 78 **O. T. Bruhns:**  
Große plastische Formänderungen - Bad Honnef 1991
- Nr. 79 **J. Makowski/J. Chrosielewski/H. Stumpf:**  
Computational Analysis of Shells Undergoing Large Elastic Deformation Part I: Theoretical Foundations
- Nr. 80 **J. Chrosielewski/J. Makowski/H. Stumpf:**  
Computational Analysis of Shells Undergoing Large Elastic Deformation Part II: Finite Element Implementation
- Nr. 81 **R. H. Frania/H. Waller:**  
Entwicklung und Anwendung spezieller finiter Elemente für Kerbspannungsprobleme im Maschinenbau
- Nr. 82 **B. Bischoff-Beiermann:**  
Zur selbstkonsistenten Berechnung von Eigenspannungen in polykristallinem Eis unter Berücksichtigung der Monokristallanisotropie
- Nr. 83 **J. Pohé:**  
Ein Beitrag zur Stoffgesetzentwicklung für polykristallines Eis
- Nr. 84 **U. Kikillus:**  
Ein Beitrag zum zyklischen Kriechverhalten von Ck 15

- Nr. 85      T. Guo:  
Untersuchung des singulären Rißspitzenfeldes bei stationärem Rißwachstum in  
verfestigendem Material
- Nr. 86      Achim Menne:  
Identifikation der dynamischen Eigenschaften von hydrodynamischen Wandlern
- Nr. 87      Uwe Folchert:  
Identifikation der dynamischen Eigenschaften Hydrodynamischer Kupplungen
- Nr. 88      Jörg Körber:  
Ein verallgemeinertes Finite-Element-Verfahren mit asymptotischer Stabilisierung angewendet  
auf viskoplastische Materialmodelle
- Nr. 89      Peer Schieße:  
Ein Beitrag zur Berechnung des Deformationsverhaltens anisotrop geschädigter Kontinua unter  
Berücksichtigung der thermoplastischen Kopplung
- Nr. 90      Egbert Schopphoff:  
Dreidimensionale mechanische Analyse der menschlichen Wirbelsäule
- Nr. 91      Christoph Beerens:  
Zur Modellierung nichtlinearer Dämpfungsphänomene in der Strukturmechanik
- Nr. 92      K. C. Le/H. Stumpf:  
Finite elastoplasticity with microstructure
- Nr. 93      O. T. Bruhns:  
Große plastische Formänderungen - Bad Honnef 1994
- Nr. 94      Armin Lenzen:  
Untersuchung von dynamischen Systemen mit der Singulärwertzerlegung - Erfassung von  
Strukturveränderungen
- Nr. 95      J. Makowski/H. Stumpf:  
Mechanics of Irregular Shell Structures
- Nr. 96      J. Chrosielewski/J. Makowski/H. Stumpf:  
Finite Elements for Irregular Nonlinear Shells



**Mitteilungen aus dem Institut für Mechanik  
RUHR-UNIVERSITÄT BOCHUM  
Nr. 96**